EXPLORING AND MODELING CARDIAC HYPERTROPHY USING H9C2 VENTRICULAR CELLS EXPOSED TO ANGIOTENSIN-II OR LIPOPOLYSACCHARIDE FOR STUDYING HEME METABOLISM REGULATION

by

Min Ji Kim

Submitted in partial fulfilment of the requirements
for the degree of Master of Science

at

Dalhousie University
Halifax, Nova Scotia
Dec 2023

Dalhousie University is located in Mi'kma'ki,
the ancestral and unceded territory of the Mi'kmaq.
We are all Treaty people.

TABLE OF CONTENTS

LIST OF TABLES

LIST OF FIGURES

ABSTRACT

Background: Hypertrophy occurs in heart failure with preserved ejection fraction (HFpEF). The extracellular signal-regulated protein kinases (Erk1/2) and heme-regulated inhibitory kinase (HRIK) regulate protein synthesis in hypertrophy.

Objective: Explore HFpEF patients for hypertrophy and identify associated disease features that may contribute to molecular mechanisms of interest: hypertrophy, heme metabolism, or estrogen signalling. Affirming these features and mechanisms of interest from a preclinical model public dataset and model hypertrophy in cell culture for hypothesis-testing.

Hypotheses: Clinical HFpEF population shows evidence of hypertrophy, features of disease that might cause metabolic, hormonal, or inflammatory stress with males exhibiting higher rates of hypertrophy, and fewer comorbid features than females. Genes regulating heme metabolism, estrogen signaling, or cardiac hypertrophy are evident in pre-clinical rat models of HFpEF. Angiotensin II or lipopolysaccharide induce hypertrophy in H9c2 myoblasts and myotubes. Either hemin or estrogen attenuate H9c2 hypertrophy through Erk1/2, Hrik, or Nfkb signalling.

Experimental Approach: 1) Define a cohort of clinical data that identifies patients with HFpEF from a cardiac surgery outcomes database; 2) Identify a preclinical rat model with HFpEF-like comorbid features, such as: diastolic dysfunction with preserved ejection fraction, hypertrophy, evidence of metabolic or inflammatory stress. Conduct a hypothesis-affirming study that identifies genes of interest associated with comorbid features of HFpEF, including, hypertrophy, heme metabolism, estrogen signalling, or inflammation, and 3) Confirm that an *in vitro* cell model of hypertrophy using H9c2 cells treated with angiotensin-II (hormones stress) and lipopolysaccharide (metabolic-inflammatory stress) can be used for hypothesis testing of treatments (e.g. hemin or estrogen) to limit hypertrophic signalling by western blotting and alter the course of cell size changes measured by immunocytochemistry and flow cytometry.

Results/Conclusion: HFpEF patients show a complex comorbid condition that could be time-dependent to acquire/contribute to features of the disease, including hypertrophy. Genes regulating heme or hypertrophy are differentially expressed in pre-clinical conditions of hypertrophy but H9c2 cells are not a reliable model of hypertrophy for hypothesis-testing.

LIST OF ABBREVIATIONS USED

AngII	Angiotensin II
ANOVA	Analysis of variance
AT_1R	Angiotensin II type 1 Receptors
ATCC	American Type Culture Collection
BMI	Body Mass Index
CBCSA	Cell Bank of the China Sciences Academy
CO	Carbon Monoxide
DAG	Diacylglycerol
DMEM	Dulbecco's Modified Eagle Medium
DMEM-HG	Dulbeco's Modified Eagle Medium-High Glucose
E/A	Early by late diastolic transmitral flow velocity
E/e'	Early by late diastolic mitral annular tissue velocity
ECACC	European Collection of Authenticated Cell Cultures
eIF2α	α subunit of eukaryotic initiation factor 2
Eif2ak1	Eukaryotic translation initiation factor 2-alpha kinase 1
Eif2ak3	Eukaryotic translation initiation factor 3
ERK1/2	Extracellular signal-regulated kinase 1/2
FBS	Fetal Bovine Serum
FCS	Foetal Calf Serum
GEO	Gene Expression Omnibus
GPCR	G-Protein-Coupled Receptors
HF	Heart Failure
HFpEF	Heart Failure with preserved Ejection Fraction
HFrEF	Heart Failure with reduced Ejection Fraction
HMOX-1	Heme Oxygenase-1
HRIK	Heme-Regulated Inhibitor Kinase (aka Eif2ak1)
HRP	Horseradish Peroxidase
IL-1β	Interleukin-1-β
IL-6	Interleukin-6
IP3	Inositol-(1,4,5)-tri-phosphate (P_3)

JNK	c-Jun N-terminal kinase
LPS	LipoPolySaccharide
LVEDP	Left Ventricular End-Diastolic Pressure
LVEF	Left Ventricular Ejection Fraction
MAPK	Mitogen-Activated Protein Kinase
mRNA	Messenger Ribonucleic acid
MyD88	Myeloid Differentiation protein 88
NCBI	National Center for Biotechnology Information
NFKB	Nuclear Factor Kappa-β
NO	Nitric Oxide
NOX	Nicotinamide adenine dinucleotide phosphate Oxidases
NYHA	New York Heart Association
OPOS	Obesity on Postoperative Outcomes
PAMP	Pattern-Associated Molecular Pattern
PBS	Phosphate-Buffered Saline
PERK	Protein kinase RNA-like endoplasmic reticulum kinase (aka. Eif2ak3)
PKC	Protein Kinase C
PLC	Phospholipase C
RAAS	Renin-Angiotensin-Aldosterone System
ROS	Reactive Oxygen Species
RTK	Receptor Tyrosine Kinases
SD	Standard Deviation
SGLT2	Sodium-Glucose Transport Protein 2
SIBCB	Shanghai Institute of Biochemistry and Cell Biology
TLR4	Toll-Like Receptor-4
TNF-α	Tumour Necrosis Factor-alpha
TRIF	Toll/Interleukin Receptor-domain containing adaptor-inducing interferon-beta

ACKNOWLEDGEMENTS

Thank you to my parents for their support and for providing me opportunity to pursue my MSc program here in Canada. I would like to express my sincere gratitude to my supervisor, Dr. Keith R. Brunt, for all the support, countless advice, and guidance, and keeping me on the right track throughout the entire process of this thesis. I learned a lot not only academically, but I learned lots of life lessons. I am deeply thankful to my committee members, Dr. Susan Howlett and Dr. Kishore Pasumarthi, for the feedback and thoughtful suggestions that greatly contributed to the refinement of this work. To Dr. Alli Murugesan, thank you for the encouragement throughout the process.

Thank you to all my lab members, faculty, and administrative staff for giving me a positive experience at DMNB. I would not have made it so far without your help. To Kyle Wells, thank you for your collegiality and friendship. Especially editing my broken English writing.

Disclaimer: The ideas conceived, experimental directions/protocols and hypotheses presented in the current work are the result of a collaboration between Min Ji Kim and Dr. Keith R. Brunt. Unless otherwise stated, Min Ji Kim designed and performed all experiments and analyzed wrote and interpreted all results.

CHAPTER 1 INTRODUCTION

1.1 Heart failure with preserved ejection fraction (HFpEF)

Heart failure (HF) is broadly defined as the heart's inability to pump enough blood to meet the metabolic needs of other organs.[1] Ejection fraction refers to the percentage of total blood pumped out of the left ventricle in the systolic phase of the cardiac cycle.[2,3] Two major classifications of heart failure are commonly referred to as: HF with reduced ejection fraction (HFrEF) or preserved ejection fraction (HFpEF). HFpEF is also known as diastolic heart failure, as it is primarily characterized by impaired relaxation and filling of the heart ventricle during the diastole phase.[4,5] In HFpEF the ventricle does not adequately fill with blood either due to: 1) low elasticity or high amounts of stiffness in the ventricle due to passive relaxation deficits, or 2) reduced ventricle filling volume during diastole due to hypertrophy and/or impaired calcium reuptake or myofilament dysfunction typical of active relaxation deficits.[6]

In HFpEF patients, the ejection fraction is preserved or maintained at near-normal levels (greater than or equal to 50 percent).[1] This is contrasted with HFrEF where the ejection fraction is markedly decreased.[1] This indicates that the heart has the capacity to move the blood volume in the ventricle forward into the systemic circulation. This implies that there may not be systolic dysfunction in the left ventricle muscle as is the case with HFrEF. A major problem for HFpEF patients lies in the impaired ability of the ventricle to relax during diastole and fill with enough blood, causing an insufficient blood volume to accumulate in the chamber to be pumped out to rest of the body during systole. This becomes particularly apparent upon strenuous exertion-like exercise and so HFpEF patients experience symptoms more acutely when they are physically active or performing daily activities. This can be exacerbated when the myocardium hypertrophies, further restricting chamber blood volume, impairing calcium-myofilament physiology, and can precipitate mortality.

Symptoms of HF are similar regardless of ejection fraction etiology (e.g., HFrEF and HFpEF). These symptoms include shortness of breath (dyspnea) during exertion or at rest, fatigue, exercise intolerance, chest discomfort, and swelling of the lower extremities. Common causes and risk factors or comorbid features (not exhaustive) for HFpEF include: older age, obesity, diabetes, coronary artery disease or microvascular dysfunction, hypertension, atrial fibrillation, pulmonary hypertension with left ventricle dysfunction, renal dysfunction, and anemia.[7–10] Clinical diagnosis of HFpEF involves a medical history assessment, physical examination, echocardiography, and additional assessments to evaluate heart function and rule out other potential causes of symptoms.[11]

Unlike HFrEF which has several therapeutic options to alleviate symptoms and reduce mortality, there are currently no medical therapies that have shown a significant reduction in mortality for HFpEF, despite medical management of disease features.[12] It could be that the various features of disease which can be categorized as hormonal, metabolic and inflammatory continue to drive hypertrophy, alone or concurrently despite best medical efforts. Current treatment options for HFpEF are limited, and guideline recommendations primarily focus on managing congestion with loop diuretics, controlling blood pressure, and treating the associated comorbid conditions (e.g. hypertension and diabetes). Diuretics have been found to effectively reduce symptoms and improve the quality of life in HFpEF patients.[13,14] Evidence from randomized clinical trials has suggested that mineralocorticoid receptor antagonists may reduce cardiovascular death amongst women and hospitalization rates across both sexes[14,15], and secondary analyses of a clinical study considering angiotensin receptor blockers (candesartan) versus placebo in HF with ejection fraction >40 appeared to show a moderate reduction in hospitalizations in a HFpEF population.[16] The 2022 American College of Cardiology/American Heart Association Joint Committee Guidelines have added SGLT2 inhibitors (Empagliflozin)[17] and angiotensin receptor-neprilysin inhibitors (Entresto, a combination of sacubitril and valsartan) to the list of treatment options for HFpEF patients but

strong evidence has not been achieved[18], possibly as not all HFpEF patients present similarly or have consistent disease features or associated comorbidities.[19]

HFpEF is a disease with complex features. It is characterized by impaired diastolic function, which can be measured by hemodynamic measurements such as elevated left ventricular end-diastolic pressure (LVEDP), or by echocardiography measures of early by late diastolic transmitral flow velocity (E/A) or diastolic mitral annular tissue velocity (E/e') that indirectly relate to filling pressure.[20] HFpEF accounts for at least 50% of all heart failure cases and exhibits higher morbidity rates in females and higher mortality rates in males.[16,21,22] The reasons for these sex differences remain to be fully elucidated, but in part are attributed to changes in estrogen signalling (protections) either by aging or comorbidity. Hypertension is reportedly more prevalent in females with HFpEF versus males.[23] There are also likely gender influences, where women present or are assessed differently by healthcare professionals, or social determinants of being a women negatively impact medical management or inclusion in clinical trials.[18,24] Yet, how these sex and/or gender differences occurs demonstrates a wide gap in the pharmacological management within a deeper understanding of the molecular mechanisms that cause HFpEF that remain unclear.[21,25] Despite its growing prevalence and clinical importance, the pathophysiology of HFpEF remains poorly understood. HFpEF is difficult to model experimentally due to lack of well accepted *in vivo* and *in vitro* models.[5] However, breaking down and studying the individual features of HFpEF can provide valuable insights into its underlying mechanisms,[26,27] and can be used to rule in or rule out potential molecular mechanisms or identify potential new experimental therapeutics or targets of therapy.

1.2 Maladaptive cardiac hypertrophy

One of the key pathological features observed in HFpEF is hypertrophy, which refers to the thickening and enlargement of the ventricle due to the increased size of cardiomyocytes.[28] This structural change typically occurs as a compensatory response to the increased workload and

pressure experienced by the heart. Cardiomyocytes initially undergo adaptive changes to enhance their contractile function by generating additional myofilaments that then generate the necessary contractile forces to meet the demands for increased cardiac output or to overcome elevated resistance (afterload) such as may be encountered with hypertension.

Hypertrophy can be categorized into two main types: concentric or eccentric hypertrophy. Concentric hypertrophy occurs when cardiac myocytes aligned side by side grow in size laterally to the length of the cell and orientation of stretch, which thickens the wall of the heart, thereby reducing the volume of the chamber.[29] This type of hypertrophy typically results from increased pressure overload or elevated hormones (like Angiotensin II) due to low renal perfusion and is commonly observed in HFpEF.[14,29] Eccentric hypertrophy is where cardiac myocytes lengthen in the direction of the stretch, which elongates the wall of the heart, sometimes increasing chamber volume.[30] This type of hypertrophy typically results from increased volume overload, or changes in myocardial elastance.[29,30] This type of hypertrophy is more commonly associated with HFrEF.[30] However, while either concentric or eccentric may be more common in certain causes of heart failure, they can both occur in the heart depending on the location and stimuli driving hypertrophy.[31,32]

Adaptive hypertrophy of the cardiac muscle can be observed in professional athletes or during pregnancy, and it is reversible when the underlying stimulus is removed.[33–35] However, in HFpEF, the hypertrophy is maladaptive generally considered irreversible and accompanied by dysfunctional calcium handling in the cardiomyocyte.[29] This hypertrophy represents an abnormal and pathological form of cardiac muscle growth associated with interstitial and perivascular fibrosis formation that further stiffens the ventricle to impair diastolic function, leading to worsening cardiac performance.[28,31]

The underlying causes of hypertrophy in HFpEF are multifactorial. Yet, several well-

established contributing factors include: microvascular dysfunction or rarefaction, chronic inflammation, elevated hormones (e.g., norepinephrine, angiotensin II), oxidative stress, hypertension (afterload), and abnormalities in cellular calcium handling and endoplasmic reticulum stress due to metabolic disease.[31,36] In this thesis, my overall goal was to associate the effects of elevated inflammation or hormones potentially causing HFpEF or HFpEF features by oxidative stress or endoplasmic reticulum stress, the relate these drivers of hypertrophy to molecular signalling and cytoprotective mechanisms that might alleviate disease by regulating hypertrophy, specifically heme metabolism or estrogen signalling.

1.3 Angiotensin II induction of hypertrophy

Angiotensin II (AngII) is a hormone generated in the lungs by angiotensin converting enzyme from angiotensin I, which is a part of the renin-angiotensin-aldosterone system (RAAS) that acts as a compensatory mechanism to maintain hemodynamic homeostasis.[37] Initially, following cardiac damage, reduced blood flow to the kidney initiates the cascade resulting in elevated AngII to increases blood pressure and positive inotropic effects, stimulating myocardial growth and promoting angiogenesis, which leads to adaptive cardiac hypertrophy.[37] However, prolonged exposure to AngII results in maladaptive cardiac hypertrophy.

AngII activates multiple signalling pathways in the cardiomyocytes that regulate cardiac hypertrophy through AngII binding to the angiotensin II type 1 receptors (AT_1R), one of G Protein-coupled receptors (GPCRs).[37] Chronic receptor activation initiates a cascade of events, such as cardiac hypertrophy, inflammation, fibrosis, and oxidative stress.[38] The hypertrophic response of cardiomyocytes to Ang II involves AT_1R stimulating phospholipase C (PLC), which generates diacylglycerol (DAG) and inositol 1,4,5-triphosphate (IP3).[37] DAG activates protein kinase C (PKC), which in turn activates mitogen-activated protein kinases (MAPK), including extracellular signal-regulated kinase 1/2 (Erk1/2).[37] Erk1/2 is a diverse kinase pathway regulating cardiomyocyte

survival, development, and growth,[39] phosphorylates various transcription factors and induces gene expression associated with protein synthesis, leading to cardiac hypertrophy.[37,40,41]

Besides the direct activation of Erk1/2 by AngII, it can also induce cardiac hypertrophy through a secondary mechanism by the production of reactive oxygen species (ROS) mediated by nicotinamide adenine dinucleotide phosphate oxidases (NOX).[37] ROS contributes to the hypertrophic effects, in cardiomyocytes by Erk1/2 and to increased inflammatory responses by activating nuclear factor-κB (Nfkb) signalling pathways which further promote production of AngII.[37] Thus AngII activation plays an essential role in inducing cardiomyocyte hypertrophy. A schematic representation of relevant hypertrophic response from AngII is shown in Figure 1.1.

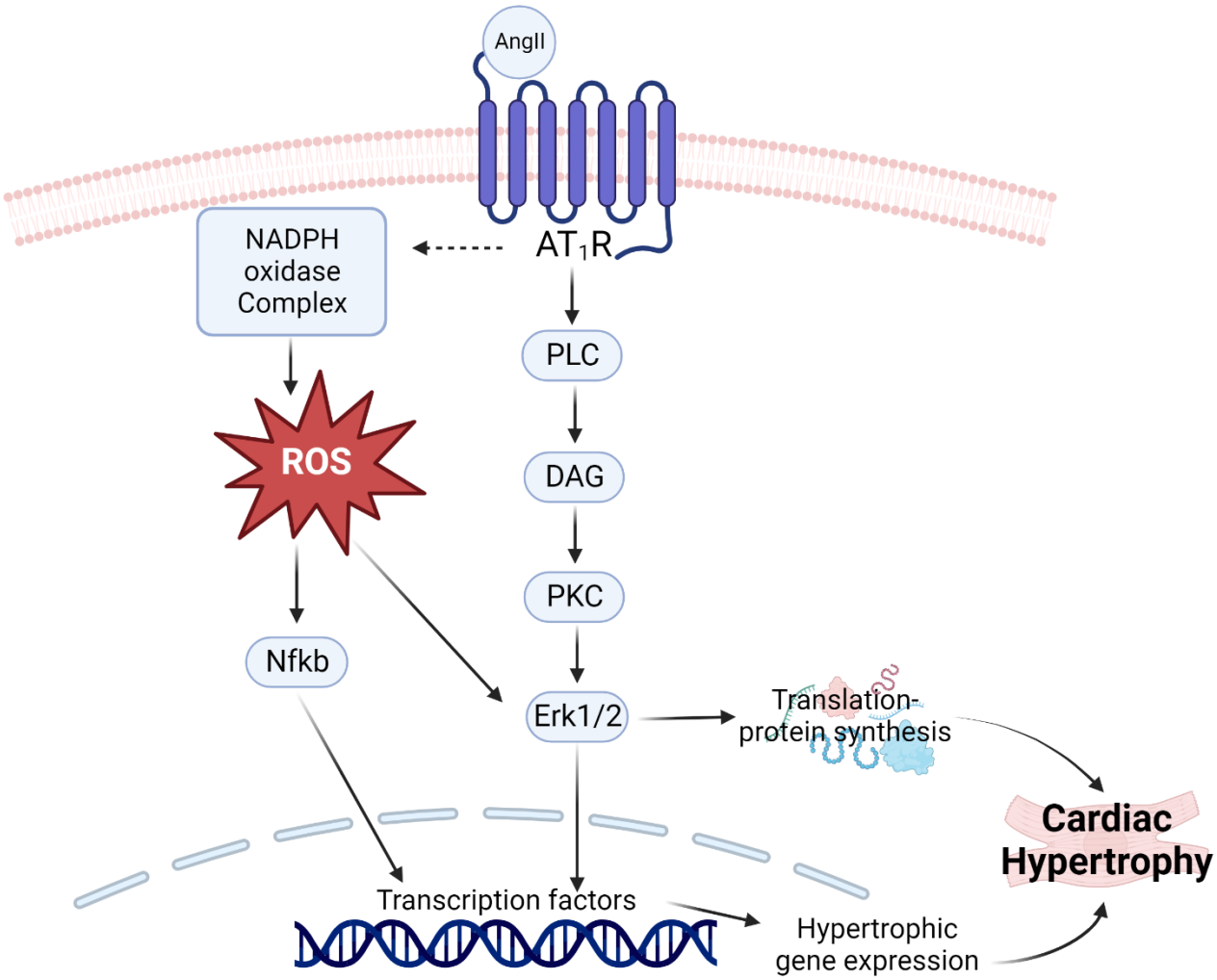

Figure 1.1. Cell signalling pathway for AngII-induced hypertrophy.
The hypertrophic response of cardiomyocytes to Ang II involves AT_1R stimulating PLC/DAG/PKC pathway, and activates MAPK, including Erk1/2. Erk1/2 phosphorylates various transcription factors and induces gene expression associated with protein synthesis, leading to cardiac hypertrophy. A secondary mechanism, production of ROS mediated by NADPH oxidase complex is involved as well, activates Erk1/2 and Nfkb signalling pathways. The figure created with BioRender.com.

1.4 Lipopolysaccharide induced hypertrophy

Lipopolysaccharide (LPS) is extracted from Gram-negative bacterial cell walls, and it is commonly used for activating inflammatory pathways.[42] LPS is one of the major components of the Gram-negative bacterial cell wall.[42] LPS has been well studied for its role as a pattern-associated molecular pattern (PAMP), which serves as a signal to the innate immune system to induce the inflammatory response through binding to the toll-like receptor-4 (TLR4).[43] TLR4, has been identified as a crucial regulator in the pathogenesis of cardiovascular diseases.[44] A wide body of evidence has been published connecting TLR4 to cardiac hypertrophy. Such studies include Ha et al.[45], who used an *in vivo* mouse model to knockout Tlr4, which reported reductions in cell size and development of cardiac hypertrophy, and Ehrentraut et al.[46] used pharmacological antagonism at the Tlr4 receptor, concluding there was a decrease in the left ventricle to body weight ratio, and a decrease in genes for hypertrophic markers, and pro-inflammatory cytokines. Moreover, increased expression of Tlr4 has been observed in ischemic heart disease, heart failure, and in ischemia/reperfusion injury[45].

To activate the signalling cascade, LPS first binds to LPS-binding protein, which then binds to cluster of differentiation which then transfers LPS to the TLR4.[47,48] Activation of TLR4 on the cell by its ligand LPS activates one of two downstream signalling pathways: myeloid differentiation protein 88 (MyD88) dependent, or TIR-domain containing adaptor-inducing interferon-beta (TRIF) dependent. The MyD88 pathway activates Nfkb, a downstream transcription factor which when activated enters the cell nucleus and promotes expression of pro-inflammatory cytokine genes that mediate the inflammatory response.[43] These genes control the release of pro-inflammatory cytokines like tumour necrosis factor-alpha (TNF-α), interleukin-1-β (IL-1β), and interleukin-6 (IL-6).[49] These same cytokines can also contribute to chronic systemic inflammatory conditions (e.g., type 2 diabetes, obesity, anemia, etc.) associated with the HFpEF phenotype.

Another MyD88 associated downstream signalling pathway activated by TLR4 are the MAPKs, which coordinate many cellular processes (i.e., cell differentiation, proliferation, cell survival, and inflammation). A number of these MAPK signalling cascade pathways have been identified playing a role in cardiac hypertrophy, such as the Erk 1/2, p38 MAPK, and c-Jun N-terminal kinase (Jnk).[50] A brief schematic representation of relevant hypertrophic response from LPS is shown in Figure 1.2.

The focus here, will be placed on Erk1/2, which plays a key role in the cardiomyocyte as an intracellular transducer of extracellular signals. Three major cell receptors within the cell respond and modulate via increased Erk1/2 signalling downstream of Tlr4 activation by its ligand[51]: integrins, GPCRs, and Receptor tyrosine kinases (RTKs).

Integrins are membrane-bound receptors involved in mechanotransduction of the extracellular matrix and cytoskeletal components because of mechanical stress to the cell, eliciting changes in structure and function. Researchers have explored the role of integrins in cardiomyocyte stretch *in vitro* under conditions of Erk activation and found that if they blocked specific isoforms of integrin, the subsequent stretch-induced release of brain natriuretic peptide was dependent on integrins.[52] This interaction contributes to the hypertrophic phenotype in cardiomyocytes.

GPCRs are also a complex target of Erk1/2 signalling, with many mediators of cardiomyocyte hypertrophy (i.e., angiotensin II, endothelin I) acting via these important transmembrane receptors. Previous work has established an the interaction of Erk1/2 with the GPCR causes an overexpression of the Gaq subunit[53] which is more robustly able to respond to local stimuli carrying maladaptive signals forward. Other studies have proposed that the beta subunit may also be modulated by Erk1/2 signalling, and that introducing regulator proteins that block the interaction of Erk1/2 with the GPCR, the response to hypertrophic stimuli produced is attenuated.[54] Despite, variability reported across the literature on which subunit of the GPCR is

being affected by Erk1/2, it remains clear that the interaction of these receptors is critical for maintaining a hypertrophic response in the cardiomyocyte, so this provides a central effector molecular mechanism to monitor during the induction of hypertrophy.

RTKs, also play an important role in converting extracellular signals to modulate intracellular processes. After Erk1/2 activation, multiple studies have noted crosstalk between GPCRs and growth factor receptors which have a role in cellular proliferation.[51] A few examples of receptors that are RTKs that depend on this Erk1/2 signallinginclude phosphorylation of the platelet derived growth factor receptor post AngII exposure[55], and the insulin-like growth factor 1 receptor which coincides with modulated Erk1/2 interaction.[56] While the literature reports that these signalling interactions contribute to maintaining cardiomyocyte homeostasis under stress conditions, they also are contributors to the maladaptive hypertrophy observed in the HFpEF phenotype.

Because LPS serves as a ligand of TLR4 introducing the inflammatory cascade as discussed above, which has been associated with the HFpEF phenotype , and due to its well reported use to model inflammatory pathways[42], we chose to use LPS as a ligand to attempt to elicit inflammatory mediated hypertrophy in our model H9c2 cells. Targeting specific components of the LPS-induced hypertrophic pathway may provide opportunities for the development of novel treatments aimed at attenuating or preventing the progression of cardiac hypertrophy in these conditions.

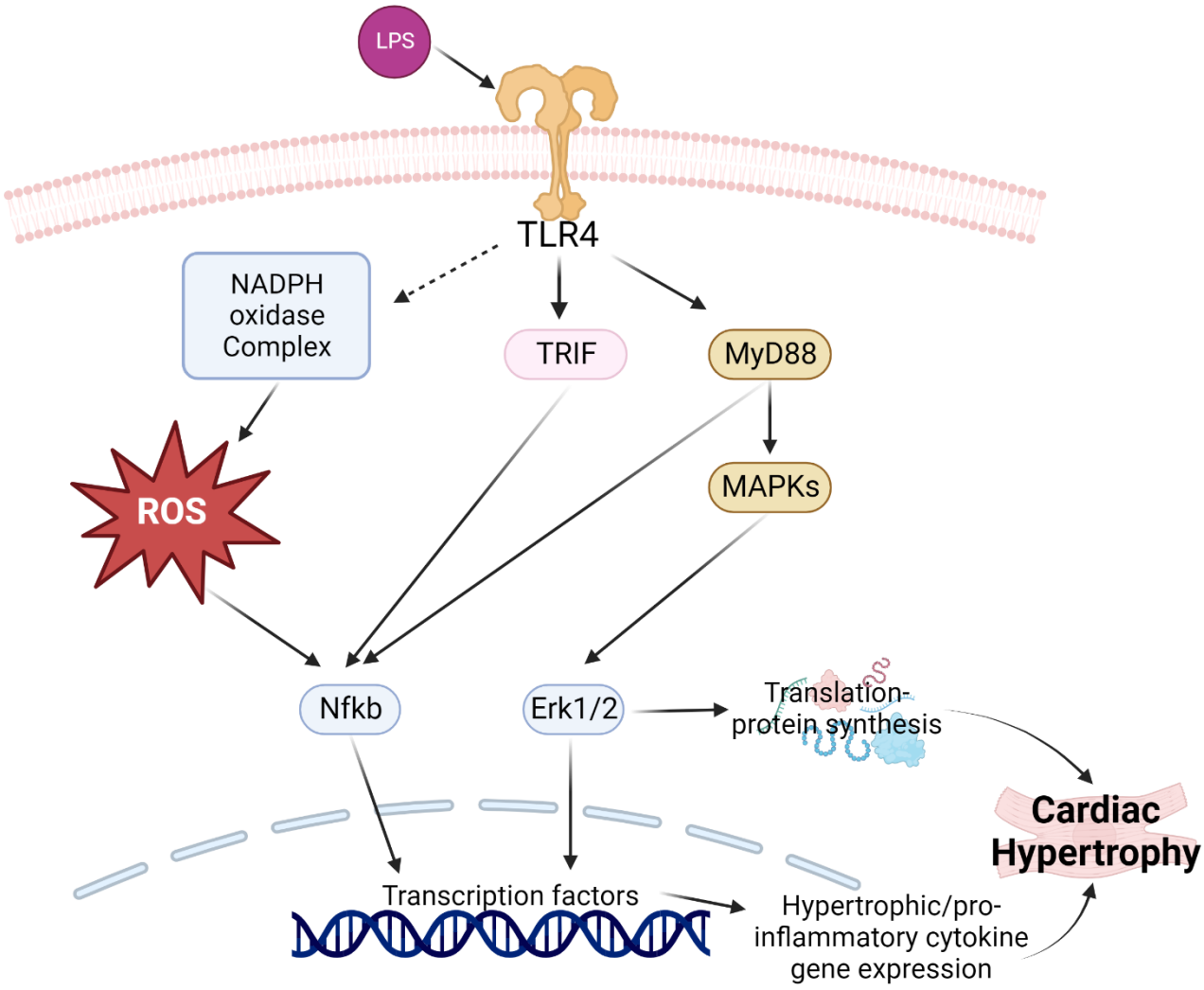

Figure 1.2. Cell signalling pathway for LPS-induced hypertrophy.
Activation of TLR4 on the cell by its ligand LPS, activates two downstream signalling pathways: MyD88 dependent, or TRIF dependent pathway. The MyD88 pathway mediates inflammatory response via activates Nfkb, which when activated enters the cell nucleus and promotes expression of pro-inflammatory cytokine genes. Another MyD88 associated downstream signalling pathway are the MAPKs, which coordinate many cellular processes. A number of these MAPK signalling cascade pathways have been identified playing a role in cardiac hypertrophy, such as the Erk 1/2. The figure created with BioRender.com.

1.5 Role of heme bioavailability in protein synthesis

Heme metabolism can also play a role in cardiac hypertrophy. In neonatal rat cardiomyocytes, overexpression of heme oxygenase-1 (Hmox-1) and incubation with biliverdin or carbon monoxide (CO)-releasing molecule suppressed the activation of Erk1/2 and the calcineurin/nuclear factor of activated T cells signalling pathway, both of which are involved in cardiac hypertrophy. Additionally, metabolomics analysis of mouse models of pressure overload-induced cardiac hypertrophy and coronary ligation demonstrated increased heme levels in hypertrophied murine hearts.[57]

Heme plays an essential role in protein synthesis by serving as a critical component of hemoproteins, which are proteins that contain heme as a prosthetic group.[58] Hemoproteins are involved in various cellular processes, including oxygen transport, electron transfer, and enzymatic reactions. One of the key functions of heme in protein synthesis is its involvement in the regulation of translation initiation. Heme-regulated inhibitor kinase (Hrik) is a kinase that is activated in response to heme deficiency. When cellular heme levels are low, Hrik is activated by autophosphorylation, leading to the phosphorylation of the α subunit of eukaryotic initiation factor 2 (eIF2α). This phosphorylation event reduces the availability of active eIF2-GTP-tRNA ternary complex, which is required for the recruitment of initiator methionyl-tRNA to the ribosome and the subsequent initiation of translation. As a result, where heme levels are low, protein synthesis (necessary for cellular hypertrophy) could be attenuated, possibly to conserve cellular resources and maintain cellular homeostasis. However, the basis of these molecular phosphor-interactions remain to be defined in myocytes. Interestingly, Hrik can also be activated by oxidative stress and can interact with NO or CO (wherein NO enhances Hrik activation, while CO suppresses Hrik activation).[59] Yet, the expression of Hmox1, which degrades heme and releases CO as a byproduct has been shown to limit cellular hypertrophy caused by oxidative stress.[60] The evaluation of heme

content, HRI expression, and HRI phosphorylation have not been characterized in cardiomyocytes under normal or stress conditions that induce hypertrophy.[61]As such, there is an opportunity to explore whether heme and or Hrik are able to regulate hypertrophy or hypertrophic signallingas means of developing novel therapeutic targets to alleviate HFpEF associated hypertrophy.

The role of heme in protein synthesis is particularly relevant in conditions where heme availability or heme synthesis is disrupted, such as certain types of anemia or heme-related disorders, including heart failure.[62–64] Alterations in heme levels can have significant impacts on cellular protein synthesis and overall protein homeostasis but also is critical to cytoprotection and maintenance of intracellular metabolism. Since anemia is a common feature of HFpEF, it may be that heme bioavailability is limited in those patients and a contributing factor to hypertrophy.

1.6 Role of estrogen with protein synthesis

Estrogen, a hormone primarily associated with female reproductive and endocrine function, plays a multifaceted role in regulating protein synthesis in various tissues throughout the body, predominantly in females. Estrogen signalling is present in both females and males, and the ratio of estrogen and testosterone signalling is potentially relevant to both sexes in hypertrophic onset or development.[65–67] Estrogen has been shown to stimulate protein synthesis in several tissues, including skeletal muscle, liver, and the cardiovascular system.

Estrogen plays a complex and multifaceted role in cardiac hypertrophy, and its effects on the Erk1/2 pathway are implicated in this process. Estrogen can exert both beneficial and detrimental effects on cardiac hypertrophy, depending on the specific context, duration of exposure, and the presence of other signalling factors. In certain conditions, estrogen has been shown to attenuate cardiac hypertrophy through its interaction with the Erk1/2 pathway.[40,68,69] Activation of Erk1/2 by estrogen can trigger a cascade of events that lead to the activation of anti-hypertrophic signalling pathways. This differs from pregnancy, where estrogen in late pregnancy is associated with

eccentric hypertrophy and diastolic dysfunction attributed to volume load stretch, which is mimicked by estrogen in ovariectomized mice causing a reduction in cardiac potassium channels and kinase activity.[70] Yet, estrogen-induced Erk1/2 activation can stimulate the production and release of anti-hypertrophic factors such as nitric oxide (NO)[71] and atrial natriuretic peptide (ANP).[72] These factors can counteract the hypertrophic stimuli and promote cardiac relaxation and vasodilation, thus preventing or reducing hypertrophy.

Overall, the role of estrogen in the Erk1/2 pathway during cardiac hypertrophy is complex and context-dependent. Estrogen can modulate Erk1/2 signalling to promote both anti-hypertrophic and pro-hypertrophic effects, depending on the specific conditions.[73] Further research is needed to elucidate the precise mechanisms by which estrogen influences the Erk1/2 pathway in the context of cardiac hypertrophy and to better understand how these interactions can be targeted for therapeutic interventions.

1.7 Rationale, hypothesis, and objectives

Hypertrophy is part of normal development and adaptation to complex stimuli or resistance in the peripheral arterial system. It can also limit the compliance of the heart and its ability to relax properly. Increased protein synthesis and higher energy demands of hypertrophied cells occurs as a direct result of generating myofilament proteins. This is controlled mainly through growth signals mediated by extracellular signal-regulated protein kinases 1 and 2 (Erk1/2) that increase protein synthesis. Erk1/2 is a key player regulating cardiac hypertrophy. Protein synthesis is also partly regulated by heme bioavailability. This occurs through phosphorylation via heme regulated inhibitory kinase (Hrik, aka. Eif2ak1), which controls protein translation through eukaryotic initiation factor 2 alpha (eif2alpha) protein. These pathways can be modified by features of HFpEF disease that contribute to hypertrophic signalling, including anemia (heme metabolism), inflammation, and hormonal signalling that potentially instigate (AngII) or regulate (estrogen)

hypertrophy.

It is important to recognize that females are more prone to living with HFpEF (morbidity), whereas males are more prone to dying from HFpEF (mortality). [25,74] Estrogen receptors regulate Erk1/2 to reduce hypertrophy in the heart.[40] It is not known what effect estrogen has on heme metabolism in cardiomyocytes undergoing hypertrophy. Whether these mechanisms can explain why there are differences in diastolic function and hypertrophy between the sexes remains has not been explored sufficiently.

The H9c2 cell line could be used in this as *in vitro* model to conduct hypothesis-testing on the molecular mechanisms regulating hypertrophy as they relate to hormone signaling, inflammation, or heme metabolism. The H9c2 cell line was originally derived from embryonic rat ventricular tissue.[75,76] H9c2 cells are commonly used as an *in vitro* model to study the cardiotoxic effect of several agents such as doxorubicin, LPS, and H_2O_2.[77]

In this thesis, I will compare stress-induced hypertrophy via hormone (HFrEF & HFpEF like) or inflammatory (HFpEF like) induced stimuli. By analyzing the hypertrophic responses and changes in molecular proteins associated with hypertrophy and diastolic dysfunction in animal models, it may be possible to affirm that these pathways have common signals or stressors related to hypertrophy. The overarching research question for this thesis is to identify and model the molecular mechanisms that regulate cardiomyocyte hypertrophy; relates this information to features of HFpEF and determine how these features and molecular mechanisms influence the sex differences between males and females with HFpEF.

For this thesis, I hypothesize that:

1. Hypertrophy is evident in a clinical population of HFpEF, and males have higher rates of hypertrophy but fewer other comorbid features associated with HFpEF than females.
2. Molecular mechanisms regulating cardiac hypertrophy, heme metabolism, or estrogen

signalling are evident (hypothesis-affirming) in a pre-clinical rat model of HFpEF determined from a public-sourced microarray dataset.

3. Exposure to AngII or LPS induces hypertrophy in rat H9c2 myoblast and/or myotubes to provide a reliable *in vitro* model for hypothesis-testing experiments related to the molecular mechanisms of hypertrophy, heme metabolism, or estrogen signalling.
4. Either hemin or estrogen will attenuate H9c2 induced hypertrophy and hypertrophic signalling through Erk1/2, Hrik, or Nfkb associated molecular mechanisms.

The overarching objectives of this thesis were to develop a connection between HFpEF and hypertrophy using the associated features of HFpEF (e.g. hypertension, anemia, metabolic/inflammation stress) that may contribute to hypertrophy or be associated with molecular mechanisms of interest: hypertrophy, heme metabolism, or estrogen signalling; thereafter affirming with a preclinical model that similar features are associated with our molecular mechanisms of interest, and finally, to model hypertrophy in cell culture for hypothesis-testing focusing on the associated molecular mechanisms regulating hypertrophy (e.g. Erk1/2, Nfkb, and Hrik).

The first objective was to identify patients where HFpEF was clinically apparent from an established clinical databank of diverse cardiac surgical samples, with a focus on records of symptoms, diastolic dysfunction, and meta-inflammatory disease features associated with HFpEF presentation. The second objective was to determine the incidence of hypertrophy based on these collected data and identify any potential for sex differences. The third objective was to determine, in addition to hypertrophy, any sex differences in HFpEF disease features that might contribute to either comorbid risks or stimuli for hypertrophy.

With these data, our fourth objective was to use a pre-clinical public dataset to support the rationale that HFpEF with hypertrophy and other HFpEF features are likely to cause changes in molecular mechanisms of interest relating to hypertrophy, heme metabolism, and/or estrogen

signalling. Our fifth objective was to compare the relative magnitude of change in gene associated with these molecular mechanisms to provide hypothesis-affirming evidence supporting *in vitro* cellular models of hypertrophy of these molecular mechanisms.

With the support that our hypotheses for molecular mechanisms were affirmed as being likely affected in a pre-clinical model, our sixth objective was to confirm and validate that rat H9c2 ventricular cells are a reliable model of cellular hypertrophy by inducing hypertrophy using AngII or LPS. The last objective would then test the hypothesis that hemin and estrogen attenuate hypertrophic signalling mediated by Erk1/2, Hrik, or Nfkb-associated pathways, notably associated with hormone signalling, heme metabolism, and inflammation.

CHAPTER 2 MATERIALS AND METHODS

2.1 Clinical database identification of HFpEF patients with hypertrophy

Obesity on Postoperative Outcomes following cardiac Surgery (OPOS) clinical database was established a registered clinical research study at the New Brunswick Heart Center (NCT: trials NCT03248921) [78]. The purpose of this study was to evaluate the impact of obesity on cardiac outcomes. Patients undergoing elective, scheduled (i.e. non-emergent) cardiac surgery were consented to participate in this observational study which involved detailed clinical review, diagnostic or prognostic evaluation and data collated with functional and clinical chemistry analyses. Blood, atrial appendage, and adipose tissue were collected intraoperatively as part of standard of care in cardiac surgery for biomarker analysis. Functional capacity, quality of life, and physical assessment measures were documented in case report forms. Clinical variables were collected from patient files, electronic medical records, and from the New Brunswick cardiac surgery registry. Clinical variables related to cardiac catheterization hemodynamic assessments and cardiac surgery procedures were collected during the standard care procedures and recorded in the APPROACH database or in patient charts that were later abstracted. Sex, body mass index (BMI), diabetes, and New York Heart Association (NYHA) functional classification were collected from the patient history section of the patient charts or documented during the normal intake for cardiac catheterization procedure approximately 6-12 months prior to being scheduled for cardiac surgery. Left ventricular ejection fraction (LVEF) and LVEDP variables were charted from pre-operative cardiac catheterization hemodynamic assessment. Whole blood analysis was performed as a routine standard of care procedures, where pre-operative hematocrit and hemoglobin values were collected from the electronic health record. This database was created, curated and linked by members of the IMPART investigator team.

For our analyses, classification of heart failure in HFpEF was practically considered present

where there are NYHA symptoms but where the LVEF is typical and in range but here we further defined its likely presence based on three clinically associated features: 1) function (LVEF ≥50% &/or LVEDP≥12mmHg),[79,80] 2) symptom presentation (NYHA classification II-IV), and 3) presence of indicative metabolic-inflammation (meta-inflammation) disease or risk factors indicated as having one or more of these conditions: obesity (defined as BMI>30, or belonging to obese classes I to III), type II diabetes (graded according to Centers for Disease Control and Prevention, Hgb-A1c level <6% = Normal, 6-6.4% = Prediabetes, >6.4% = diabetes), anemia (defined by WHO as <12.0g/dL in women/females and <13.0g/dL in men/males,[81] and graded clinically according to the National Cancer Institute, as follows: in female, 120-160g/L = Normal, 100-120g/L = Mild, 80-100g/L = Moderate, 65-80g/L = Severe; in male, 140-170g/L = Normal, 100-140g/L = Mild, 80-100g/L = Moderate, 65-80g/L = Severe)) or (Figure 2.1.).

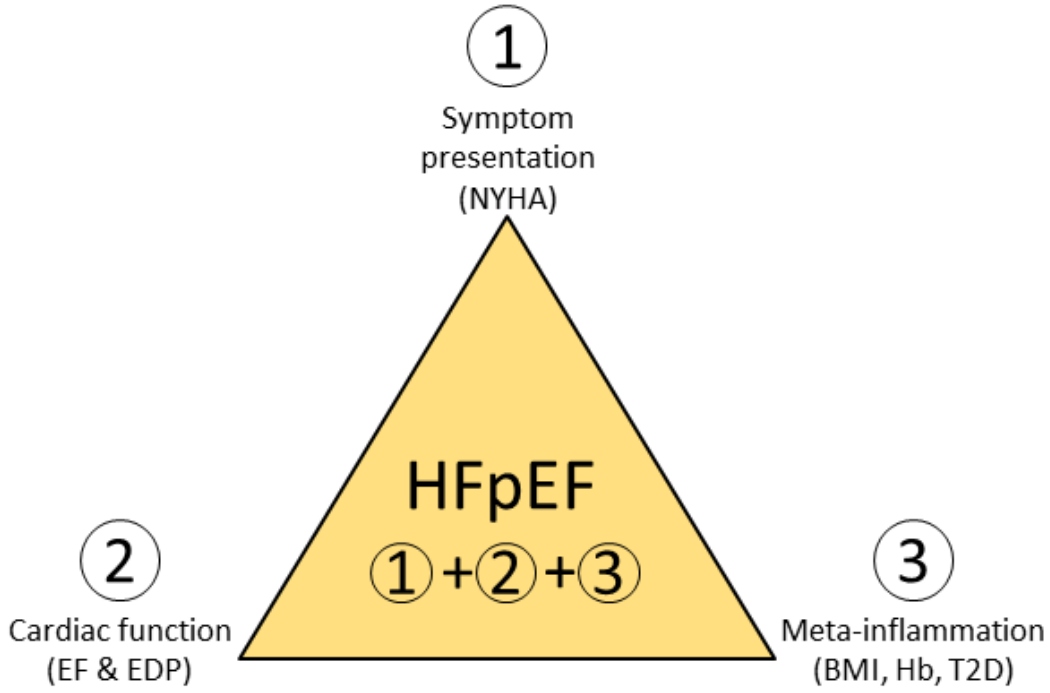

Figure 2.1. Triangulating HFpEF patients from the "Obesity on Postoperative Outcomes following cardiac Surgery (OPOS)" Database.
HFpEF is defined as patients with EF≥50%, NYHA Class II-IV, and have one or more of these conditions: type 2 diabetes, anemia, obesity class 1-3 (N=105/341 assessed; male=78, female=27). NYHA indicates New York Heart Association; EF, ejection fraction; EDP, end diastolic pressure; BMI, body mass index; Hb, Hemoglobin; T2D, type 2 diabetes.

2.2 Gene Expression Omnibus (GEO) database dataset evaluation

The Gene expression Omnibus (GEO) data was originally collected and deposited by Zhang et al[82] where the data was made public as GSE126062 and obtained through the open-access data deposited in the National Center for Biotechnology Information's (NCBI's) Gene Expression Omnibus DataSets website (http://www.ncbi.nlm.nih.gov/geoprofiles/). The available GEO DataSets were identified by searching the GEO database using the keywords "HFpEF", "Rattus norvegicus", and "Series" as an entry type. The dataset was originally generated by using an Agilent 028282 Whole Rat Genome Microarray 4x44K v3 and expressed as normalized mRNA presented in a log-transformed manner with a range from 0 to +/- 1.5 fold change in a cluster based heat map.

Gene expression values (expressed as normalized signal intensity) were extracted by GEO2R, an interactive web tool available on the NCBI website (https://www-ncbi-nlm-nih-gov.ezproxy.library.dal.ca/geo/geo2r/). The samples were defined by group-effect as "control" or "HFpEF" based on the original treatment classification of low-salt (LS) and high-salt (HS) intake in Dahl salt-sensitive (DSS) rats originally reported and phenotyped as having features of HFpEF, including diastolic dysfunction with normal EF, and HFpEF features of hypertrophy, inflammation, impaired myocardial calcium handling and metabolic dysfunction. Under the "Profile graph" tab, genes of interest were searched individually to identify the expression profile graph by entering the corresponding ID name in the GSE126062 dataset. Each animal's corresponding data value for a gene of interest that was related to hypertrophy, heme metabolism, estrogen signalling, or inflammation. The extracted data values were entered into excel for analysis to determine the group mean of samples. Given the wide variation in raw data, we utilized a log2-fold change transformation (=Log(HFpEF_Mean/Control_Mean, 2) for the purpose of data visualization (in GraphPad) of the molecular mechanism pathways of interest and clustered genes of interest related to hypertrophy, heme metabolism, estrogen signaling, or inflammation. The *a priori* prediction was

that genes related to hypertrophy, heme metabolism, or inflammation would be upregulated and therefore a one-tailed t-test was applied if the change was positive in the HFpEF group. The a priori prediction was that genes related to estrogen signalling could either be upregulated or downregulated and therefore performed a two-tailed t-test. We considered any gene with a difference of $p<0.05$ as hypothesis-affirming, as the original data was intended only for hypothesis-discovery. The data and any changes for reordering the figures to represent the groups as "Control" or "HFpEF" are defined in the figure legend and reproduced in accordance with the creative common copyright licence (CC BY 4.0 Deed, Attribution 4.0 International license, https://creativecommons.org/licenses/by/4.0/) and the journals (https://www.ncbi.nlm.nih.gov/pmc/articles/PMC7247709/) open access policy as stated (https://www.mdpi.com/openaccess#Permissions).

2.3 Cell culture

H9c2 embryonic rat ventricle cardiomyoblasts (CRL-1446, American Type Culture Collection) were expanded from frozen cryovials and maintained in Dulbeco's Modified Eagle Medium-High Glucose (DMEM-HG, Gibco, 4500 mg/L glucose) supplemented with 10% Fetal Bovine Serum (FBS, Gibco). These cells were culture expanded to 80% confluency at 37°C in a 95% air, 5% CO_2 humidified atmosphere. Cells were passaged by rinsing with 1x PBS, then 0.25% Trypsin was added to cell culture dishes; incubated at 37°C for 5 minutes to detach cells, collected by centrifugation at 500 rcf for 5 minutes, counted in a hemacytometer and then re-seeded at ~25% confluency with the seeded number proportioned according to cell culture ware for expansion into the effective growth areas. All cells were passaged at least once from the frozen cryovials and cultured for a minimum of 24h after second passage before experimental treatments. Cells used in the experiments did not exceed 20 passages and cell numbers were counted by a hemocytometer. To differentiate cardiomyoblasts to cardiomyotubes, cells were culture expanded to 80% confluency,

then the media was changed to DMEM-HG without FBS every 3 days, with media changed 2 times while maintained at 37°C in a 95% air, 5% CO_2 humidified atmosphere. For inducing hypertrophy, H9c2 cells were seeded at $2x10^5$ cells onto 35mm dish (for 24hrs prior to treatments for myoblasts or an additional 6 days without serum for myotubules) or 100mm dish (for flow cytometry) to achieve ~80-90% confluency at the time of collection for analysis. Cells were incubated at 37°C in a 95% air, 5% CO_2 humidified atmosphere for 24h, afterwards the media was changed to fresh DMEM-HG containing AngII (Sigma, Catalogue #A9525) or LPS (Enzo Life Sciences, R515 (Re), Catalogue #ALX-581-007-L002 or Sigma, O111:B4, Catalogue #L2630, as specified in Figure 3.10 as treatment). Hemin (Sigma, Catalogue #51280) was prepared as a stock solution in DMSO at 5mM, then diluted to a working solution into media at 2.5µM (5µl into 10ml, for 0.05% DMSO vehicle); and cells were treated after being seeded for 24hrs (myoblasts with 10%FBS) or 6 days (myotubules without FBS) for 24hrs then for 24hrs then harvested as a cell lysate for immunoblotting.

2.4 Resazurin (PrestoBlue™) cell metabolic activity assay

H9c2 cells were seeded in a 96-well plate as 100 µl cell media mixture/well (10,000 cells/well or 5,000 cells/well), and incubated at 37°C in a 95% air, 5% CO_2 humidified atmosphere for 24h. After treatments, 10 µl of 0.3mg/ml resazurin (Life Tech, R12204) was added to each well. The plate was incubated at 37°C for 3h with resazurin. Fluorescence (560 nm, 590 nm) and spectral absorbance (570nm, 600nm) were measured using a Synergy H4 Hybrid Reader (Biotek). An additional Resazurin supplier was required due to supply chain breakdown for cell viability based on identical chemistry principles, the PrestoBlue cell viability assay (Invitrogen, Catalogue #A13261) achieved similar results, though media compatibility for solubility had to be redetermined Appendix-A for compatibility table; requiring the addition of 0.5% FBS with the PrestoBlue during the incubation period on otherwise serum free myotubes). According to the manufacturer's

specification, 10 µl of PrestoBlue cell viability reagent was added to each well and incubated at 37°C for 1h. Fluorescence (560 nm, 590 nm) and spectral absorbance (570nm, 600nm) were measured using a Synergy H4 Hybrid Reader (Biotek) and similar data were achieved after 1h with PrestoBlue by either fluorescent or absorbent measures (Appendix-A). Cell viability was calculated by the ratio of 560nm/590nm (or 570nm/600nm) by subtracting the value of a no-cell control in all groups and then normalizing each cell treatment group to an untreated cell control group.

2.5 Immunocytochemistry and measuring cell surface size

Seventy percent alcohol was used to sterilize glass coverslips prior to placing the coverslip in a 35mm cell culture plate under sterile conditions in a biosafety cabinet. H9c2 cells in media were dropped carefully by pipetting onto the coverslips to allow attachment for 15 minutes then additional media volume was added for cell incubation. Following treatments, media was aspirated carefully, and the plate was washed with 1xPBS three times. Then, 200µl of 2% paraformaldehyde in PBS was used for fixation of cells per coverslip. The plates were incubated for 5 min at room temperature. 0.25% Triton X-100 in 1xPBS for cell permeabilization for 10 minutes. The plates were washed three times for 5 minutes in 1xPBS. To block non-specific binding, 1% BSA in 1xPBS 0.1% Tween 20 was used as a blocking buffer for 20 minutes. The plates were then washed three times for 5 minutes in 1xPBS. Phalloidin Alexa 488 (A12379, Invitrogen, 1:1000 in PBS) was added and incubated in a dark chamber for 30 minutes at room temperature. The plates were then washed three times for 5 minutes in 1xPBS. For counterstaining, Hoechst (33342, Thermo, 1:3000 in 1xPBS) was used to identify nuclei. After adding the Hoechst, the plates were incubated in a dark chamber for 1 minute at room temperature. The plates were then washed three times for 5 minutes in 1xPBS. For mounting, 10 µl of mixed glycerol and PBS in a 50:50 ratio was dropped onto a glass slide. The edges of the coverslip were sealed with clear nail polish, and the slides were allowed to dry in a dark place for 24h and cell images were obtained using a ZEISS microscope. The cell

surface area of the selected H9c2 cells were traced and quantified by ImageJ as a plug-in application for the microscope ZEISS software.

2.6 Flow cytometry and measure cell size by volume

H9c2 cells ($2x10^5$) were seeded in 100mm cell culture dish and incubated at 37°C in a 95% air, 5% CO_2 humidified atmosphere for 24h, afterward the media was changed with fresh DMEM-HG containing AngII (Sigma, A9525) or LPS (Enzo Life Sciences, R515 (Re), ALX-581-007-L002; Sigma, O111:B4, L2630) for 24h or 48h (as specified in Figure 3.10). Cells were then washed with 1x PBS, and 0.25% Trypsin was added to cell culture dishes; incubated at 37°C for 5 minutes to detach cells, and collected by centrifugation at 500 rcf for 5 minutes. The cell pellets were washed with 1xPBS by gentle pipetting up and down, and collected by centrifugation at 500 rcf for 5 minutes. The cell pellets were then resuspended in 1 ml of fresh 1xPBS by gentle pipetting up and down and the cell suspension was transferred to a flow cytometry tube (5ml). Cell size was measured by flow cytometry (Beckman Coulter) by forward scatter (FS) after collecting 75,000 cells/events and then gated for single cells for analysis. The data was analyzed by Kaluza Analysis Software.

2.7 Immunoblotting

2.7.1 Cell Collection and Lysate Preparation

Following treatment, H9c2 cells in 35mm plates were placed on ice. The media was removed by aspiration, and washed with 1xPBS, then cells were scraped into 60 µl of lysis buffer. The lysis buffer was prepared freshly before use, and consisted of 10µl protease inhibitor cocktail (VWR, m250), 10µl phosphatase inhibitor cocktail (EMD Millipore, 524628), and 10µl activated sodium orthovanadate per 100µl lysis buffer stock (20mM Tris, 5mM EDTA, 10 mM Na4P2O7, 100mM NaCl, 1% NP-40, pH=7.41). Cell lysates were transferred to 1.5ml tubes and incubated on ice for 30 minutes. Cell lysates were then sonicated for 10 seconds at 20kHz, 30% amplitude using

the QSonicator. Total protein concentrations were quantified by bicinchonic acid (BCA) protein assay kit (Pierce™). Protein samples (8µg) were denatured by heating samples at 99°C for 5 minutes in 4X Laemmli Buffer with dithiothreitol (DTT).

2.7.2 Western blotting

Denatured protein samples (8µg) were separated and resolved via 10% Mini-protein sodium dodecyl sulfate-polyacrylamide gel electrophoresis (SDS-PAGE) or by 4-20% Criterion™ TGX™ PreCast Gels (BioRad). 1µl of Precision Plus Protein™ Standards Kaleidoscope™ ladder (BioRad) and samples were loaded into the left-most empty lane (without Laemmli buffer). Mini-Protein self-cast gels were run at 90V at room temperature in 1X Tris/Glycine/SDS Electrophoresis Buffer (BioRad); Criterion™ gels were run at 90V for 30 minutes and 120V in an external ice bath to maintain temperature. Gels were run until the dye front migrated to the bottom edge of the gel. Samples were transferred to nitrocellulose (BioRad) at 100V for 1 hour 30 minutes at 4°C. Membranes were rinsed in ddH_2O and then incubated in Pierce® Reversible Memcode Stain for 5 min to confirm even transfer and measure total protein. The stained blot was labeled with indelible marker for date, lanes, experimental name, and other identifiers and then imaged using a ChemiDoc™ MP Imaging System. The membrane stain was removed using Pierce® Stain Eraser. Membranes were then protein blocked in 5% skim-milk in 1X Tris-Buffered-Saline-Tween 20 (TBS-T) for 45 minutes. Membranes were incubated in a 50ml tube or sealed plastic bags on a roller at 4°C overnight in primary antibody (1% skim-milk in TBS-T with 0.1% sodium azide) targeting Hmox1 (1:1000, H4535, Sigma), phospho-Nfkb (1:1000, CST3033S, Cell Signalling Technology), Nfkb (1:1000, CST8242S, Cell Signalling Technology), phospho Erk1/2 (1:1000, CS9101S, Cell Signalling Technology), Erk1/2 (1:1000, CS9102S, Cell Signalling Technology), Eif2ak1 (Hrikk, 1:1000, 20499-1-AP, Proteintech) or Myh7b (1:2000, ab172967, Abcam). Membranes were incubated with secondary horseradish peroxidase (HRP)-conjugated HRP-conjugated anti-mouse

(1:2000, #sc-2055, Santa Cruz), or HRP-conjugated anti-rabbit (1:2000-5000, #sc-2054, Santa Cruz) IgG for 2h in 5% skim-milk in TBS-T at room temperature on a roller. Membranes were washed three times in TBS-T and then immunoreactivity was detected using Clarity™ Western Enhanced Chemiluminescence Substrate (BioRad) or SuperSignal® West Dura Extended Duration Substrate with a ChemiDoc™ MP Imaging System. Membranes were then stripped between different primary antibodies by incubating in 25ml 0.5M Tris-HCl/SDS buffer supplemented with 125µl β-mercaptoethanol (OmniPur®) for 1 hour. Densitometry measurements were completed using ImageLab™ Software v6.1 (BioRad). Relative integrated density was calculated by the density of the target protein normalized to the total protein density of the respective memcode-stained lane. Where digital rearrangement of bands from within an individual blot was necessary for presentation this was denoted by a vertical dashed line.

2.8 Statistical analysis

Results are expressed as mean ± standard deviation (SD) unless otherwise stated. Statistical analyses were done using Excel (for GEO data only) and GraphPad Prism 9 (GraphPad Software Inc.). Unpaired student's t-Test was used on two groups with normality (or a Mann-Whitney test if data were not normally distributed). One-way analysis of variance (ANOVA) was used on three or more groups. The results were tested for normality by Shapiro-Wilk test. Where data were considered normally distributed they were analyzed by one-way ANOVA followed by Tukey's multiple comparison test. If the results did not pass the normality test, ANOVA was used with the Kruskal-Wallis test and Dunn's multiple comparisons test. P-value of less than 0.05 was considered statistically significant.

CHAPTER 3 RESULTS

3.1 Comorbidities, including hypertrophy, are not uniform in HFpEF patients

Using our criteria to triangulate HFpEF from the OPOS database, we were able to identify 105 patients out of 341 complete datasets that make up a cohort that presented clinically as having HFpEF at the time of inclusion in the study. HFpEF patients exhibited many features associated as comorbid clinical conditions, though not all are reliably present in every patient. Among the HFpEF patients, a majority exhibited high left ventricular end-diastolic pressure (LVEDP) as expected due to our use of this measure as inclusion criteria. The typical (normal) range of LVEDP is 4-12mmHg[83], and there were 9 patients at 12mmHg, with 96 patients that were above of the typical (normal) range (Figure 3.1). The left ventricular ejection fraction (LVEF) of the patients fell within the typical (normal) range (50%-70%) as expected by inclusion criteria and HFpEF definition[84], with a subset (22.2% in female, 12.8% in male, Figure 3.2) showing values typically associated with left ventricle hypertrophy (greater than 70%)[84]. Hypertrophy is often the result of hypertension, with increasing age.[85] We identified that the hypertrophic (LVEF>70%) females (N=7) had an age range from 56 to 74 years old with a median age of 69 years; 86% of these patients had hypertension (N=6). Nonhypertrophic females (N=20) had an age range from 39 to 74 years old with a median age of 65 years, 60% of these patients had hypertension (N=12). In hypertrophic males (N=13), had an age range from 48 to 73 years old with a median age of 67 years; 84.6% of the group had hypertension (N=11). Nonhypertrophic males (N=65) had an age range of 40 to 75 years old with a median of 64 years; 86.2% of these patients had hypertension (N=56). As an empirical observation of limited results, females with hypertrophy trend older with greater probability of hypertension, whereas males with hypertrophy showed no appreciable difference in age or incidence of hypertension.

In terms of body mass index (BMI)[86], HFpEF patients were predominantly overweight or

obese (greater than 24.9), although a few were within the typical (normal) range (Figure 3.3). Hemoglobin A1c (Hgb-A1c) was collected as an indicator of diabetes (not well medically managed) and followed the guideline from Centers for Disease Control and Prevention[87]. Approximately 45% of male HFpEF patients displayed elevated hemoglobin A1c levels which suggests presence of prediabetes or diabetes, while nearly 30% of female HFpEF patients exhibited similar elevations (Figure 3.4B&C). Since, diabetes can contribute to hypertension,[88–90] we observed that among females with diabetes 88% had hypertension (N=7/8) compared to 56% of females that were nondiabetic (N=10/18). Whereas, 89% of males with diabetes also had hypertension (N=31/35), but this was similar to non-diabetic males, of which 85% had hypertension(N=33/39). As an empirical observation of limited results, females with hypertension may be more likely to have diabetes (uncontrolled), whereas no appreciable difference was observed with the incidence of diabetes (uncontrolled) or hypertension in males.

Pre-operative hemoglobin levels were collected as an indication of anemia, and grading of anemia was done in accordance to the National Cancer Institute classification.[91,92] HFpEF patients displayed low hemoglobin levels (Figure 3.5), and males patients (48.7%) were about double compared to females patients (22.2%). Anemia can be a consequence of renal end organ damage contributing to hypertension and hypertrophy.[93–95] Females with anemia had a hypertension incidence of 80% (N=4/5) and 20% of anemic females had hypertrophy (N=1/5), compared to nonanemic females where 64% had hypertension (N=14/22) and 27% had hypertrophy (N=6/22). Anemia in males with hypertension was 94% (N=33/35) but just 17% of anemic males (N=6/35) had hypertrophy compared to non-anemic males with incidence of hypertension of 79% (N=34/43) or hypertrophy of 16% (N=7/43). As an empirical observation of limited results, both sexes may be more likely to have both anemia with hypertension, with slightly more males than females having coinciding features; yet both sexes are similar with anemia and hypertrophy.

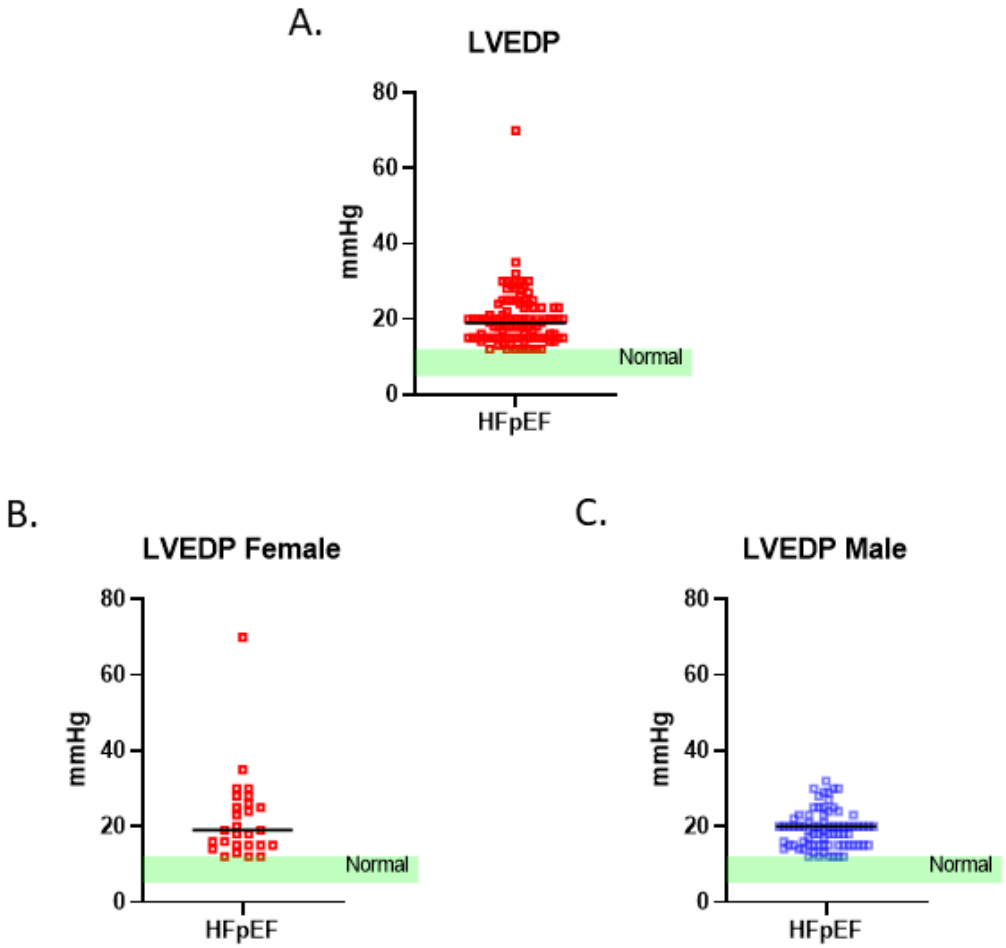

Figure 3.1. Evidence of diastolic dysfunction in HFpEF patients.
(A) LVEDP of total HFpEF patients. (B) LVEDP of Female HFpEF patients. (C) LVEDP of Male HFpEF patients. Normal range of LVEDP is 4-12mmHg.

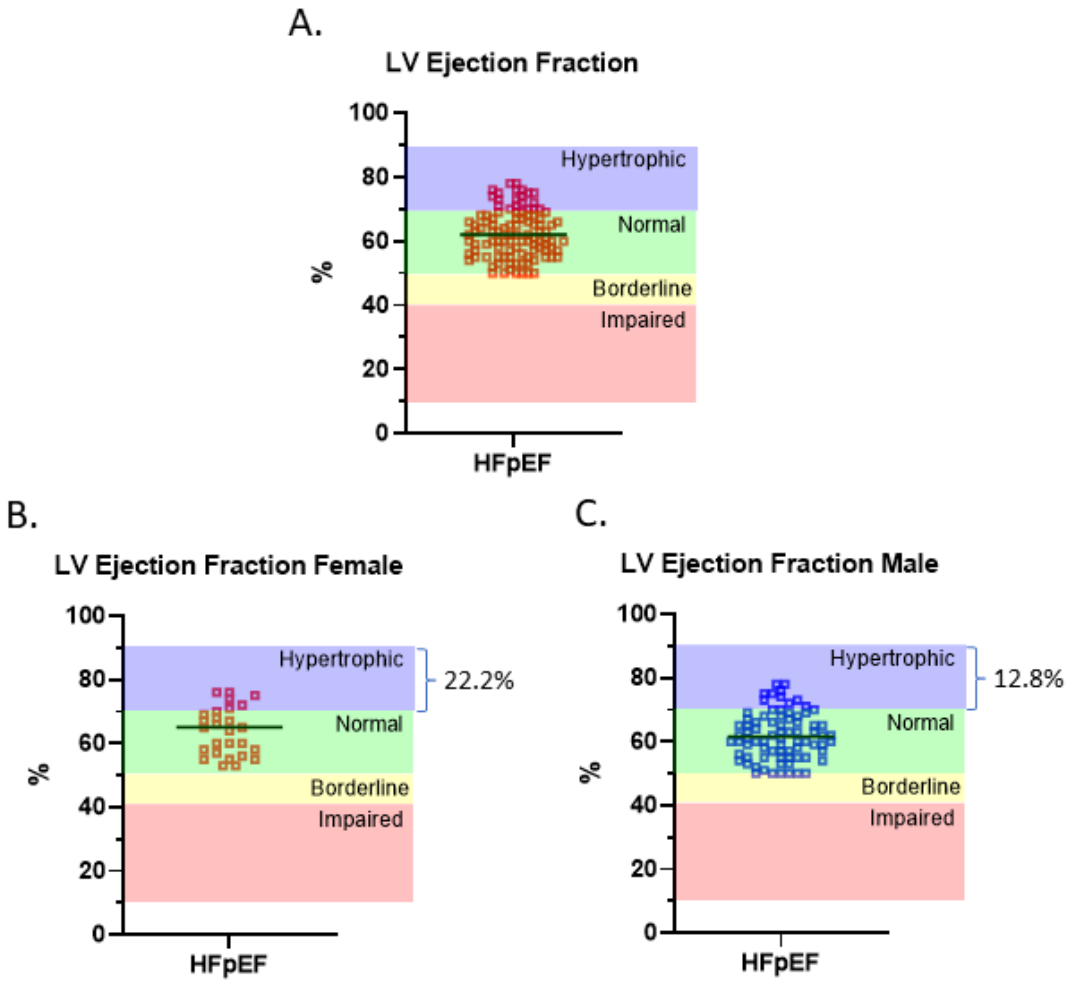

Figure 3.2. Evidence of hypertrophy in HFpEF patients.
(A) LVEF of the total HFpEF patients. (B) LVEF of Female HFpEF patients. (C) LVEF of Male HFpEF patients. LVEF classification from American College of Cardiology that is used clinically, >70% = Hypertrophic, 50%-70% = Normal, 40%-49% = Borderline, <40% = Impaired.

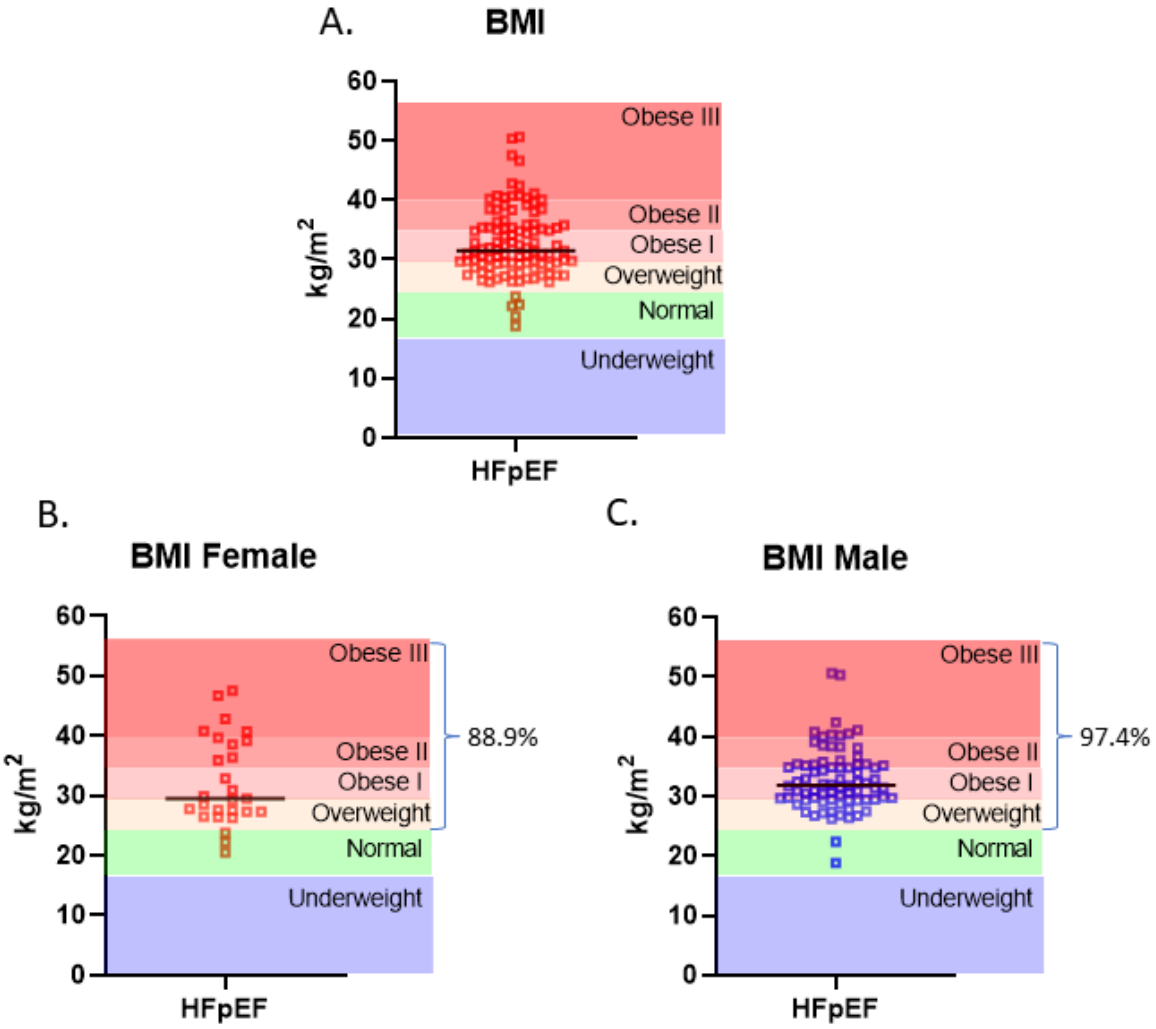

Figure 3.3. Evidence of obesity in HFpEF patients.
(A) BMI of total HFpEF patients. (B) BMI of Female HFpEF patients. (C) BMI of Male HFpEF patients. The BMI guideline from World Health Organization, the BMI below 18.5 = underweight, 18.5-24.9 = Normal, 25.0-29.9 = Overweight, 30.0-34.9 = Obesity class I, 35.0-39.9 = Obesity class II, >40 = Obesity class III.

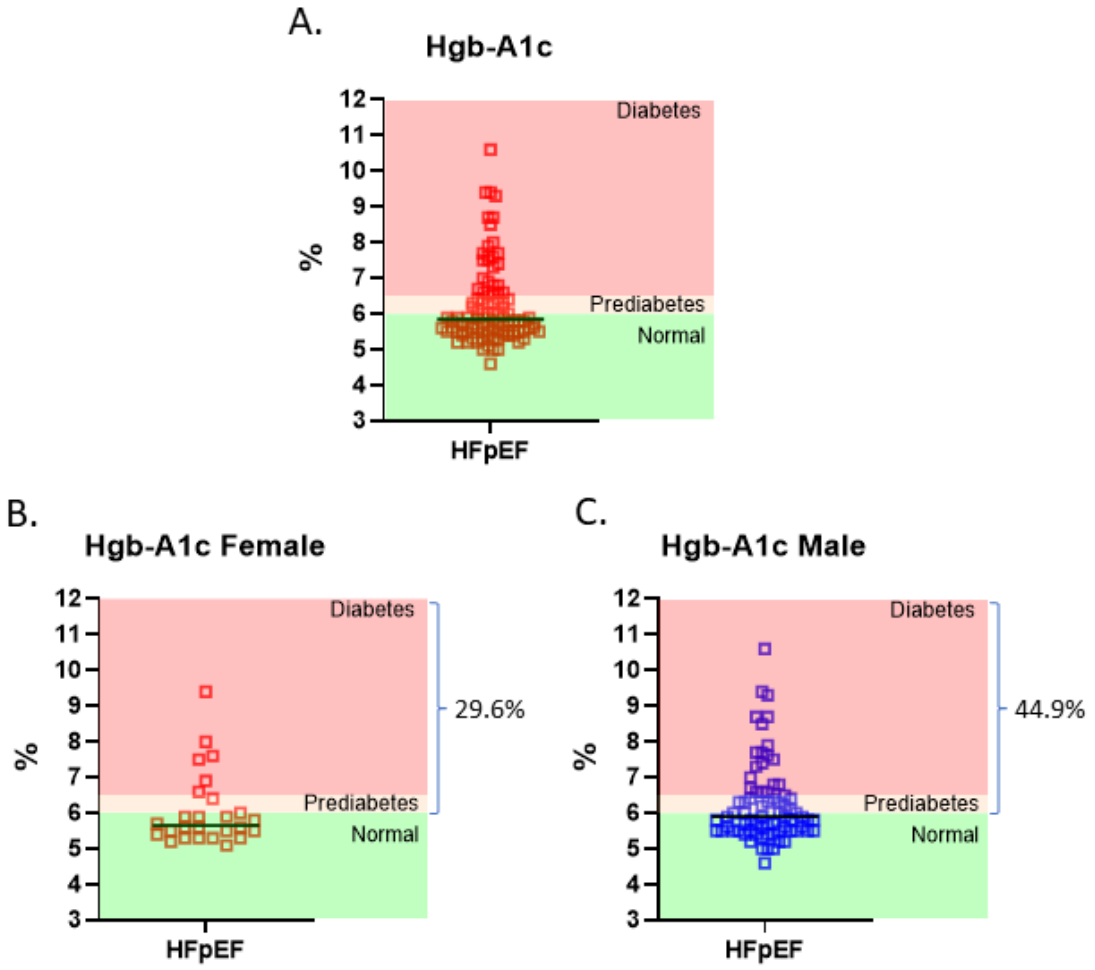

Figure 3.4. Evidence of uncontrolled (type 2) diabetes in HFpEF patients.
(A) Hgb-A1c of total HFpEF patients. (B) Hgb-A1c of Female HFpEF patients. (C) Hgb-A1c of Male HFpEF patients. The range guideline from Centers for Disease Control and Prevention, Hgb-A1c level <6% = Normal, 6-6.4% = Prediabetes, >6.4% = diabetes.

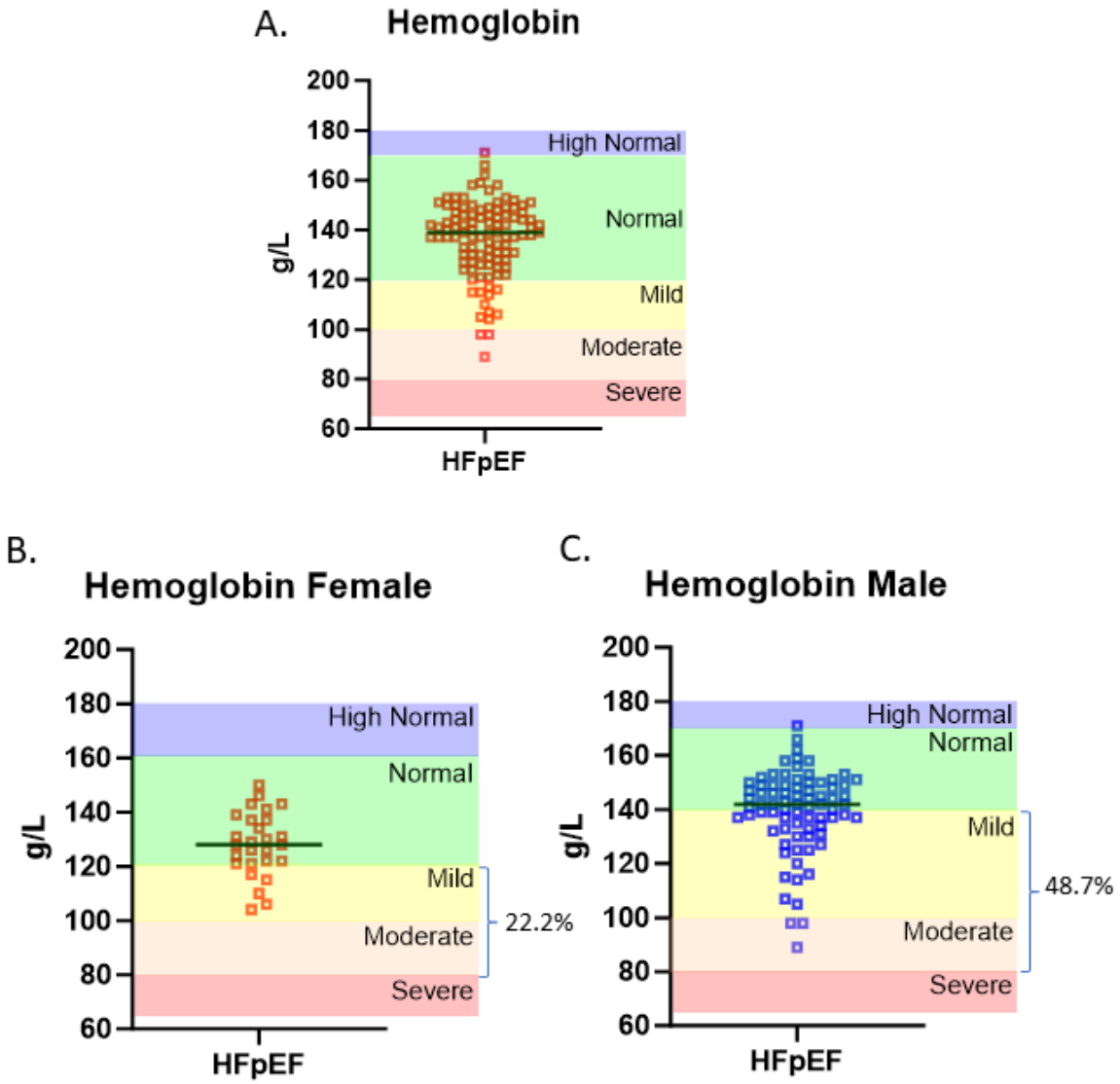

Figure 3.5. Evidence of anemia in HFpEF patients.
(A) Hemoglobin level of total HFpEF patients. (B) Hemoglobin level of female HFpEF patients. (C) Hemoglobin level of male HFpEF patients. According to the National Cancer Institute, the grading of anemia as follow: in female, 120-160g/L = Normal, 100-120g/L = Mild, 80-100g/L = Moderate, 65-80g/L = Severe; in male, 140-170g/L = Normal, 100-140g/L = Mild, 80-100g/L = Moderate, 65-80g/L = Severe.

3.2 Preclinical HFpEF model GEO data support the rationale for exploring the heme metabolism, estrogen, and inflammation mechanisms

To further investigate the molecular changes underlying HFpEF, we analyzed a preclinical model found in open-access microarray datasets from Entrez Gene Expression Omnibus (GEO). A preclinical model of HFpEF shared by Zhang et al[82] (GSE126062) induced hypertrophy by high-salt diet, successfully replicating some key features observed in HFpEF (Figure 3.6.A). Zhang et al.[82] evaluated the EF of the rats, which fell within the normal range (Figure 3.6.A). Lower E/A ratios indicated diastolic dysfunction, corroborating the presence of impaired relaxation and filling of the heart. Immunofluorescence images of myocytes stained with wheat germ agglutinin revealed an increased cross-sectional area, confirming the occurrence of hypertrophy. Some genes related to the HFpEF phenotype and heme metabolism were selected and extracted from the Agilent Whole Rat Genome Microarray database, with p-values based on the normalized signal intensity shared by Zhang et al, and the fold change used for visualization.

Among the heme-related genes, Hmox1, Hebp1, Hrik (Eif2ak1) showed significant upregulation of RNA expression in the HFpEF preclinical rat model (Figure 3.6.B). However, no significant changes were observed in the expression of Hmox2, Alas1, Alas2, Hebp2, and Perk (Eif2ak3) (Figure 3.6.B). Although the preclinical modeling was done in male rats, it is interesting to note that changes were observed in estrogen regulated genes, with Esrrg (estrogen-related receptor gamma) expression being significantly upregulated, while Ste2 (estrogen sulfotransferase) expression was significantly down regulated in the HFpEF rat preclinical model (Figure 3.6.C). However, no significant changes were observed in the expression of other sex related genes such as Rerg (RAS-like, estrogen-regulated, growth-inhibitor), Esrrb, Gper, Esr1, Esr2, and Esrra (Appendix-B).

Genes related to inflammation appeared to be a major driver in the preclinical model, as IL-

1b, Tnf-a, Nfkb (p65), and Tlr4 showed significant upregulation (Figure 3.6.D). However, no significant changes were observed in the expression of IL-6 and IL-10 (Figure 3.6.D). Additionally, genes related to hypertrophy were examined, and of the genes examined: Nppa, Nppb, Nkx2-5 Tbx5/Tbx20, Gata4, Myh6, Myh7, and Hand2 show no significant change in gene expression (Figure 3.6.E).

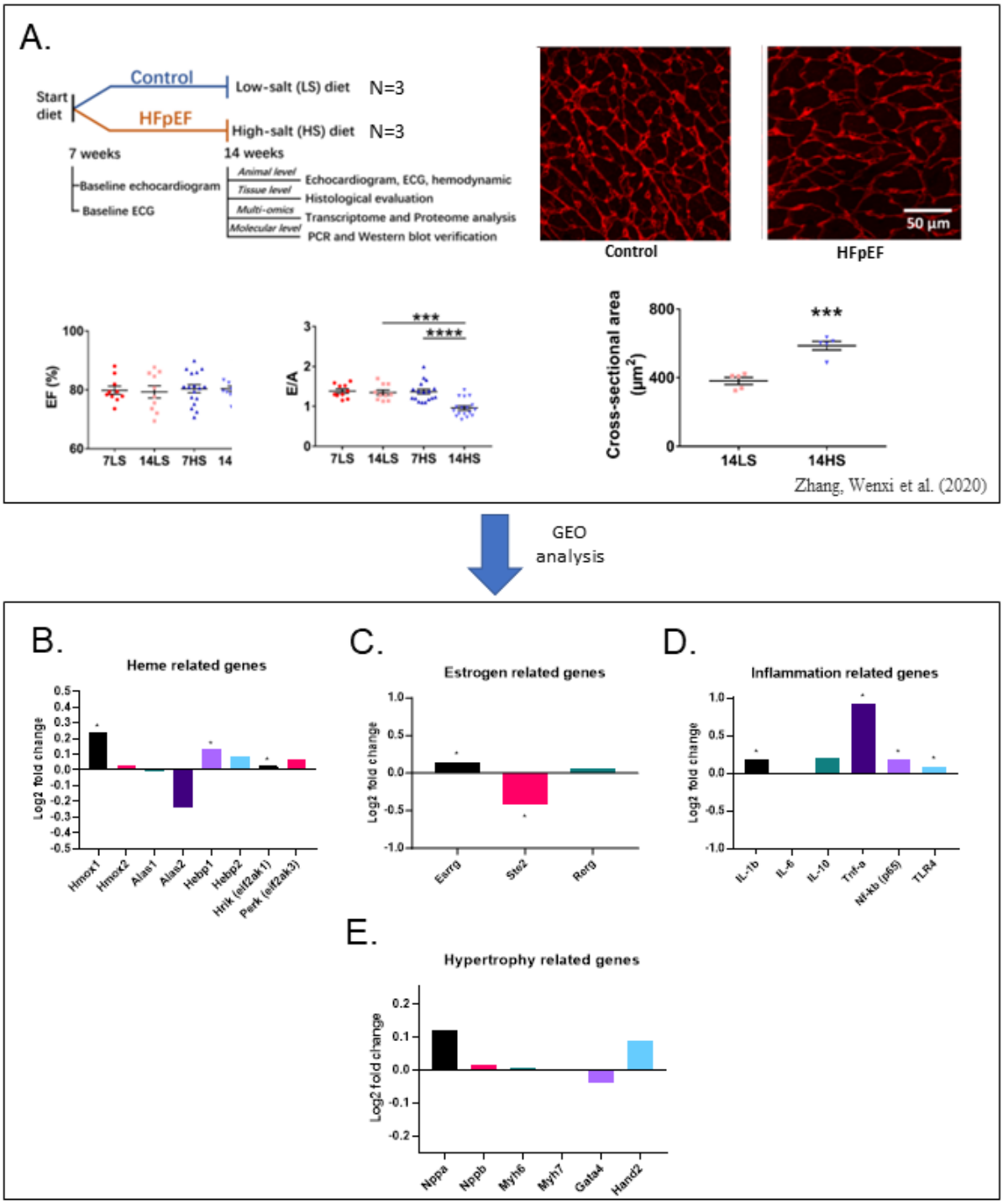

Figure 3.6. Retrieval of rat preclinical HFpEF model GEO profiles via the NCBI database. (A) A schematic representative of experimental protocol from GEO DataSets (GSE126062) induced HFpEF by high-salt diet (N=3) on Dahl salt-sensitive (DSS) rats. Ejection fraction (EF (%) mean ± SE) in the two groups at the age of 7 and 14 weeks; histological evaluation showed increase in size, and E/A. (B) Heme related genes expression. (C) Sex related genes expression. (D) Inflammation related genes expression. (E) Hypertrophy related gene expression. *, significant, one-tailed t-test; estrogen related genes used two-tailed t-test.

3.3 *In vitro* data

3.3.1 Heme treatment increases Hmox1 protein expression in H9c2 myoblasts and myotubes

Prior dose finding studies in our laboratory have shown that 2.5μM hemin is a well-tolerated therapeutically cytoprotective concentration that upregulates Hmox1. To validate the effect of hemin treatment on Hmox1 levels in H9c2 myoblasts and myotubes, cells were exposed to 2.5μM hemin for 24 hours so as to evaluate relevant feature biomarkers by western blot. Eif2ak1, Nfkb, and Hmox1 were tested with H9c2 myoblast (Figure 3.7.A). Eif2ak1 levels did not change significantly as compared to control levels in response to hemin treatments in myoblasts (Figure 3.7B). Nfkb showed no significant change compared to control as well (Figure 3.7.C). Hmox1 expression was significantly increased in both H9c2 myoblasts and myotubes in response to hemin treatment (Figure 3.7.D & 3.8.D). In the myotubes, Erk1/2, Nfkb, and Hmox1 were tested (Figure 3.8.A). Erk1/2 levels were not significantly different between control cells and 2.5 μM hemin treatment (Figure 3.8.B). However, with hemin treatment on myotubes, Nfkb levels were significantly reduced in myotube cells as compared to controls (Figure 3.8.C).

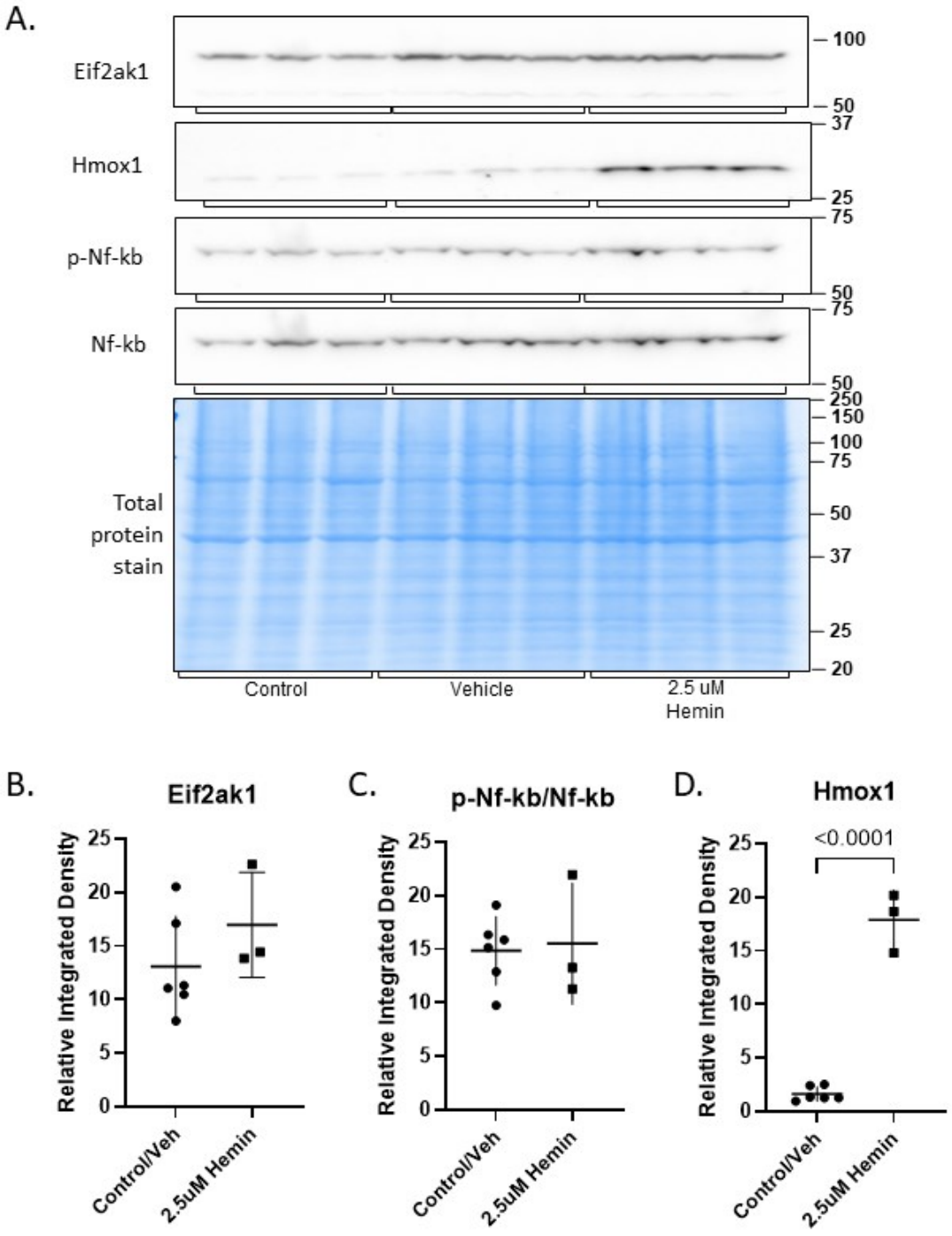

Figure 3.7. Hemin treatment increased Hmox1 expression but did not change Eif2ak1 (Hrik) or NFkB expression in H9c2 myoblasts.
H9c2 myoblast incubated for 24hr from seeding and exposed to 2.5uM Hemin for 24h. A) Representative Eif2ak1, Hmox1, NFkB probed membrane with total protein stains. B) Eif2ak1 did not differ significantly with Hemin treatment. C) NFkB did not differ significantly with Hemin treatment. D) Hmox1 was significantly increased with Hemin treatment.

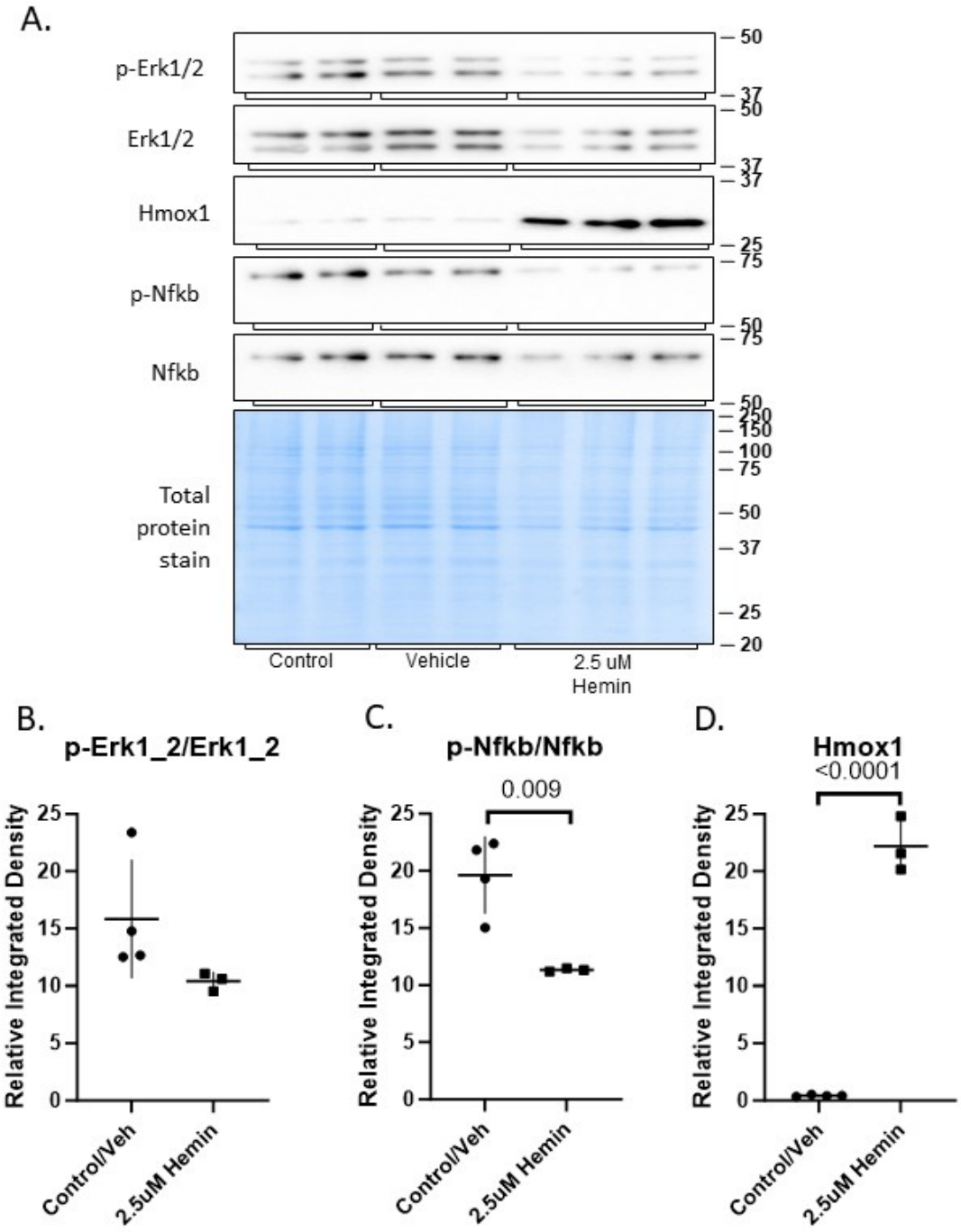

Figure 3.8. Hemin treatment increased Hmox1 expression and reduced Nfkb expression in H9c2 myotubes.

H9c2 myotubes differentiated for 7 days from seeding and exposed to 2.5uM Hemin for 24h. A) Representative p-Erk1/2, Erk1/2, Hmox1, pNfkb, Nfkb probed membrane with total protein stains. B) Erk1/2 did not differ significantly with Hemin treatment. C) Nfkb significantly reduced with Hemin treatment. D) Hmox1 was significantly increased with Hemin treatment.

3.3.2 H9c2 myoblasts and myotubes tolerate high doses of AngII or LPS

According to prior reporting studies in the literature, the dose and treatment time of AngII and LPS varies considerably but has been reported as a reliable means to induce hypertrophy in H9c2 and other myocyte cultures. To determine the optimal dose and time treatments to induce hypertrophy, H9c2 myoblasts and myotubes were treated with various concentrations of known hypertrophic inducing agents: AngII: 100nM-1mM; LPS: 1µg/ml-100µg/ml (Figure 3.9).

H9c2 myoblasts were exposed to AngII (100nM-1mM) for either 24hrs or 48hrs (Figure 3.9A & B). H_2O_2 was used as a positive control for cell stress. H9c2 myotubes were exposed to 500nM-100µM of AngII for 48hrs (Figure 3.9.C). The results showed high doses of AngII do not negatively influence the cell viability of the H9c2 myoblast or myotubes, and even increased the cell metabolic activity in some cases (Figure 3.9.C). These findings were inconsistent with the previously published data. [96–98] Time dependent dose of 500nM AngII was tested on H9c2 myotubes, and 48hrs of incubation increased the cell metabolic activity (Figure 3.9D).

Additionally, H9c2 myoblasts were exposed to varying concentrations of LPS (1µg/ml-100µg/ml) for 48hrs, with 1mM H_2O_2 as a positive control to confirm loss of cell viability and test validity (Figure 3.9E). Also. H9c2 myoblasts were exposed for 24hrs at different concentrations of LPS (0.5µg/ml-50 µg/ml), which showed no significant decrease in cell viability (Figure 3.9F). High doses of AngII or LPS showed either no effect or an increase in metabolic activity in both H9c2 myoblasts and myotubes (Figure 3.9), without any indication of cellular toxicity. These data confirm that a broad range of AngII or LPS can be used safely to effect a change in cell metabolism that may lead to hypertrophic cellular remodeling.

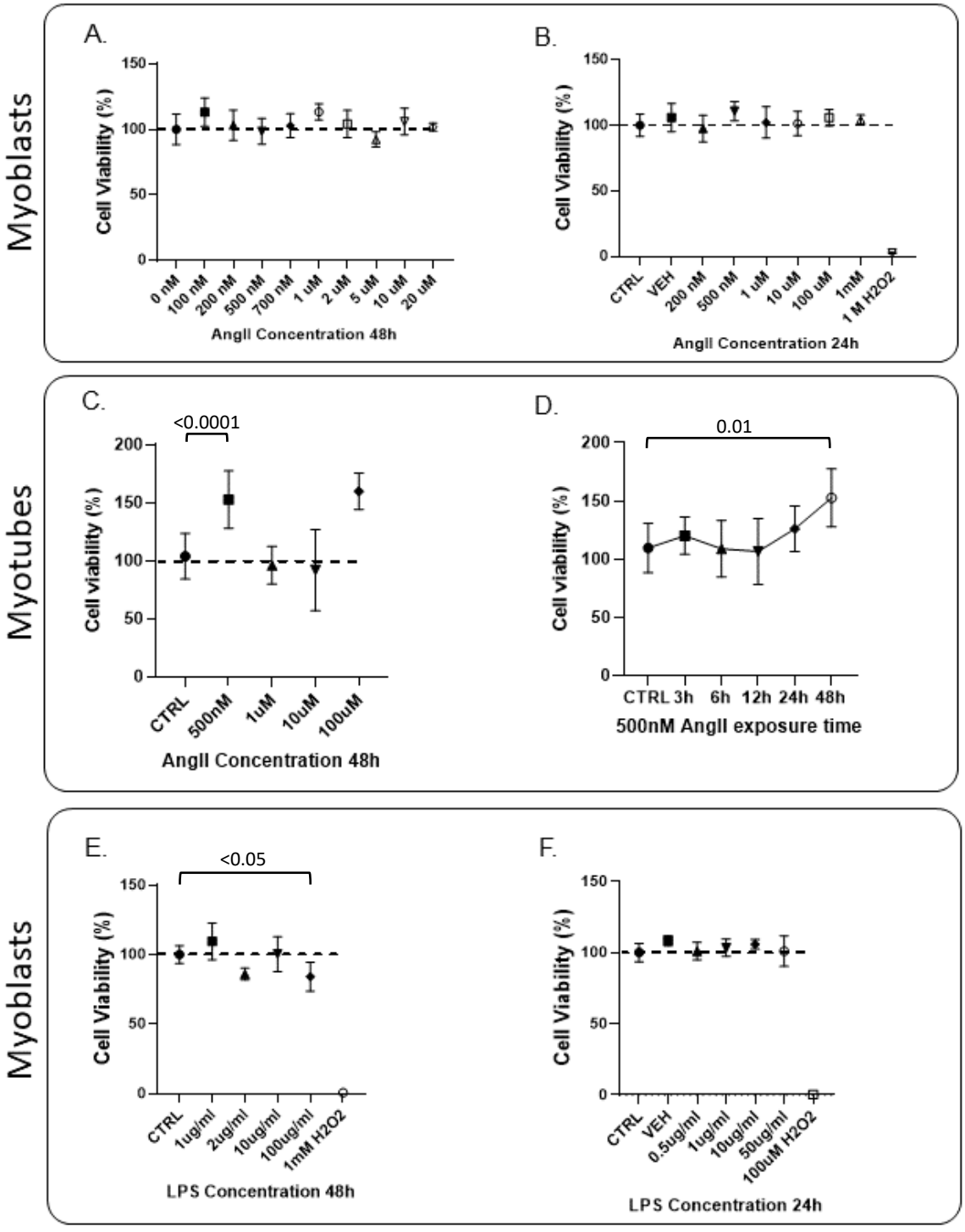

Figure 3.9. Resazurin cell viability dose and time effect of AngII and LPS on H9c2 myoblasts and myotubes.

(A) AngII dose dependent for 48h on H9c2 myoblasts, 10,000 cells/well. (B) AngII dose dependent for 24h on H9c2 myoblasts, 5,000 cells/well, 1M H2O2 as positive control. (C) AngII dose dependent 48h on H9c2 myotubes. (D) 500nM AngII time dependent on H9c2 myotubes. (E) LPS dose dependent 48h on H9c2 myoblasts. (F) LPS dose dependent 24h on H9c2 myoblasts.

3.3.3 H9c2 myoblasts show no dose-response increase in cell size to AngII evaluated by immunocytochemistry

To elicit cellular hypertrophy, the cell surface area of myoblasts was measured by immunocytochemical staining after exposure to AngII. The treatment timeline is presented in Figure 3.10.A. H9c2 myoblasts were stained for f-actin with phalloidin (green) and the nucleus with Hoechst (blue), then cell surface area was measured by Image J software (Figure 3.11A). Compared to the control, only 1 cell was larger than 10,000 μm^2 after 500nM treatment; there were 6 cells in the 1,000nM AngII group and 5 cells in the 2,000nM AngII group, that were larger than 10,000μm^2. While trending towards larger cell sizes, this is not sufficient to be indicative of hypertrophy in the cell population. Overall, there were no statistically significant changes observed in the cell surface area of H9c2 myoblasts treated with 500nM, 1µM, and 2µM AngII for 48hrs (Figure 3.11B).

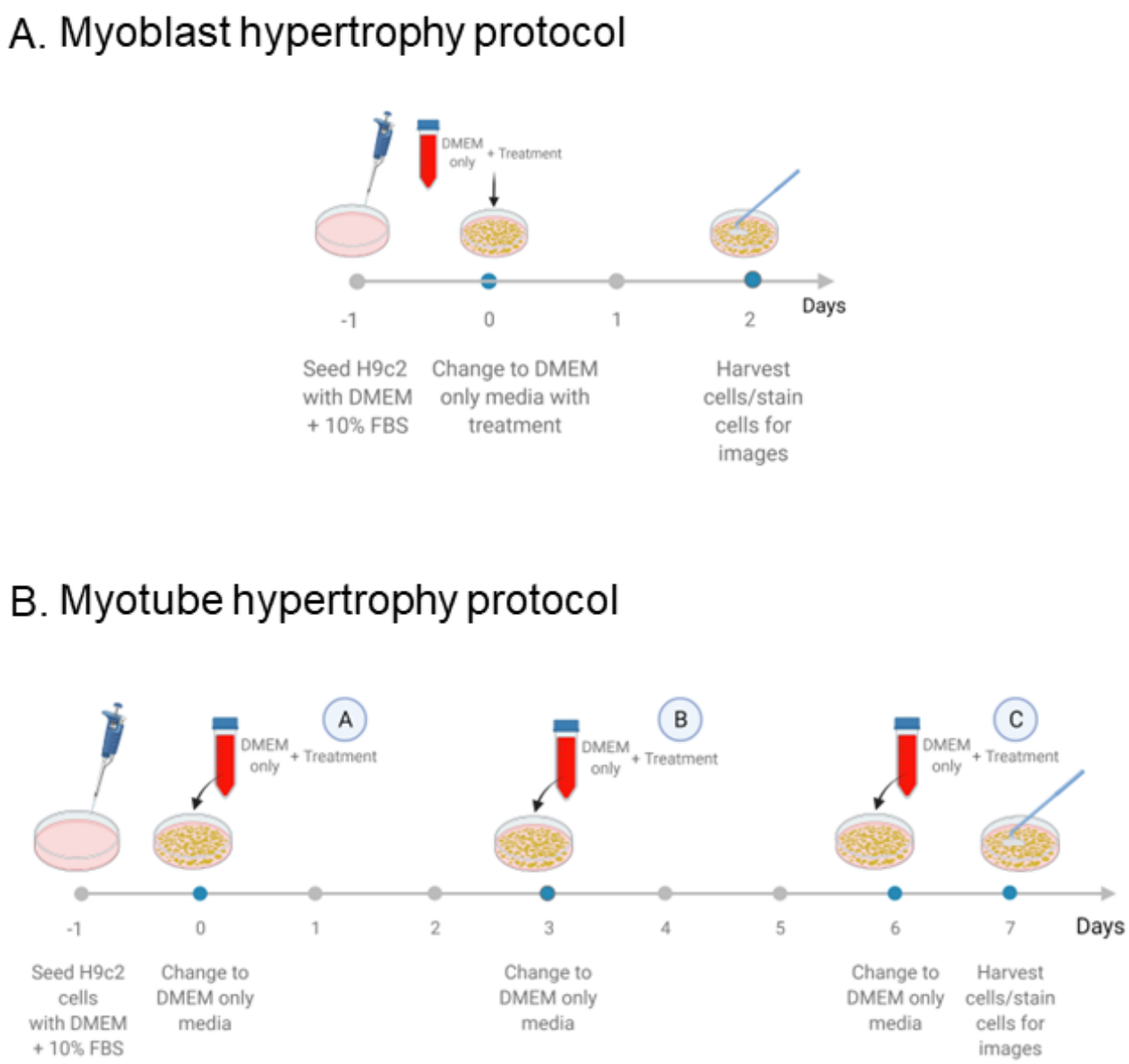

Figure 3.10. Experimental design induction of hypertrophy in the H9c2 cell line.
Cultured in high-glucose DMEM and treated with: AngII & LPS. A) myoblast B) myotube

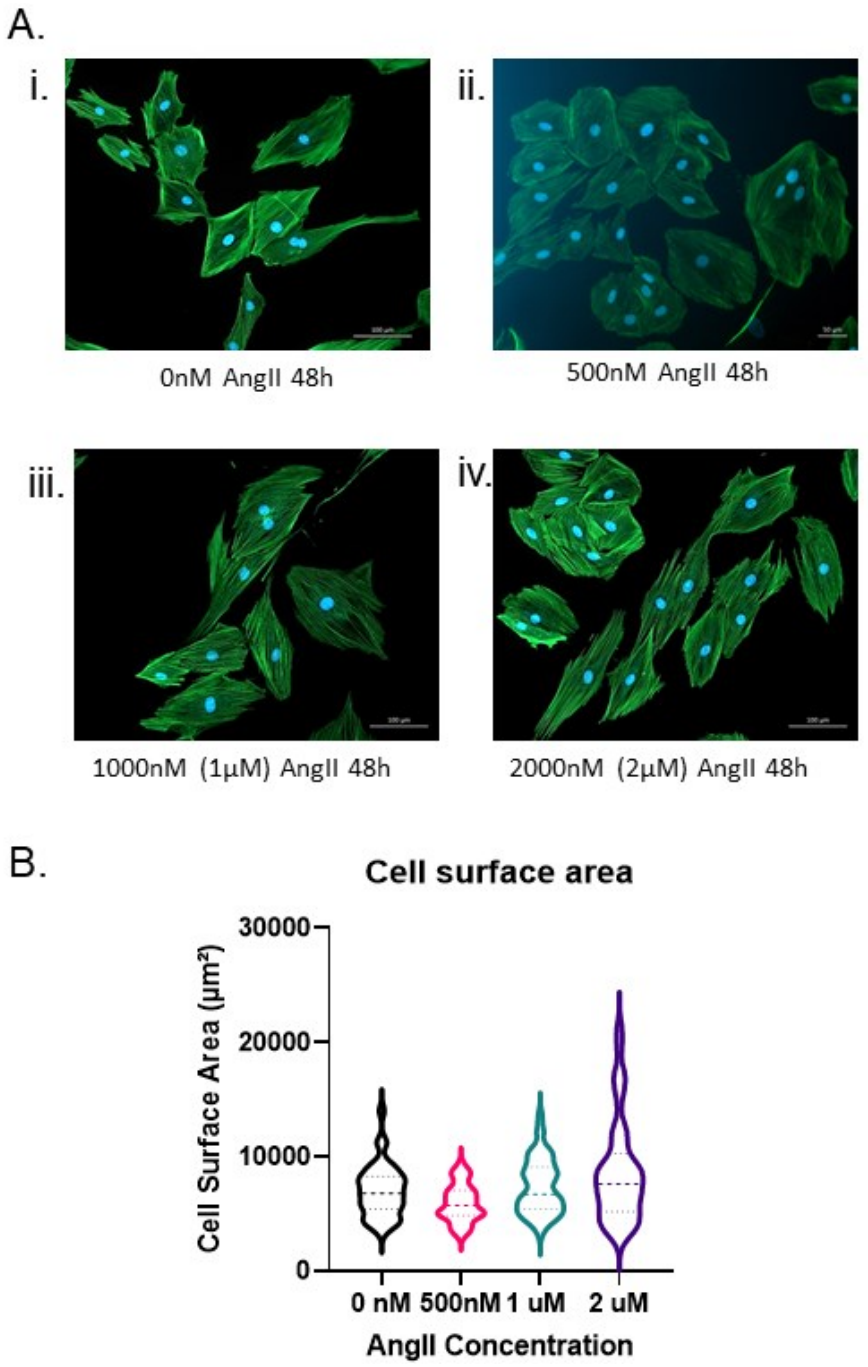

Figure 3.11. Immunocytochemistry, cell surface area of H9c2 myoblasts treated with AngII. (A.i-iv) H9c2 myoblasts stained for F-actin with phalloidin (green) and nuclear stain Hoechst 33342 (blue). Then photographed using a slide scanner. (B) Cell surface area was measured and analyzed with ImageJ software. The data are expressed as the median and quartiles. Cells treated with different concentration of Angiotensin II for 48h (0nM, 500nM, 1000nM, and 2000nM). The experiment ran on 2 individual plates, 6 randomly selected fields, counted cell numbers are 42 for each group.

3.3.4 H9c2 myoblasts show no dose-response increase in cell size to AngII evaluated by flow cytometry

This series of studies was designed to explore whether measuring 3D volume of cells size, could increase the power of cell population analysis, and eliminate unconscious selection bias, by using flow cytometry. Forward scatter (FS) and side scatter (SS) was recorded for each cell to determine the relative size and granularity, respectively (Figure 3.12.A-F). Based on Deckman flow cytometry manual guide, FS intensity is proportional to the diameter of the cell. This is the most robust method for determining an increase in cell size (hypertrophy) quantitatively in a mixed cell population. After filtering out cell debris, ~45-50,000 cells were analyzed (Figure 3.12.G). From the FS histograms, H9c2 myoblasts treated with 200nM, 500nM, 1μM, 10μM, and 100μM of AngII for 48hrs, no shift of the histogram was observed compared to control (Figure 3.12.A-F). Flow sytometry-derived geometric means of H9c2 myoblasts showed less than 5% changes across treatment groups as compared to control (Figure 3.12.G).

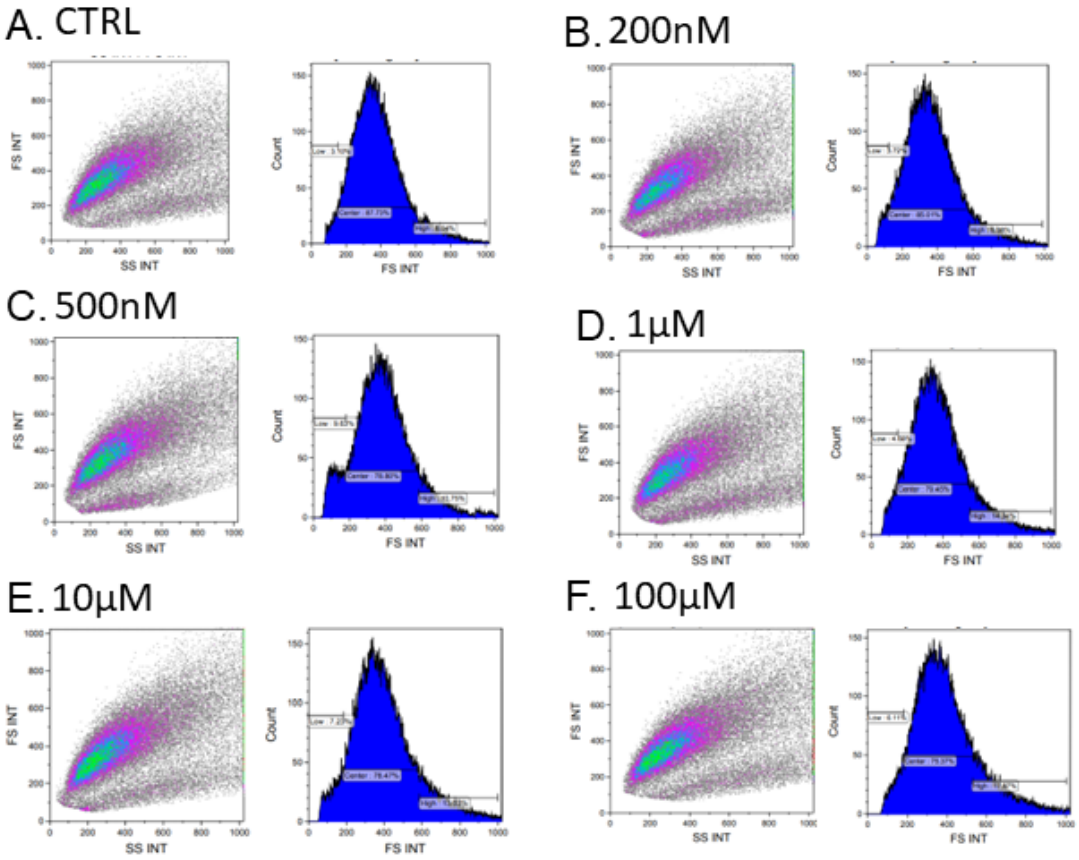

G.

Treatment group	Cell number	% Total	Median	Geometric means
CTRL	45,718	87.55	365.56	355.53
200nM	46,895	91.35	352.90	338.26
500nM	45,954	88.58	376.98	351.89
1μM	49,631	91.25	360.85	349.91
10μM	49,542	91.22	379.49	368.50
100μM	47.393	90.59	374.72	369.60

Figure 3.12. Flow cytometry analysis of H9c2 myoblasts treated with AngII.
The treatment time is 48hrs. (A) H9c2 myoblast CTRL 0nM. (B) H9c2 myoblast with 200nM of AngII. (C) H9c2 myoblasts with 500nM of AngII. (D) H9c2 myoblast with 1μM of AngII, (E) H9c2 myoblast with 10μM AngII. (F) H9c2 myoblast with 100μM. (G) statistical information on H9c2 myoblasts treated with different concentration of AngII.

3.3.5 H9c2 myotubes show no dose-response increase in cell size to AngII evaluated by flow cytometry

Since myoblasts are actively in a state of cell replication, this may not model well non-proliferating (quiescent) cardiomyocytes, and could be limiting the induction of hypertrophy. To determine if hypertrophy could be confirmed visually at the cellular level, microscopy and immunocytochemical staining were used on quiescent differentiated H9c2 myotubes. Additionally, repeated exposure to AngII may be required to chronically elicit hypertrophy *in vitro*. H9c2 myotubes were stained for f-actin with phalloidin (green) and nucleus with Hoechst (blue) (Figure 3.13) and being treated with 500nM of AngII repeatedly after initiating differentiation in serum free media (Figure 3.10 B). 500nM of AngII was commonly used in literature and Figure 3.9A,C,D showed the dose did not reduce the cell viability, therefore, the 500nM of AngII was used in these myotubes treatment. Group A got AngII treatment on the day 0 only for 48h, Group B got AngII treatment on the day 3 only for 48h, Group C got AngII treatment on the day 6 only for 48h, Group A+B+C got AngII treatment on the day 0, day 3, and day 6, with each media change total 3 times of the treatments for 7days (Figure 3.10B). Representative phase contrast microscopy of H9c2 myotubes after AngII exposure showed preservation of morphology (Figure 3.13). Due to the spindle morphology of these cells, it is impractical to trace single cell myotube H9c2, so the cell size was measured after dissociation by flow cytometry. Figure 3.14A-E shows FS by SS, and FS histograms of H9c2 myotubes cell size by volume treated with 500nM of AngII at different time points. After filtering out cell debris, ~60,000 cells were analyzed (Figure 3.14.F). There was no shift of FS histogram observed compared to control (Figure 3.105A-E). FACS-derived geometric means of H9c2 myotubes showed less than 5% changes across treatment groups as compared to control (Figure 3.14F). Neither the differentiation of H9c2 nor the repeated exposure to AngII were able to elicit cellular hypertrophy.

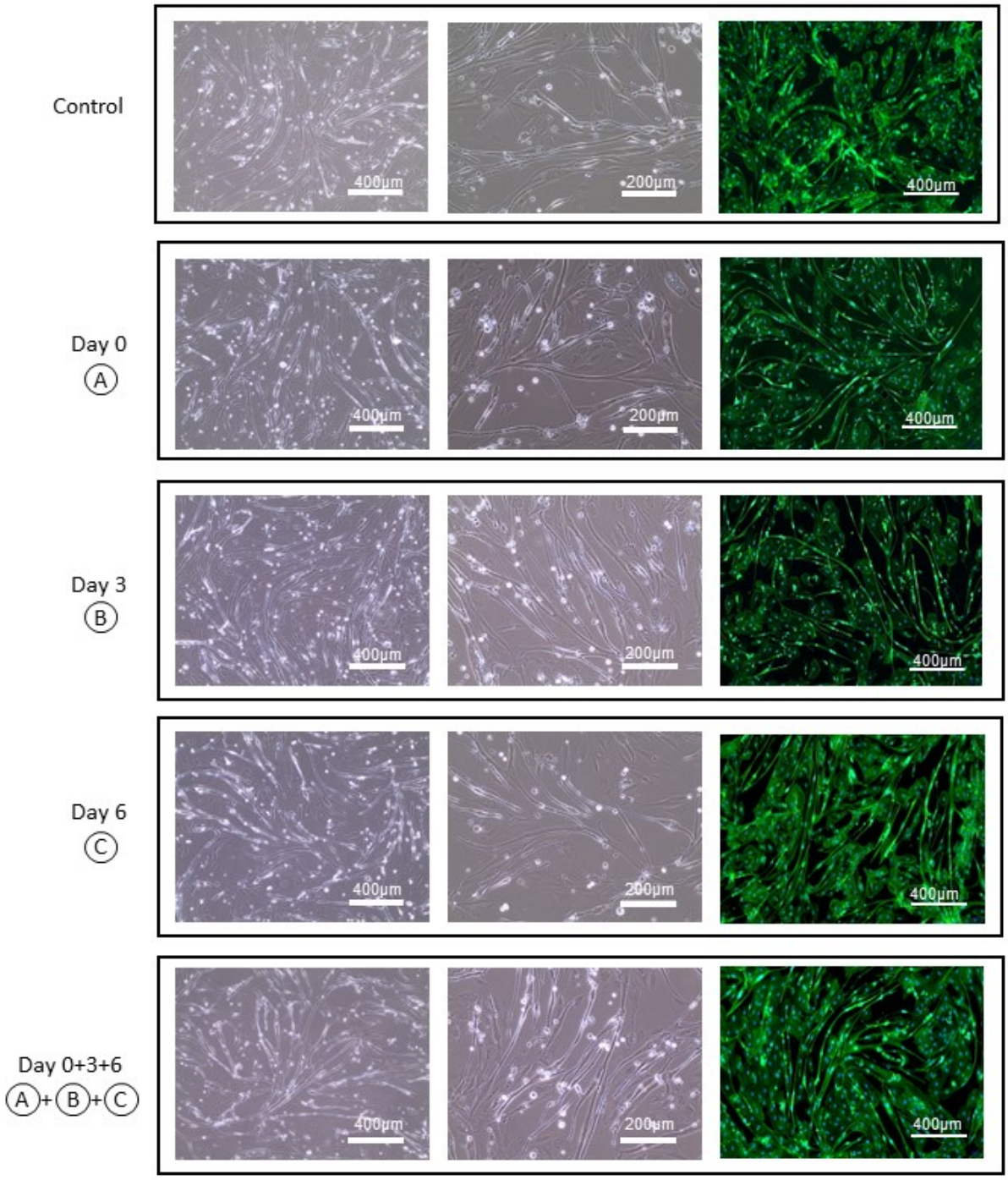

Figure 3.13. Representative phase contrast microscopy of H9c2 myotubes after treated with AngII.

Myotubes were treated with 500nM of AngII. Group A got AngII treatment on the day 0 only, Group B got AngII treatment on the day 3 only, Group C got AngII treatment on the day 6 only, Group A+B+C got AngII treatment on the day 0, day 3, and day 6, total 3 times of the treatments.

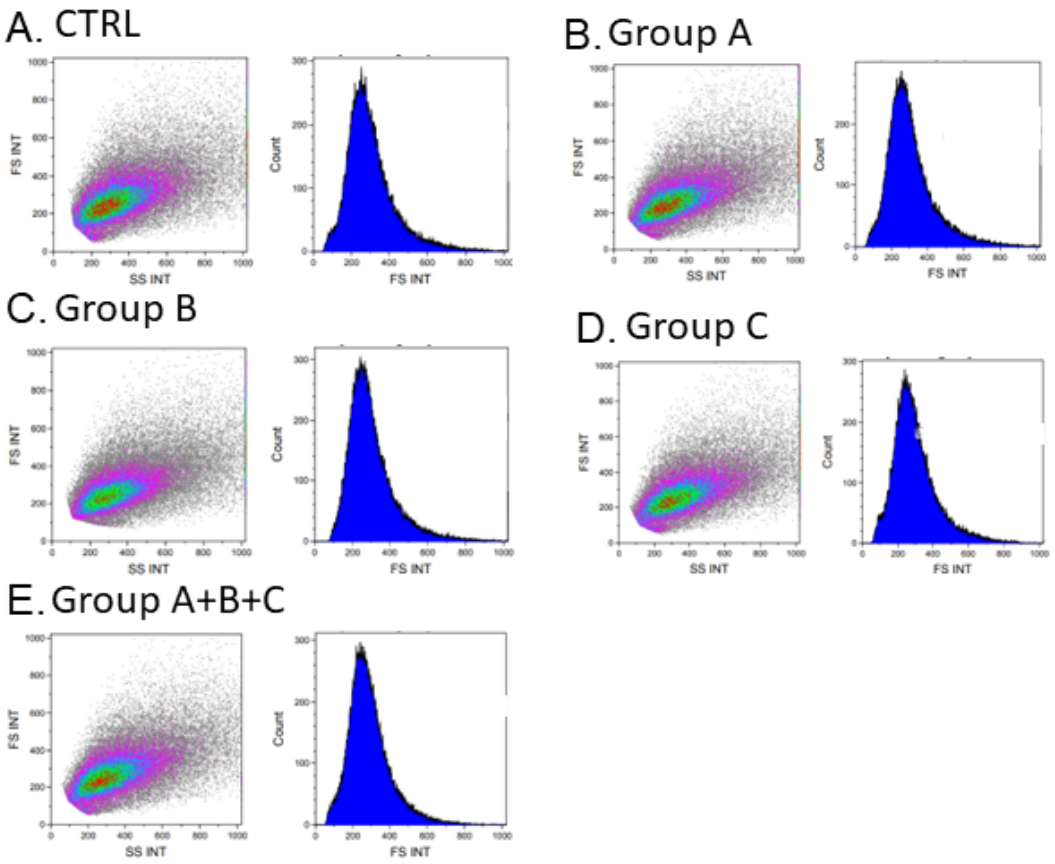

F.

Treatment group	Cell number	% Total	Median	Geometric means
CTRL	60,709	80.95	279.02	280.79
Group A	62,961	83.95	282.27	285.24
Group B	63,090	84.12	275.24	280.15
Group C	61,471	81.96	276.39	275.75
Group A+B+C	61,558	82.08	272.00	269.43

Figure 3.14. Flow cytometry analysis of H9c2 myotubes treated with AngII.
500nM of AngII was used in the experiment, except for CTRL. (A) H9c2 myotubes CTRL, 0nM of AngII. (B) H9c2 myotubes Group A got AngII treatment on the day 0 only. (C) H9c2 myotubes Group B got AngII treatment on the day 3 only. (D) H9c2 myotubes Group C got AngII treatment on the day 6 only. (E) H9c2 myotubes Group A+B+C got AngII treatment on the day 0, day 3, and day 6, total 3 times of the treatments. (F) Statistical information on H9c2 myotubes treated with 500nM of AngII at different time points.

3.3.6 Molecular expression and phosphorylation of hypertrophy-associated proteins are inconsistent after exposure to AngII from a single source supplier with different reagent lot numbers

To reconcile these results with the reported literature,[96,99–104] we explored intracellular molecular patterns associated with AngII and tested an alternate lot of AngII (Lot#2). To identify potential biomarkers of hypertrophy at the molecular level, western blots were run on H9c2 myoblasts treated in different AngII doses for 48hrs, and the timeline showed on Figure 3.10.A. Hypertrophy associated proteins were myosin heavy chain 7B (Myh7b), Erk1/2, and Nfkb were measured (Figure 3.15.A). Of these proteins of interest, only Nfkb showed significant increase at 250nM and 500nM treatment for 48hrs compared to control (Figure 3.15.D). Myh7b was elevated slightly with 500nM exposure of AngII treatment for 48hrs, but the changes were not significant as compared to control. (Figure 3.15.B). Erk1/2 showed slight increase at 250nM of AngII treatment, and then a decrease with higher doses, and the changes were not significant as compared to control (Figure 3.15.C). Hmox1 were measured as well, but no protein signals detected, suggesting AngII may not be induced sufficient cellular stress in H9c2 cells.

Amongst different lot numbers of AngII reagents, there were some slight variations in the molecular hypertrophic pattern (Figure 3.15.B-D). In the H9c2 group treated with Lot#2, Myh7b showed no changes; Erk1/2 showed a slight increase but was not significant compared to control; Nfkb showed a slight increase and peak at 1000nM (1μM) of AngII. Hmox1 were measured as well, and no protein signals detected.

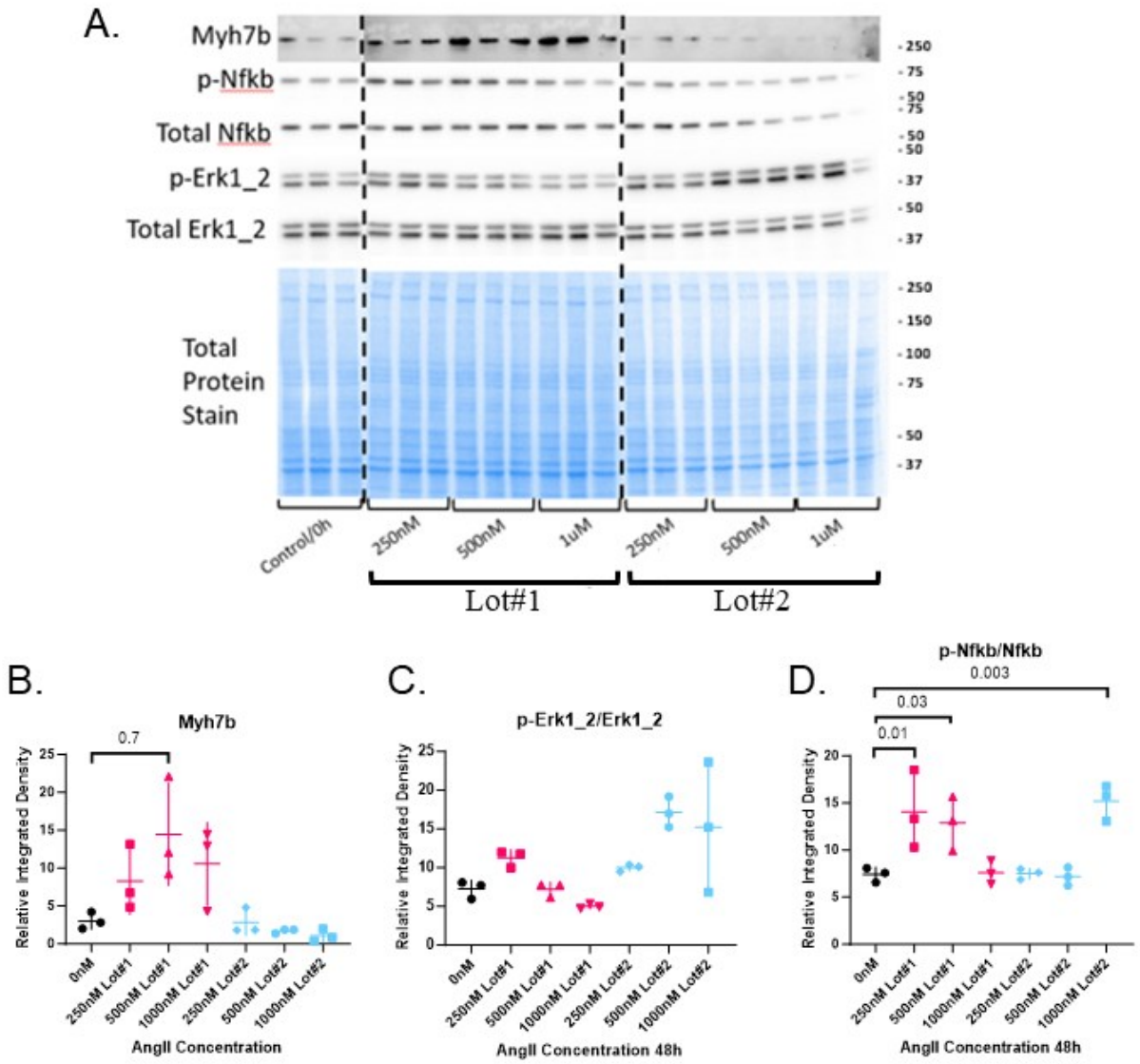

Figure 3.15. Comparison of different lots of AngII product show different molecular changes from H9c2 myoblasts.

(A) representative Myh7b, Nfkb, Erk1/2 probed membrane with total protein stains. (B) Myh7b did not differ significantly with both lot# of AngII treatments. (C) Erk1/2 did not differ significantly with both lot# of AngII treatments (D) Nfkb elevated on low dose of Lot#1, high dose of Lot#2.

3.3.7 H9c2 myoblasts show no dose-response increase in cell size to LPS evaluated by immunocytochemistry

As hypertrophy is often associated with hormone or inflammatory stress, to determine whether an inflammatory insult could better induce hypertrophy, we explored another commonly used stimulus, LPS. Cells were visually examined at the cellular level, cell surface area of myoblasts was measured by immunocytochemical staining. H9c2 myoblasts were stained with phalloidin (green) for f-actin and nuclear stain Hoechst (blue) after treated with different concentration of LPS (Figure 3.16.A). The treatment timeline could be found in Figure 3.10.A. Cell surface area was measured by tracing the cell outline and analysis by Image J software (Figure 3.16.B). Compared to the control (1 cell >10,000 μm^2) there were 6 cells in the 1µg/ml LPS group and 4 cells in the 10µg/ml LPS group, that were larger than 10,000μm^2, while trending towards larger cell sizes, this is not sufficient to be analytically indicative of cellular hypertrophy. Overall, there were no statistically significant changes observed in the cell surface area of H9c2 myoblasts treated with 1µg/ml, or 10µg/ml LPS for 48hrs (Figure 3.16.B). There was a significant effect by the ddH_2O vehicle. Despite there being no changes in the means across the doses tested, the 1µg/ml, and 10µg/ml LPS groups showed some skewedness toward larger cells (Figure 3.16.B), but not hypertrophy was confirmed that could not be attributed to cell flattening, swelling, or isolated random events.

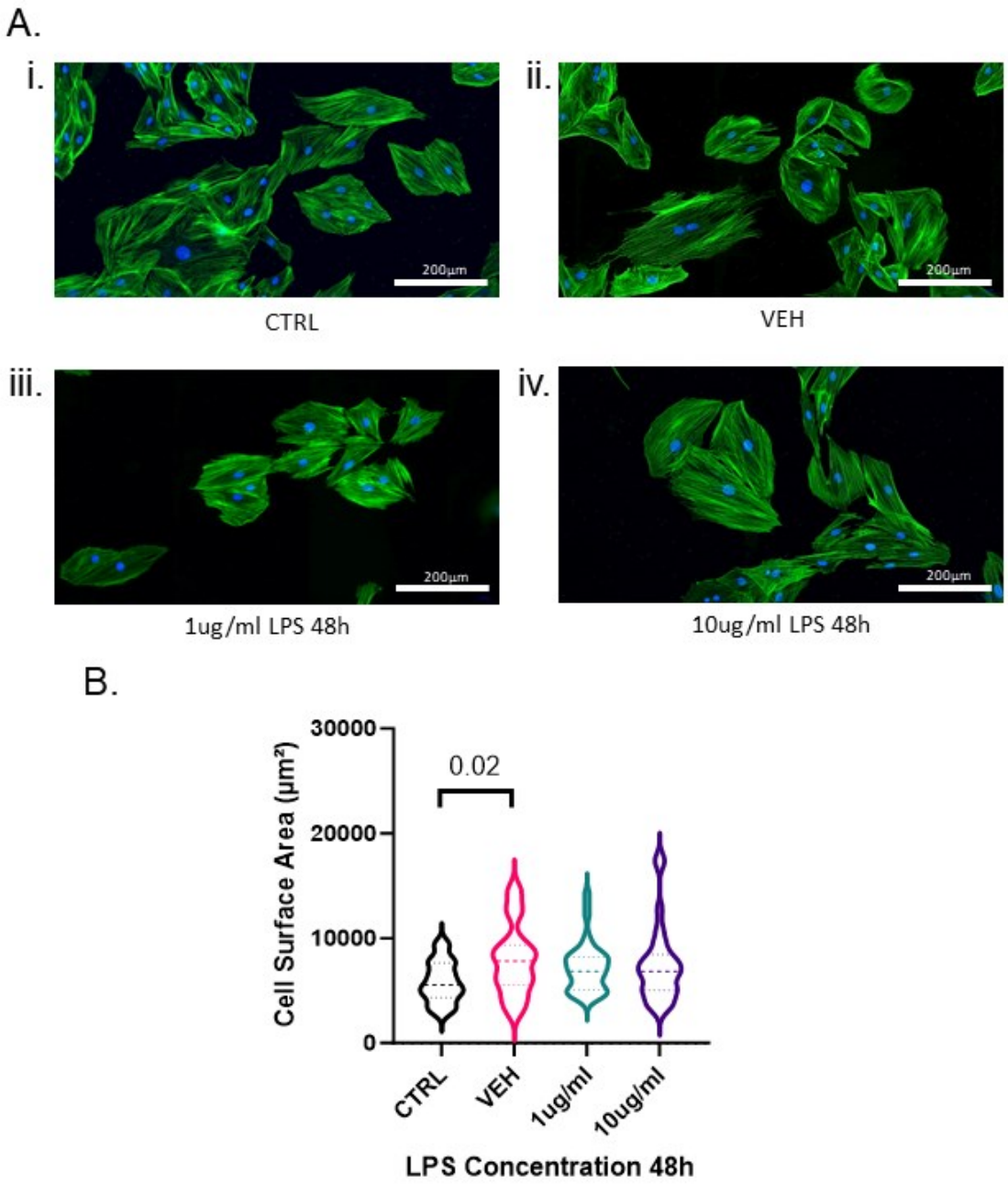

Figure 3.16. H9c2 myoblast treated with 1µg/ml and 10µg/ml concentration of LPS for 48h. (A.i-iv) H9c2 myoblasts stained for F-actin with phalloidin (green) and nuclear stain Hoechst 33342 (blue). Then photographed using a slide scanner. (B) Cell surface area was measured and analyzed with ImageJ software. The data are expressed as the median and quartiles. The experiment ran in 2 individual plates, 2 randomly selected field, counted cell numbers are 30 (CTRL), 32 (VEH), 29 (1µg/ml), 30 (10µg/ml). VEH, treated with 80µl of ddH2O.

3.3.8 H9c2 myoblasts show no dose-response increase in cell size to LPS evaluated by flow cytometry

To measure 3D volume of cells size, increase power of cell population analysis, increase stimulus and eliminate any unconscious selection bias, flow cytometry analysis was used. FS and SS was recorded for each cell to determine the relative size and density, respectively (Figure 3.17.A-D). After using cell gates to filter out cell debris, more than 70,000 cells were measured (Figure 3.17E). From the FS histograms of H9c2 myoblasts treated with 1µg/ml, or 50µg/ml of LPS, no shift of histogram was observed compared to control (Figure 3.17A-D). FACS-derived median and geometric means of H9c2 myoblasts showed less than 6% increase and no shift in whole cell population size compared to control (Figure 3.17E). These findings were inconsistent with the literature reporting LPS induced hypertrophy in H9c2, even at concentrations 50-fold higher than what has been previously established.[105–107]

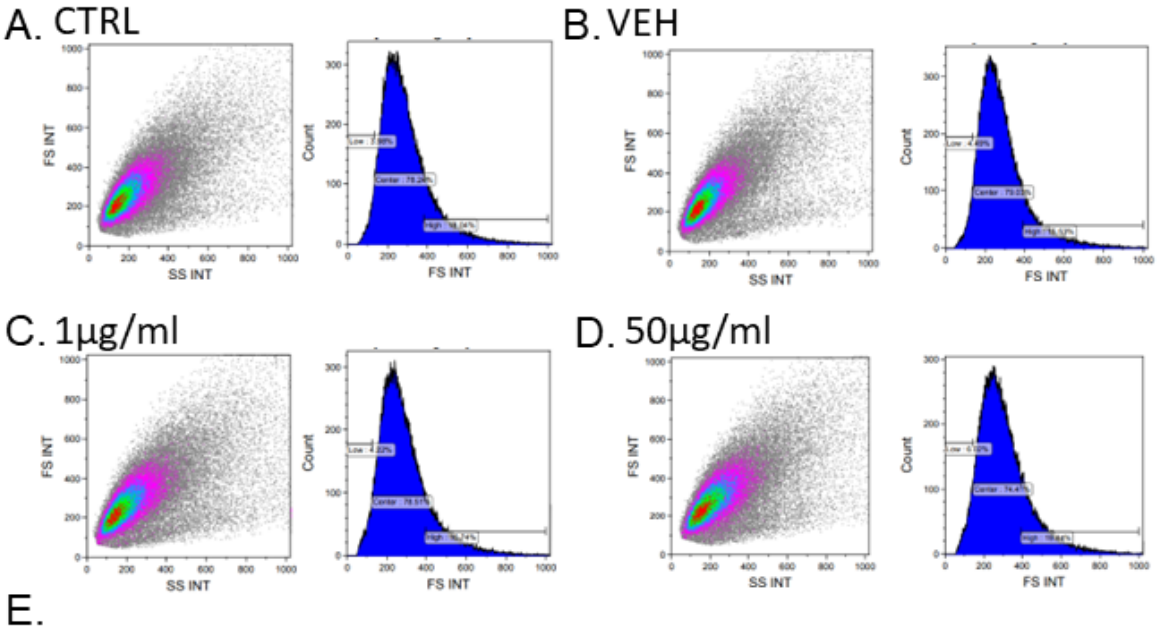

E.

Treatment group	Cell number	% Total	Median	Geometric means
CTRL	72,127	96.17	264.27	266.45
VEH	72,631	96.84	262.85	266.11
1µg/ml	70,061	93.41	262.99	264.11
50µg/ml	70,956	94.61	280.57	279.99

Figure 3.17. Flow cytometry analysis of H9c2 myoblasts treated with LPS.
The LPS source is Enzo, and the treatment time is 48hrs. (A) H9c2 myoblast CTRL 0nM of LPS. (B) Vehicle control, H9c2 myoblast with 100µl of ddH2O. (C) H9c2 myoblasts with 1µg/ml of LPS. (D) H9c2 myoblast with 50µg/ml of LPS, (E) Statistical information on H9c2 myoblasts treated with different concentration of LPS.

3.3.9 Molecular expression and phosphorylation of hypertrophy-associated proteins are inconsistent after exposure to LPS from a different source suppliers

To explore the potential for biomarkers of hypertrophy at the molecular level, H9c2 myoblasts were treated with 1µg/ml LPS incubated in different treatment times. Hypertrophy associated proteins, Myh7b, Erk1/2, and Nfkb were measured by western blot (Figure 3.18.A). Of these proteins of interest, only Erk1/2, a biomarker for protein synthesis, showed elevated signalling and significant increase at 12hrs treatment with 1µg/ml LPS (Figure 3.18.C, blue). Myh7b showed no changes (Figure 3.18.B, blue). Of concern to the underlying assumption of how LPS signals inflammation biomarkers, Nfkb, showed no changes over the time (Figure 3.18.D, blue). Heme related enzyme, Hmox1 also showed no changes overtime suggesting 1µg/ml was insufficient to induce cell stress or activate inflammation cell signalling (Figure 3.18.E, blue). This suggested that perhaps the LPS (sourced from Enzo) was compromised and unable to elicit expected signaling.

To confirm that LPS could be effective at inducing cell stress and inflammation, and alternative source of LPS reagents was sourced from Sigma, and this generated a different pattern of cell signalling (Figure 3.18.B-E). In the sample group treated with the reagent from Sigma, Myh7b showed no significant changes (due to normality of data distribution across groups) compared to control, but did show an elevated expression pattern after 12h ($P<0.001$ if normality were presumed) which wasn't observed in the group treated with LPS from Enzo (Figure 3.18.B); Erk1/2 showed a similar expression pattern with the reagents from Enzo or Sigma and both showed significant increase of phosphoErk1/2 to Erk1/2 at 12hrs treatment compared to control (Figure 3.18.C); Nfkb elevated phosphorylation at 3hrs treatment that slightly decreased overtime which wasn't observed in the group treated with LPS from Enzo (Figure 3.18.D); Hmox1 was elevated at 3hrs after treatment with Sigma LPS and expression decreased overtime where no change in Hmox1 was observed in the group treated with LPS from Enzo (Figure 3.18.E). Taken together, Sigma

sourced LPS was able to show some evidence of cellular stress by Hmox1 elevation and induce an inflammation pattern by elevated Nfkb phosphorylation and effect a change in Myh7b.

Encouraged by these findings that were consistent with expectations to elicit hypertrophy by inflammatory stress, we then repeated the prior FACS analysis in H9c2 myoblasts treated with LPS sourced from Sigma. The FS by SS was recorded for each cell measured to determine relative size and density, granularity, respectively (Figure 3.19.A-D). FS intensity is proportional to the diameter of the cell. After using cell gates to filter out cell debris, about 70,000 cells were measured (Figure 3.19.E). The FS histograms of H9c2 myoblasts treated with 1µg/ml, and 50µg/ml of LPS from Sigma, however, did not demonstrate a shift in the histogram compared to the control group (Figure 3.19.A-D). Flow cytometry-derived median and geometric means of H9c2 myoblasts showed an increase in the whole cell population of less than 8% compared to the control group (Figure 3.19.E). Again, these findings were inconsistent with the literature, and together with the molecular signalling patterns for hypertrophy, indicate that H9c2 myoblast may not be a reliable cell to model hypertrophy.

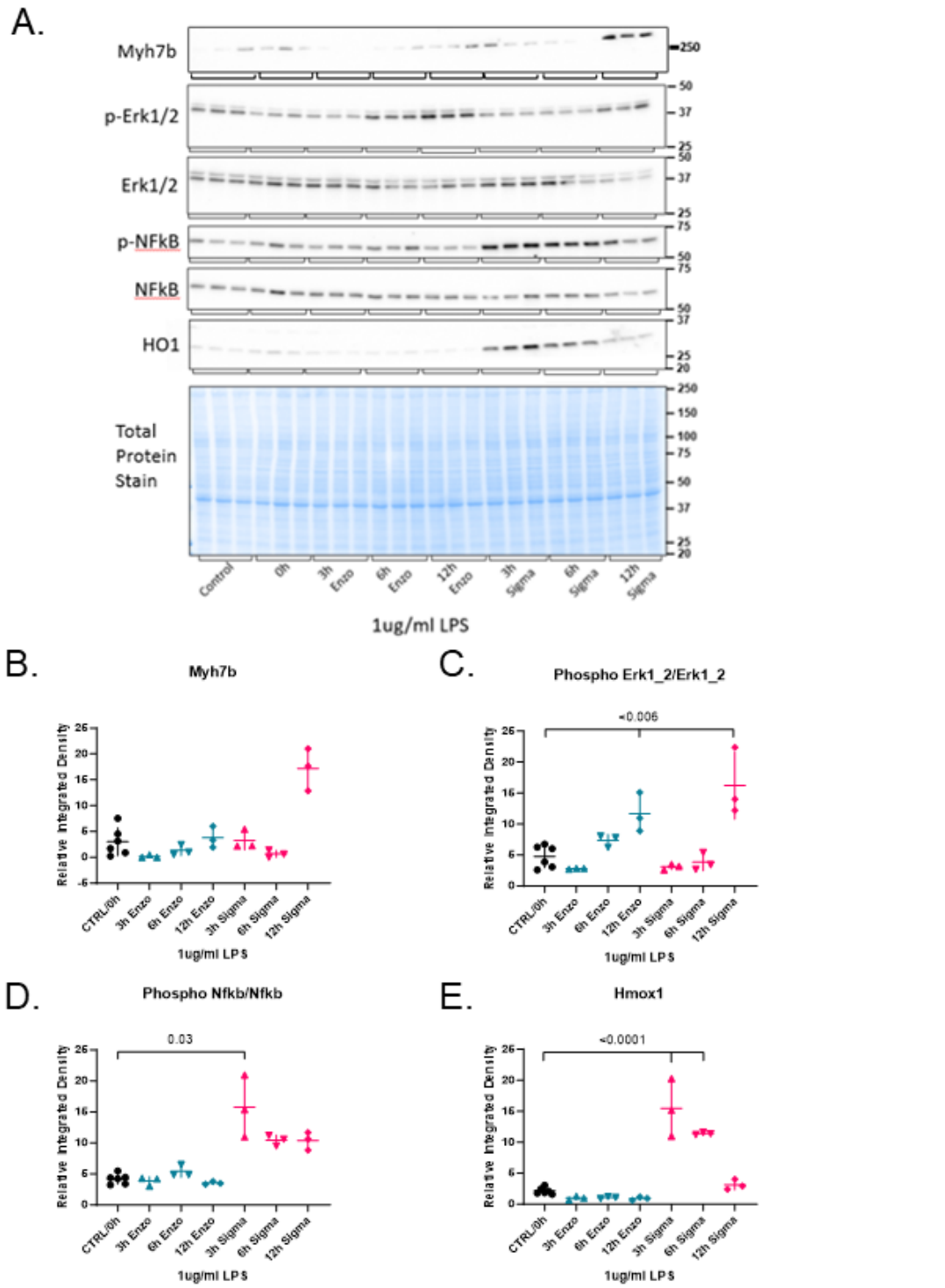

Figure 3.18. Time-dependent change in protein expressions of H9c2 myoblasts treated with variable lot source of LPS

(A) representative Myh7b, Erk1/2, Nfkb, Hmox1 probed membrane with total protein stains. (B) Myh7b did not differ significantly with treatment times except 12h treatment from Sigma. (C) Erk1/2 elevated with treatment time and showed significantly differ with 12h treatment in both source of LPS. (D) Nfkb elevated only with treatment from Sigma. (E) Hmox1 elevated only with treatment from Sigma, 3h and 6h treatment showed significantly difference from control.

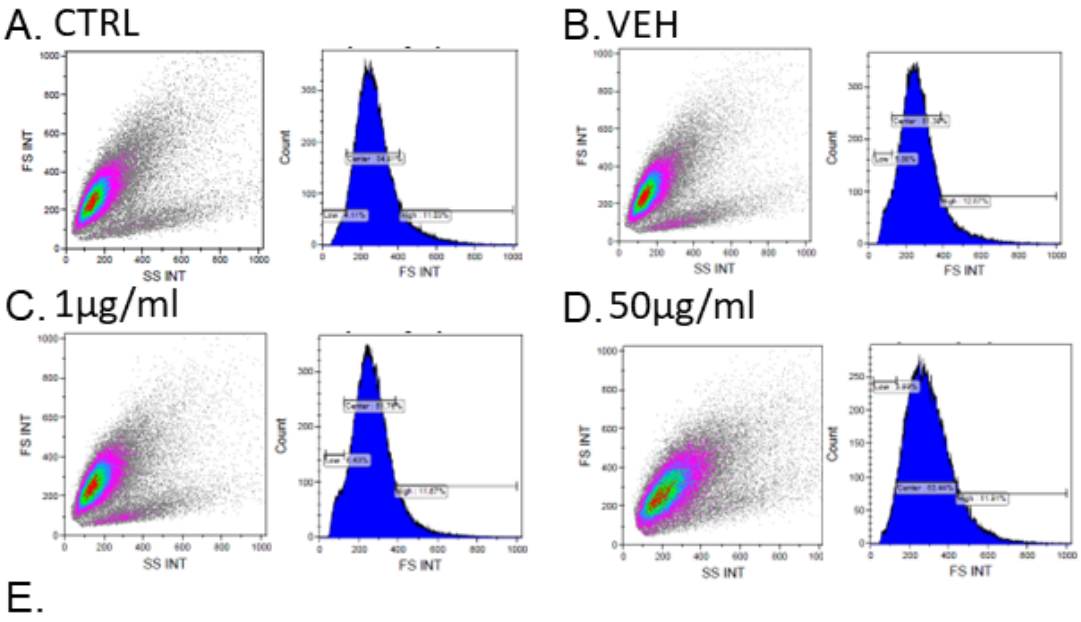

E.

Treatment group	Cell number	% Total	Median	Geometric means
CTRL	73,196	97.59	261.86	259.23
VEH	73,504	98.01	256.39	249.40
1µg/ml	73,184	97.58	257.63	247.06
50µg/ml	71,386	95.18	283.70	275.71

Figure 3.19. Flow cytometry analysis of H9c2 myoblasts treated with LPS.
The LPS source is from Sigma, the treatment time is 48hrs. (A) H9c2 myoblast CTRL 0nM of LPS. (B) Vehicle control, H9c2 myoblast with 100µl of ddH2O. (C) H9c2 myoblasts with 1µg/ml of LPS. (D) H9c2 myoblast with 50µg/ml of LPS, (E) Statistical information on H9c2 myoblasts treated with different concentration of LPS.

CHAPTER 4 DISCUSSION

4.1 Summary of Findings

HFpEF is a complicated disease with many pathophysiological and clinical features. Hypertrophy is one feature, and can be associated with other features potentially with interactions of significance that deserve more study, particularly as they relate to the underlying molecular mechanisms regulating cardiomyocyte hypertrophy and diastolic dysfunction.[6] Despite having affirmed an association of our molecular pathways of interest from a preclinical model that shared features of HFpEF, including hypertrophy, we did not confirm that H9c2 are a reliable cell model for hypertrophy to sufficiently to test our hypotheses using either AngII or LPS as stimuli. This led to a disappointing moot end to test pharmacologically our hypothesis for hemin or estrogen alone or together being able to attenuate hypertrophy at the cellular level as originally planned. However, we have collected some interesting hypothesis-generating data for future studies that might overcome the experimental limitations encountered here.

We completed our first objective and were able to identify a cohort of HFpEF patients from a cardiac surgical outcomes clinical database to discern insights into the features of HFpEF. Caution should be taken however as the original study design was not intended to enroll HFpEF patients per se, but given the focus on obesity, which is a feature of HFpEF, the probability of HFpEF patients presenting was expected. There is a high degree of selection bias for obesity in this study and males outnumbered females, all patients were scheduled (stable) not unscheduled (emergent) for surgery, and these were all patients requiring cardiac surgery, so don't represent all heart failure patients being managed by cardiology in the general population. As such, our cohort may not be representative of the broader HFpEF-afflicted population (by disease progression/severity, sex, or features of disease to be broadly applicable), nor would it be sufficiently powered to make

statistically determined conclusions clinically at this time. Despite these limitations, there was still a reasonable number (N=105) of HFpEF patients to make detailed observations with potential qualitative or empirical value. With these considerations including with reflection upon the literature introduced, we observed a null hypothesis, as we predicted that males would show a higher rate of hypertrophy with fewer comorbid features than females. Rather, females (22%) more than males (13%) had LVEF indicative of hypertrophy. Those females tended to be older than females without hypertrophy and had comorbid hypertension and uncontrolled diabetes associated with hypertension. Both sexes appeared to share risk of anemia and hypertension. Yet, it was males that showed a slightly higher rate of uncontrolled diabetes and anemia overall, not females as we hypothesized. If future studies explore these as covariates, there might be potential to discover undertreatment of females for diabetes or hypertension that is not yet fully recognized.

HFpEF patients exhibited a variety of comorbid clinical conditions, and some have common pathophysiological features, though not all conditions were present in every patient. To define HFpEF patients, a combination of three clinical conditions/features was utilized, including symptom presentation (based on NYHA guidelines), cardiac function parameters (LVEDP & LVEF), and markers of inflammation and metabolic stress (obesity, diabetes, and anemia). Future studies might add features of heme bioavailability or sex differences, or definitive biomarkers like pro-NT-BNP to facilitate a more detailed elucidation of the underlying physiological mechanisms of HFpEF, thereby enabling a refinement of targeted management strategies than what is currently available.

The observation of low hemoglobin levels in HFpEF patients may suggest reduced heme bioavailability, though no direct measures of heme or heme-regulating proteins have been made in the plasma/serum or in myocardial tissues yet and this could be useful to analyze to determine if anemia is a feature indicative of heme bioavailability. Given the HFpEF outcome differences by sex, monitoring sex hormones and their ratio (e.g. estrogen to testosterone) in both sexes may add

value as a biomarker to the course of HFpEF. Future investigations should consider molecular markers of these sex differences, but also gender effects that are socially determined that might lead to under-treatment or under-diagnosis of hypertrophy, hypertension, diabetes or anemia to better understand the underlying mechanisms and tailor management strategies accordingly.[108]

While the literature suggests that females have a higher morbidity than males, the higher levels of hypertrophy and associated features like hypertension and diabetes are concerning since they can precede mortality events in HFpEF due to sudden cardiac death, arrythmia-to-stroke, and cardiac failure.[109] However, there are fewer female patients in this clinical database to study. It could be that female patients are moving from stable (on waitlist) to emergent and so are not included in our patient catchment or that biological sex hormones still enable them to be stable on the waitlist longer than males with less need for surgery. It is difficult to speculate based on limited information at this time. Future studies that explore all HFpEF patients, ensuring diagnosis is not limited by sex or gender effects could enable larger studies to resolve these suppositions. Additionally, where males are recruited more often then females, bootstrapping analysis by resampling the data to randomly select equal numbers of males to compare to females might provide further insight or confidence to comparisons by sex effect.

Translating information from clinical observation to pre-clinical models is a challenge, particularly for HFpEF where no single model has achieved consensus. However, we were able to conduct a hypothesis-affirming study on a public dataset that aligned with the same species (rat) as our in vitro cell model of interest. This provided a bridge to research delve into some of the molecular mechanisms of interest using a preclinical HFpEF model, with gene expression data available in the GEO database. Surprisingly, despite evidence that the model has hypertrophy, only small changes (Nppa and Hand2) were determined in the genes typically used as biomarkers for hypertrophy. The often-utilized discriminators Myh7 and Myh6 for example were equivalent

between control and HFpEF. It may therefore be that hypertrophy in HFpEF where LVEF is preserved and hypertrophy apparent follows a different molecular pattern of hypertrophy. The change in heme-related genes were more apparent, including Hmox1, Hebp1, and Hrik (Eif2ak1), suggesting that heme bioavailability may be altered in HFpEF, potentially contributing to the pathophysiology of the disease. The potential for estrogen-regulated genes changes associated with HFpEF, such as Esrrg and Ste2, even in these male rats, further highlights the potential influence of estrogen signalling previously reported in HFpEF.[110,111] We did not explore androgen signaling, nor was it part of our objective or hypotheses but acknowledge this as an oversight and limitation that could be reconciled in future. However, the elevated expression affirmed with inflammatory mediator genes, including Il-1b, Tnf-a, Nfkb (p65), and Tlr4, underscored the role of inflammation in HFpEF development and progression, particularly, given that the model showed hypertrophy.[112,113] These findings align with previous studies implicating inflammation as a key contributor to cardiac remodelling and diastolic dysfunction in HFpEF.[114] These findings also provide some, albeit limited, reassurance supporting the exploration of the molecular changes associated with HFpEF future exploration of the role of heme bioavailability and sex differences in HFpEF as we originally hypothesized to do if not for experimental approaches that limited our hypothesis-testing.

Our investigation extended into an *in vitro* experimentation intended to model cellular hypertrophy based on several papers achieving similar hypertrophic effects (Table 1 and Table 2), where the effects of a surrogate treatment (Hemin)or estrogen on H9c2 myoblasts and myotubes could assessed as hypertrophic regulators. Hemin treatment demonstrate to increase Hmox1 protein expression, which has been associated with cytoprotection, with limited direct interaction on related hypertrophic pathways (Erk1/2 and Nfkb), though some reduction in Nfkb signaling was noted with hemin alone, suggesting it may pre-empt inflammation or Nfkb hypertrophic signaling. This study

then looked to confirm that a hypertrophic response in H9c2 cell lines could be achieved by AngII (stress-induced hypertrophy via hormone) or LPS (inflammatory-induced stimuli), two agents widely used to induce hypertrophy (Table 1 and Table 2). Unexpectedly, even at high doses (supraphysiological) these agents did not effectively induce hypertrophy in H9c2 cells, regardless if they were myoblast or differentiated into myotubules.

In troubleshooting this experimental setup, it was also discovered that the reagents themselves can also be implicated in the failure to elicit stress sufficient to induce hypertrophy in H9c2 cells. Further, variations of reagents could have resulted in conscious or unconscious bias of analysis in prior studies, though it is nearly impossible to determine this from other variables at play. By using an alternative lot, or changing sources of hypertrophic agents, we observed different cellular signalling patterns in hypertrophy proteins, some that might imply activation of hypertrophic signaling. We did not measure protein synthesis directly, which might be a useful additional parameter to consider as it is a precursor to increased total cell mass/volume when proliferation is controlled for. Since, Erk1/2 is not solely a hypertrophic regulator, but can regulate cell survival, proliferation and metabolic pathways, care should be taken in assuming that its expression or lack of expression are definitive to hypertrophy. As such, while some molecular patterns of hypertrophy could be elicited by AngII or LPS the results were neither reliably nor consistently dose-dependent or affirmed by various lots of AngII or sources of LPS that were otherwise prepared identically and sourced from a common supplier or alternative. As such, it may be that low purity, contaminants, lot-to-lot variation, and/or storage duration impacts the stability, effectiveness, and reliability of AngII or LPS as an inducer of in vitro H9c2 hypertrophy signalling, but as this is not overcome by dose escalation, degradation from mishandling is unlikely.

Yet no matter whether cells were assessed cells by 2D immunocytochemistry or total 3D cell size by flow cytometry analysis, not variable or troubleshooting attempt was able to yield

substantial changes in cell size indicative of hypertrophy or reliable molecular patterns associated with hypertrophy, thereby casting doubt on the reliability of H9c2 myoblasts or myotubules as a model for studying hypertrophy *in vitro*. It may be that other agents, like non-toxic levels of H2O2 that more directly cause oxidative stress might elicit hypertrophy.[60] Similarly, more targeted cytokines, like Tnf-a or Il-1b, might also generate more direct and reliable induction of inflammation to cause stress and hypertrophy. Further, the use of metabolic stress alone or in combination, such as by insulin with high glucose media or the addition of lipid stress, such as palmitate, might offer avenues that reliable generate hypertrophy in H9c2 cells. Finally, these cells have not experienced any mechanical load and do not cycle calcium or contract spontaneously (like true adult cardiomyocytes), so these features or modeling them may be key to eliciting a hypertrophic cell phenotype.

4.2 Comparison with the literatures and future directions

Table 1 and Table 2 were compiled to compare the findings of this thesis with prior of published literature that conducted on studies by inducing hypertrophy in H9c2 cells with AngII and LPS. Table 1 summarizes the dose and time of AngII treatment reported in the literature, along with the media and supplementation used, use of antibiotics, and methods used to analyse hypertrophy. These could be variables that are relevant to eliciting hypertrophy, or in revealing biases or uncontrolled variables to consider, in addition to randomization and blinding of analysis or other unconscious bias in methods of analyses used. Most studies commonly used the American Type Culture Collection (ATCC) as the original cell line source, but some of the studies used cells from the European Collection of Authenticated Cell Cultures (ECACC), Cell Bank of the China Sciences Academy (CBCSA), and one reported using cells from LGC Promochem. Although sex information for the cell lines were not avaible from CBCSA and LGC Promochem, H9c2 cells from ECACC are

female[115], and from ATCC are male[116]. The sex of a cell line might influence the hypertrophic response derived from the cells, and this information should be considered in any future studies carried out using H9c2 cells. In conducting experiments with FBS, carbon filtration of media to remove any trace sex hormones might also be necessary to prevent uncontrolled variables.

In the literature, AngII was mainly sourced from Sigma, and few studies gave specific lot or catalog numbers. As the cell signalling pattern was different between the lot numbers in this project from the same supplier, in future studies, it may be useful to test the consistency of reagents before use when carrying out experimentation or validate assumptions based on the induction of cell stress by measuring oxidative stress first for example. All the studies used DMEM as media for cell culture, with differences found in the serum, and in supplementation of glucose, or usage of antibiotics (Table 1). The most common reagent used was AngII amongst papers and the dose most often examined to induce hypertrophy in H9c2 cells was 1μM, with treatment times ranging from 4 to 48hrs depending on the study (Table 1). These results suggest hypertrophic response can be influenced by a wide variety of parameters, including the length of the hypertrophic stimulus, strength of the hypertrophic stimulus, and cell culture conditions.

Table 2 summarizes the dose and time of LPS treatment reported in the literature, along with the media and supplementation used, usage of antibiotic, and hypertrophy analysis methods. Amongst these papers the common source of the cell line was ATCC, except one study using cells from Cell Bank of the Chinese Academy of Science (Table 2). LPS was sourced from Sigma, but no information was available about which germ-negative bacteria species and strains were used in production, and details of purity were lacking. According to Pulendran et al.[117] they found LPS from different bacteria activate different inflammatory signalling pathways, which may suggest LPS derived from certain strains or bacterial species may better activate certain inflammatory pathways and so present another compound variable to limit replication. As such, while LPS is likely to elicit

inflammation, more defined cytokines might provide more consistent and reproducible results in future.

The methods used in many of the prior literature studies to analyze hypertrophy were limited to 2D sizing, which relied on manual cell planimetry using actin staining. This might suggest there is unconscious selection bias, towards picking bigger and brighter cells. Moreover, cells can take up variable surface area without an actual increase in total cell size (i.e., flattening or swelling). This study used flow cytometry as an unbiased method to measure the 3D volume of cells was determined, thereby greatly increasing the power of cell population analysis, and reducing the risk of unconscious selection bias, as the input sample was a truer representation of the population as a whole.

Since both hormones and inflammatory pathways indirectly rely on intracellular oxidative stress as a means of inducing hypertrophy, any future studies should examine the effect of using a direct oxidative stimulus, such as H_2O_2 to induce hypertrophy. It may also be valuable to consider combining stimuli or evaluating whether confounding factors, such as antibiotic use in cell culture media, may contribute to the downstream signalling required to induce hypertrophy occurring alongside hypertrophic stimuli. Using insulin, lipotoxicity, or anemic-hypoxia or a combination thereof could also be considered as a means of inducing hypertrophy to better model HFpEF preclinically, as it is a complex clinical syndrome with many pathophysiological stimuli. Different cell lines should also be considered for a model, like primary neonatal cardiomyocyte cells (NRCM)[75,118] or human AC16 cardiomyocyte cell line.[119]

Highlighting the importance of cell model selection, a study by Onodi et al. assessed the response to hypertrophic stimuli (100, 500, 1000 nM of AngII or isoprenaline for 24 hrs) on H9c2 cells along with other cardiac cell lines and primary NRCMs.[118] Onodi et al found that neither AngII nor isoprenaline treatments altered the hypertrophy markers (Nppb, Ctgf, Col1a1, and Col3a1) in

H9c2 cell lines.[118] Cell surface area was measured as well, and H9c2 did not show significant hypertrophy but NRCM did show a significant increase in cell surface area.[118] As such, we are not the first to identify potential limitations for the use of H9c2 cells as a model of hypertrophy.

Table 1. The dose and time effect of AngII treatment on H9c2 cell line to induce hypertrophy compared to reported literature.

Cell line (state & source)	Ang II source	Ang II dose	Treatment time	Media and supplementation	Antibiotic	% increase of cell size	Hypertrophy analysis	PMID
H9c2 (myoblasts, myotubes; ATCC)	Sigma (A9525)	100, 200, 250, 500, 700nM, 1, 2, 5, 10, 20, 100µM	24hrs, 48hrs	DMEM HG (Gibco) with 10% FBS (Gibco), serum-free DMEM for experiments.	Did not use	<5%	2D sizing (actin stain) 3D sizing (Flow cytomertry) ↑ Nfkb, n/c: Mhy7b, Erk1/2, (WB)	Kim et al (This thesis)
H9c2 (myoblasts; ECACC)	Sigma (A9525)	200nM	48hrs, 4hrs for RNA	DMEM HG with 10% FCS, 4 mM glutamine (Supplier not reported), serum-free DMEM for experiments	p/s 100U/ml	170%	↑ Bnp n/c: Anf, Acta, Mlc2v, Hprt (qPCR) 2D sizing (actin stain)	21082279[75]
H9c2 (CBCSA)	Sigma (Cat # not reported)	100nM, 1, 10µM	12hrs, 24hrs, or 48hrs	DMEM HG with 10% FBS *FBS reduced to 1% for Experiments.* (Thermo)	p/s	250%	↑ Vpo1, Nox2, Nox4, Bnp, Anf (qPCR) ↑Vpo1, Nox2, Erk1/2, pJnk, p38 (WB) 2D sizing (actin stain)	27651140[100]

Cell line (state & source)	Ang II source	Ang II dose	Treatment time	Media and supplementation	Antibiotic	% increase of cell size	Hypertrophy analysis	PMID
H9c2 (ATCC; CRL-1446)	Not reported	2μM	48h or 20 mins	DMEM with 10% FBS (Thermofisher)	p/s 100ug/mL	25%	↑ Anp, Bnp (qPCR) ↑ Erk, Akt, Gsk3β, Sirt3 (WB) 2D sizing (actin stain)	28296029[101]
H9c2 (ECACC)	Sigma (A9525)	1μM	48hrs	DMEM (Cat# AU-L0101) with 10% FBS (Cat# AU-S181H), 5% L-Glutamine (Cat# AU-X0550) , 5.5 mM D-Glucose	5% p/s (Cat# AU-L0022)	67%	2D sizing (actin stain)	30416452[120]
H9c2 (LGC Promochem)	Sigma (Cat# not reported)	1μM	4hrs	DMEM (Invitrogen) with 10% FCS	1% p/s	74% (biomarkers)	↑ Anf, Bnp, Myh7b, Mlc (qPCR)	18790741[99]
H9c2 (SIBCB)	Aladdin Chemicals (Cat# A107852)	1μM	24hrs for 2D sizing 6hrs for qPCR 6-48hrs for WB	DMEM (Gibco/BRL Life Technologies) with 10% FBS	100 units/mL p/s	128%	↑ Myh7b, Tgfb1, Col1a1 (qPCR) ↑ Myh7b, Tgfb1, Col1a1, Stat3 (WB) 2D sizing (actin stain)	32098592[102]

Cell line (state & source)	Ang II source	Ang II dose	Treatment time	Media and supplementation	Antibiotic	% increase of cell size	Hypertrophy analysis	PMID
H9c2 (ATCC)	EMD Millipore (Cat# not reported)	5μM	12, 24, 48hrs	DMEM HG(Corning) with 10% FBS (Gibco)	Not reported	22%, 46%, 115%	↑ Stat3, p-Jak2 (WB) ↑ Anp, Myh7b (qPCR) 2D sizing (actin stain)	28686615[103]
H9c2 (ATCC)	Sigma-Aldrich (Cat# not reported)	1μM (*Tested Viability*)	48hrs	DMEM (Gibco) with 10% FBS (Sagon Biotech Co) Serum Starved for Experiments	Penicillin 100 units/mL Streptomycin 10 ug/mL	800%	↑ Erk1/2, Akt (WB) 2D sizing (actin stain)	29750308[104]

↑, increased activity; n/c, no change; p/s, penicillin and streptomycin; WB, western blot; qPCR, quantitative real-time PCR; AngII, angiotensin II; PMID, PubMed Identifier; ATCC, american type culture collection; ECACC, european collection of authenticated cell cultures; CBCSA, cell bank of the china sciences academy; DMEM, dulbecco's modified eagle medium; HG, high glucose; FBS, fetal bovine serum; FCS, fetal calf serum; Myh7b, myosin heavy chain 7B; Erk, extracellular signal-regulated kinase; Nfkb, nuclear factor-κB; Bnp, brain natriuretic peptide; Anf, atrial natriuretic factor; Acta, alpha 1 actin; Mlc2v, ventricular myosin light chain 2; Hprt, hypoxanthine guanine phosphoribosyl transferase gene; Vpo1, vascular peroxidase 1; Nox2, NADPH oxidase2; Nox4, NADPH oxidase4; Jnk, c-Jun N-terminal kinases; Akt, protein kinase B; Gsk3β, Glycogen synthase kinase 3 beta; Mlc, myosin light chain; Tgfb1, transforming growth factor beta 1; Col1a1, collagen type I alpha 1 chain; Stat3, signal transducer and activator of transcription 3; Jak2, Janus Kinase 2.

Table 2. The dose and time effect of LPS treatment on H9c2 cell line to induce hypertrophy compared to reported literature.

Cell line (state & source)	LPS source	LPS dose	Treatment time	Media and supplementation	Antibiotic	% increase of cell size	Hypertrophy analysis	PMID
H9c2 (myoblast; ATCC)	Sigma, Enzo	0.5, 1, 10, 50μg/ml	3, 6, 12, 24, 48hrs	DMEM HG with 10% FBS	Did not use	<6%	↑ Erk1/2 n/c: Myh7b, Nfkb, Hmox1 (WB) 2D sizing (actin stain) 3D sizing (flow cytometry)	Kim et al
H9c2 (myoblast; ATCC)	Not reported	2μg/mL in serum-free medium	12hrs	DMEM with 10% CCS, 2 mM glutamine, 1 mM pyruvate	p/s (100 U/mL, 100 mg/mL)	200%	↑ Bnp (WB) 2D sizing (actin stain)	31081962[121]
H9c2 (myoblast; ATCC)	Sigma	2μg/ml	12hrs	DMEM with 10% FBS, 2 mM glutamine, 1 mM pyruvate	p/s (100 units/mL, 100 μg/mL)	120%	↑ Anp, Bnp, Gata4, Calcineurin (WB) 2D sizing (actin stain)	31714667[77]
H9c2 (myoblasts; ATCC)	Sigma	2μg/ml in serum-free medium	12hrs	DMEM with 10% CCS, 2 mM glutamine, 1 mM pyruvate	p/s (100 U/ml, 100 mg/ml)	170%	↑ Bnp (WB) 2D sizing (actin stain)	30980393[122]

Cell line (state & source)	LPS source	LPS dose	Treatment time	Media and supplementation	Antibiotic	% increase of cell size	Hypertrophy analysis	PMID
H9c2 cells (myoblasts; ATCC)	Sigma	1μg/ml	12hrs or 24hrs	DMEM with 10% FBS, 2 mM glutamine, 1 mM HEPS buffer	p/s (100 lg/ml)	130%	↑ Anp, Bnp, Gata4, nuclear Nfat3 (WB) 2D sizing (actin stain)	18398669[105]
H9c2 cells (myoblasts; ATCC)	Sigma	1μg/ml	3hrs or 24hrs	DMEM with 10% heat-inactivated FBS, 1% l-glutamine (200 mM), 1% sodium pyruvate (100 mM) 16 h before hypertrophy induction, cells were incubated in DMEM without serum.	p/s (100 IU/ml, 100 μg/ml)	25%	↑ Anp, Acta1 (qPCR) 2D sizing (actin stain)	25445045[106]
H9c2 (unspecified; Cell Bank of the Chinese Academy of Sciences)	Not reported	10μg/ml	6, 12, 24, 48hrs	DMEM with 10%FBS	Not reported	200%	↑ Anp, Bnp, Tlr4 (qPCR) ↑ Tlr4, nuclear Nfkb (WB) 2D sizing (actin stain)	33719658[123]

↑, increased activity; n/c, no change; p/s, penicillin and streptomycin; WB, western blot; qPCR, quantitative real-time PCR; AngII, angiotensin II; PMID, PubMed Identifier; ATCC, american type culture collection; DMEM, dulbecco's modified eagle medium; HG, high glucose; FBS, fetal bovine serum; CCS, Cosmic Calf Serum; Myh7b, myosin heavy chain 7B; Erk, extracellular signal-regulated kinase; Nfkb, nuclear factor-κB; Bnp, brain natriuretic peptide; Anp, atrial natriuretic peptide; Acta, alpha 1 actin; Tlr4, toll-like receptor 4.

4.3 Limitations

There are important limitations to this research thesis. The clinical data used was taken from the OPOS database, which recruited in a semi-biased manner to ensure selection of features to make comparisons across an obese sub-population, however HFpEF patients may not be obese and been negatively selected for that reason. Most of the patients had an Hgb-A1c in the normal range. However, this population may also be using diabetes medications, as there was no information about medications status, or the effect of these medications on their glycemic control charted in the database at the time of analysis. Therefore, this association may not accurately capture the effect of poor glycemic control on HFpEF development prior to drug treatment or in those who needed to change therapies to achieve better control. The study also did not measure pro-NT-BNP in patients in the OPOS database, which is often used to support the degree of myocardial dysfunction in HFpEF. Also, this clinical study was not designed to measure microvascular rarefaction, which is typically expected to occur in HFpEF patients. Future clinical studies exploring the HFpEF syndrome used to inform preclinical modeling should use a tighter selection criterion to better include parameters reflective of the disease being modeled like HFpEF.

The preclinical model used in the GEO dataset was the Dahl salt-sensitive (DSS) rat. DSS rats only models those patients that have hypertension, specifically salt-sensitive hypertension, thereby disregarding the 40-50% of the population with idiopathic hypertension that can not be linked to salt-sensitivity.[124] Also, we assumed that the data derived from GSE126062 has been normalized at the time of submission. The majority of GEO microarray data does conform to this normalization rule, however, we did not verify this extensively. Lastly, in the GEO dataset, cardiac tissues were only taken from three male animals (N=3) in the control and HFpEF phenotype. Therefore, these results are not generalizable.

This study was focused to be performed *in vitro* using the H9c2 cell line only. While this

allowed for cardiac cell specificity and direct modeling of conditions to identify molecular mechanisms, it lacks the complexity of the *in vivo* condition, with complex humoral, cellular, and molecular mechanisms interacting between various cardiac and other cell types within the heart. The cell viability findings in this study were limited somewhat by the assay used to measure viability. We used a resazurin-based assay, which more accurately measures cellular metabolic activity, based on a colorimetric change by substrate conversion, rather than a direct, binary measurement of live cell vs. dead cell assays, or cell stress assays associated with necrosis (e.g., Lactate dehydrogenase assay). This may explain in part why the cell viability read-outs do not match the findings reported in the literature using other methods of viability.

Finally, this study was limited by the types of statistical tests and replicate power used for the analysis. The normality testing (e.g., Shapiro-Wilk, Kolmogorov–Smirnov tests) upon which the further statistical tests were based, can be limited by the number of datapoints used in the modeling (i.e., statistical power, e.g. Myh7b). However, we assumed that our modelling was appropriately powered, and used the results of the normality testing based on this assumption accordingly, to decide to whether use an ANOVA or Kruskal-Wallis test with post-hoc analysis to determine p-values. This "conservative" approach to the statistical testing used in this project may have underestimated the differences between groups if the models used were not robustly powered.

4.4 Conclusions

The findings of this thesis underscore the intricate nature of HFpEF, emphasizing the need for a further investigation into how the features of the disease impact the associated molecular mechanisms that regulate the hypertrophy role of sex-specific responses. The challenges encountered in inducing hypertrophy *in vitro* raise important questions about the appropriateness of H9c2 myoblasts as a model for this purpose, calling for a re-evaluation of experimental methods in this context. In conclusion, while the H9c2 cell line is widely used for cardiomyocyte hypertrophy

studies, we have determined that inducing hypertrophy by AngII and LPS is not a reliable or reproducible approach for determining mechanisms or testing therapeutics at this time.

BIBLIOGRAPHY

1. Heidenreich, P. A. *et al.* 2022 AHA/ACC/HFSA Guideline for the Management of Heart Failure: A Report of the American College of Cardiology/American Heart Association Joint Committee on Clinical Practice Guidelines. *Circulation* **145**, e895–e1032 (2022).

2. Katz, A. M. & Rolett, E. L. Heart failure: when form fails to follow function. *Eur. Heart J.* **37**, 449–454 (2016).

3. Ejection Fraction Heart Failure Measurement. *www.heart.org* https://www.heart.org/en/health-topics/heart-failure/diagnosing-heart-failure/ejection-fraction-heart-failure-measurement.

4. Owan, T. E. *et al.* Trends in Prevalence and Outcome of Heart Failure with Preserved Ejection Fraction. *N. Engl. J. Med.* **355**, 251–259 (2006).

5. van Ham, W. B. *et al.* Clinical Phenotypes of Heart Failure With Preserved Ejection Fraction to Select Preclinical Animal Models. *JACC Basic Transl. Sci.* **7**, 844–857 (2022).

6. Ogilvie, L. M. *et al.* Hemodynamic assessment of diastolic function for experimental models. *Am. J. Physiol.-Heart Circ. Physiol.* **318**, H1139–H1158 (2020).

7. Gong, F. F. *et al.* Risk factors for incident heart failure with preserved or reduced ejection fraction, and valvular heart failure, in a community-based cohort. *Open Heart* **5**, e000782 (2018).

8. Lee, M. P. *et al.* Risk Factors for Heart Failure with Preserved or Reduced Ejection Fraction Among Medicare Beneficiaries: Application of Competing Risks Analysis and Gradient Boosted Model. *Clin. Epidemiol.* **12**, 607–616 (2020).

9. D'Amario, D. *et al.* Microvascular Dysfunction in Heart Failure With Preserved Ejection Fraction. *Front. Physiol.* **10**, 1347 (2019).

10. Guazzi, M., Ghio, S. & Adir, Y. Pulmonary Hypertension in HFpEF and HFrEF: JACC Review Topic of the Week. *J. Am. Coll. Cardiol.* **76**, 1102–1111 (2020).

11. Gazewood, J. D. & Turner, P. L. Heart Failure with Preserved Ejection Fraction: Diagnosis and Management. *Am. Fam. Physician* **96**, 582–588 (2017).

12. Kataria, R. & Van Spall, H. Pharmacologic Treatment For HFpEF: Role of Drug Therapies at the Higher End of LVEF Spectrum. *American College of Cardiology* https://www.acc.org/Latest-in-Cardiology/Articles/2022/03/08/18/51/http%3a%2f%2fwww.acc.org%2fLatest-in-Cardiology%2fArticles%2f2022%2f03%2f08%2f18%2f51%2fPharmacologic-Treatment-For-HFpEF (2022).

13. McDonagh, T. A. *et al.* 2021 ESC Guidelines for the diagnosis and treatment of acute and chronic heart failure: Developed by the Task Force for the diagnosis and treatment of acute and chronic heart failure of the European Society of Cardiology (ESC) With the special contribution of the Heart Failure Association (HFA) of the ESC. *Eur. Heart J.* **42**, 3599–3726 (2021).

14. Gevaert, A. B. *et al.* Heart failure with preserved ejection fraction: recent concepts in diagnosis, mechanisms and management. *Heart* **108**, 1342–1350 (2022).

15. Bauersachs, J. & López-Andrés, N. Mineralocorticoid receptor in cardiovascular diseases—Clinical trials and mechanistic insights. *Br. J. Pharmacol.* **179**, 3119–3134 (2022).

16. Pfeffer, M. A., Shah, A. M. & Borlaug, B. A. Heart Failure With Preserved Ejection Fraction In Perspective. *Circ. Res.* **124**, 1598–1617 (2019).

17. Anker, S. D. *et al.* Empagliflozin in Heart Failure with a Preserved Ejection Fraction. *N. Engl. J. Med.* **385**, 1451–1461 (2021).

18. Eadie, A. L., Brunt, K. R. & Herder, M. Exploring the Food and Drug Administration's review and approval of Entresto (sacubitril/valsartan). *Pharmacol. Res. Perspect.* **9**, e00794 (2021).

19. Nouraei, H. & Rabkin, S. W. A new approach to the clinical subclassification of heart failure with preserved ejection fraction. *Int. J. Cardiol.* **331**, 138–143 (2021).

20. Farris, S. D., Moussavi-Harami, F. & Stempien-Otero, A. Heart failure with preserved ejection fraction and skeletal muscle physiology. *Heart Fail. Rev.* **22**, 141–148 (2017).

21. Stolfo, D. *et al.* Sex-Based Differences in Heart Failure Across the Ejection Fraction Spectrum: Phenotyping, and Prognostic and Therapeutic Implications. *JACC Heart Fail.* **7**, 505–515 (2019).

22. Beale, A. L. *et al.* Sex Differences in Heart Failure With Preserved Ejection Fraction Pathophysiology: A Detailed Invasive Hemodynamic and Echocardiographic Analysis. *JACC Heart Fail.* **7**, 239–249 (2019).

23. Kaur, G. & Lau, E. Sex differences in heart failure with preserved ejection fraction: From traditional risk factors to sex-specific risk factors. *Womens Health* **18**, 17455057221140209 (2022).

24. Arcopinto, M., Valente, V., Giardino, F., Marra, A. M. & Cittadini, A. What have we learned so far from the sex/gender issue in heart failure? An overview of current evidence. *Intern. Emerg. Med.* **17**, 1589–1598 (2022).

25. Tamargo, J., Caballero, R. & Delpón, E. Sex-related differences in the pharmacological treatment of heart failure. *Pharmacol. Ther.* **229**, 107891 (2022).

26. Barandiarán Aizpurua, A., Schroen, B., van Bilsen, M. & van Empel, V. Targeted HFpEF therapy based on matchmaking of human and animal models. *Am. J. Physiol.-Heart Circ. Physiol.* **315**, H1670–H1683 (2018).

27. Matsiukevich, D. *et al.* Characterization of a robust mouse model of heart failure with preserved ejection fraction. *Am. J. Physiol.-Heart Circ. Physiol.* **325**, H203–H231 (2023).

28. Heinzel, F. R., Hohendanner, F., Jin, G., Sedej, S. & Edelmann, F. Myocardial hypertrophy and its role in heart failure with preserved ejection fraction. *J. Appl. Physiol.* **119**, 1233–1242 (2015).

29. Bernardo, B. C., Weeks, K. L., Pretorius, L. & McMullen, J. R. Molecular distinction between physiological and pathological cardiac hypertrophy: Experimental findings and therapeutic strategies. *Pharmacol. Ther.* **128**, 191–227 (2010).

30. Nauta, J. F. *et al.* Concentric vs. eccentric remodelling in heart failure with reduced ejection fraction: clinical characteristics, pathophysiology and response to treatment. *Eur. J. Heart Fail.* **22**, 1147–1155 (2020).

31. Simmonds, S. J., Cuijpers, I., Heymans, S. & Jones, E. A. V. Cellular and Molecular Differences between HFpEF and HFrEF: A Step Ahead in an Improved Pathological Understanding. *Cells* **9**, 242 (2020).

32. Paulus, W. J. & Tschöpe, C. A Novel Paradigm for Heart Failure With Preserved Ejection Fraction: Comorbidities Drive Myocardial Dysfunction and Remodeling Through Coronary Microvascular Endothelial Inflammation. *J. Am. Coll. Cardiol.* **62**, 263–271 (2013).

33. Mone, S. M., Sanders, S. P. & Colan, S. D. Control Mechanisms for Physiological Hypertrophy of Pregnancy. *Circulation* **94**, 667–672 (1996).

34. Schannwell, C. M. *et al.* Left Ventricular Hypertrophy and Diastolic Dysfunction in Healthy Pregnant Women. *Cardiology* **97**, 73–8 (2002).

35. Maron, B. J., Pelliccia, A., Spataro, A. & Granata, M. Reduction in left ventricular wall thickness after deconditioning in highly trained Olympic athletes. *Br. Heart J.* **69**, 125 (1993).

36. Mishra, S. & Kass, D. A. Cellular and molecular pathobiology of heart failure with preserved ejection fraction. *Nat. Rev. Cardiol.* **18**, 400–423 (2021).

37. Bhullar, S. K. & Dhalla, N. S. Angiotensin II-Induced Signal Transduction Mechanisms for Cardiac Hypertrophy. *Cells* **11**, 3336 (2022).

38. Sadoshima, J. & Izumo, S. Molecular characterization of angiotensin II--induced hypertrophy of cardiac myocytes and hyperplasia of cardiac fibroblasts. Critical role of the AT1 receptor subtype. *Circ. Res.* **73**, 413–423 (1993).

39. Clerk, A. & Sugden, P. H. Signaling through the extracellular signal-regulated kinase 1/2 cascade in cardiac myocytes. *Biochem. Cell Biol.* **82**, 603–609 (2004).

40. Bueno, O. F. & Molkentin, J. D. Involvement of Extracellular Signal-Regulated Kinases 1/2 in Cardiac Hypertrophy and Cell Death. *Circ. Res.* **91**, 776–781 (2002).

41. Yan, Z.-P., Li, J.-T., Zeng, N. & Ni, G.-X. Role of extracellular signal-regulated kinase 1/2 signaling underlying cardiac hypertrophy. *Cardiol. J.* **28**, 473–482 (2021).

42. Park, C., Cha, H.-J., Lee, H., Kim, G.-Y. & Choi, Y. H. The regulation of the TLR4/NF-κB and Nrf2/HO-1 signaling pathways is involved in the inhibition of lipopolysaccharide-induced inflammation and oxidative reactions by morroniside in RAW 264.7 macrophages. *Arch. Biochem. Biophys.* **706**, 108926 (2021).

43. Xiao, Z. *et al.* Key Player in Cardiac Hypertrophy, Emphasizing the Role of Toll-Like Receptor 4. *Front. Cardiovasc. Med.* **7**, (2020).

44. Singh, M. V. & Abboud, F. M. Toll-like receptors and hypertension. *Am. J. Physiol.-Regul. Integr. Comp. Physiol.* **307**, R501–R504 (2014).

45. Ha, T. *et al.* Reduced cardiac hypertrophy in toll-like receptor 4-deficient mice following pressure overload. *Cardiovasc. Res.* **68**, 224–234 (2005).

46. Ehrentraut, H. *et al.* The toll-like receptor 4-antagonist eritoran reduces murine cardiac hypertrophy. *Eur. J. Heart Fail.* **13**, 602–610 (2011).

47. Sumneang, N., Apaijai, N., Chattipakorn, S. C. & Chattipakorn, N. Myeloid differentiation factor 2 in the heart: Bench to bedside evidence for potential clinical benefits? *Pharmacol. Res.* **163**, 105239 (2021).

48. Płóciennikowska, A., Hromada-Judycka, A., Borzęcka, K. & Kwiatkowska, K. Co-operation of TLR4 and raft proteins in LPS-induced pro-inflammatory signaling. *Cell. Mol. Life Sci.* **72**, 557–581 (2015).

49. Zhang, Y., Wu, J., Dong, E., Wang, Z. & Xiao, H. Toll-like receptors in cardiac hypertrophy. *Front. Cardiovasc. Med.* **10**, (2023).

50. Kim, E. K. & Choi, E.-J. Compromised MAPK signaling in human diseases: an update. *Arch. Toxicol.* **89**, 867–882 (2015).

51. Gilbert, C. J., Longenecker, J. Z. & Accornero, F. ERK1/2: An Integrator of Signals That Alters Cardiac Homeostasis and Growth. *Biology* **10**, 346 (2021).

52. Liang, F., Atakilit, A. & Gardner, D. G. Integrin Dependence of Brain Natriuretic Peptide Gene Promoter Activation by Mechanical Strain*. *J. Biol. Chem.* **275**, 20355–20360 (2000).

53. Chen, J. *et al.* Specific LPA receptor subtype mediation of LPA-induced hypertrophy of cardiac myocytes and involvement of Akt and NFκB signal pathways. *J. Cell. Biochem.* **103**, 1718–1731 (2008).

54. Lorenz, K., Schmitt, J. P., Schmitteckert, E. M. & Lohse, M. J. A new type of ERK1/2 autophosphorylation causes cardiac hypertrophy. *Nat. Med.* **15**, 75–83 (2009).

55. Wang, C. *et al.* Crosstalk between angiotensin II and platelet derived growth factor-BB mediated signal pathways in cardiomyocytes. *Chin. Med. J. (Engl.)* **121**, 236 (2008).

56. Carrasco Mujica, L. *et al.* Role of heterotrimeric G protein and calcium in cardiomyocyte hypertrophy induced by IGF-1. *J. Cell. Biochem.* (2014) doi:10.1002/jcb.24712.

57. Sawicki, K. T., Chang, H. & Ardehali, H. Role of Heme in Cardiovascular Physiology and Disease. *J. Am. Heart Assoc.* **4**, e001138.

58. Mense, S. M. & Zhang, L. Heme: a versatile signaling molecule controlling the activities of diverse regulators ranging from transcription factors to MAP kinases. *Cell Res.* **16**, 681–692 (2006).

59. Uma, S., Yun, B.-G. & Matts, R. L. The Heme-regulated Eukaryotic Initiation Factor 2α Kinase: A POTENTIAL REGULATORY TARGET FOR CONTROL OF PROTEIN SYNTHESIS BY DIFFUSIBLE GASES *. *J. Biol. Chem.* **276**, 14875–14883 (2001).

60. Brunt, K. R. *et al.* Heme Oxygenase-1 Inhibits Pro-Oxidant Induced Hypertrophy in HL-1 Cardiomyocytes. *Exp. Biol. Med. Maywood NJ* **234**, 582–594 (2009).

61. Chen, J.-J. Regulation of protein synthesis by the heme-regulated eIF2α kinase: relevance to anemias. *Blood* **109**, 2693–2699 (2007).

62. Packer, M. How can sodium–glucose cotransporter 2 inhibitors stimulate erythrocytosis in patients who are iron-deficient? Implications for understanding iron homeostasis in heart failure. *Eur. J. Heart Fail.* **24**, 2287–2296 (2022).

63. Voltarelli, V. A., Alves de Souza, R. W., Miyauchi, K., Hauser, C. J. & Otterbein, L. E. Heme: The Lord of the Iron Ring. *Antioxidants* **12**, 1074 (2023).

64. Miyamoto, H. D. *et al.* Iron Overload via Heme Degradation in the Endoplasmic Reticulum Triggers Ferroptosis in Myocardial Ischemia-Reperfusion Injury. *JACC Basic Transl. Sci.* **7**, 800–819 (2022).

65. Bell, J. R., Bernasochi, G. B., Varma, U., Raaijmakers, A. J. A. & Delbridge, L. M. D. Sex and sex hormones in cardiac stress—Mechanistic insights. *J. Steroid Biochem. Mol. Biol.* **137**, 124–135 (2013).

66. Hayward, C. S., Webb, C. M. & Collins, P. Effect of sex hormones on cardiac mass. *The Lancet* **357**, 1354–1356 (2001).

67. Regitz-Zagrosek, V. & Seeland, U. Sex and gender differences in myocardial hypertrophy and heart failure. *Wien. Med. Wochenschr. 1946* **161**, 109–116 (2011).

68. van Eickels, M. *et al.* 17β-Estradiol Attenuates the Development of Pressure-Overload Hypertrophy. *Circulation* **104**, 1419–1423 (2001).

69. Pedram, A. *et al.* Estrogen Inhibits Cardiac Hypertrophy: Role of Estrogen Receptor-β to Inhibit Calcineurin. *Endocrinology* **149**, 3361–3369 (2008).

70. Eghbali, M. *et al.* Molecular and Functional Signature of Heart Hypertrophy During Pregnancy. *Circ. Res.* **96**, 1208–1216 (2005).

71. Chen, Z. *et al.* Estrogen receptor α mediates the nongenomic activation of endothelial nitric oxide synthase by estrogen. *J. Clin. Invest.* **103**, 401–406 (1999).

72. Jankowski, M., Rachelska, G., Donghao, W., McCann, S. M. & Gutkowska, J. Estrogen receptors activate atrial natriuretic peptide in the rat heart. *Proc. Natl. Acad. Sci.* **98**, 11765–11770 (2001).

73. Kilić, A., Javadov, S. & Karmazyn, M. Estrogen exerts concentration-dependent pro-and anti-hypertrophic effects on adult cultured ventricular myocytes. Role of NHE-1 in estrogen-induced hypertrophy. *J. Mol. Cell. Cardiol.* **46**, 360–369 (2009).

74. Deswal, A. & Bozkurt, B. Comparison of Morbidity in Women Versus Men With Heart Failure and Preserved Ejection Fraction. *Am. J. Cardiol.* **97**, 1228–1231 (2006).

75. Watkins, S. J., Borthwick, G. M. & Arthur, H. M. The H9C2 cell line and primary neonatal cardiomyocyte cells show similar hypertrophic responses in vitro. *Vitro Cell. Dev. Biol. - Anim.* **47**, 125–131 (2011).

76. Kimes, B. W. & Brandt, B. L. Properties of a clonal muscle cell line from rat heart. *Exp. Cell Res.* **98**, 367–381 (1976).

77. Tung, C.-L. *et al.* LPS-enhanced IGF-IIR pathway to induce H9c2 cardiomyoblast cell hypertrophy was attenuated by Carthamus tinctorius extract via IGF-IR activation. *Environ. Toxicol.* **35**, 145–151 (2020).

78. Aguiar, C. *et al.* Impact of Obesity on Postoperative Outcomes following cardiac Surgery (The OPOS study): rationale and design of an investigator-initiated prospective study. *BMJ Open* **9**, (2019).

79. Mascherbauer, J. *et al.* Wedge Pressure Rather Than Left Ventricular End-Diastolic Pressure Predicts Outcome in Heart Failure With Preserved Ejection Fraction. *JACC Heart Fail.* **5**, 795–801 (2017).

80. Oh, J. K., Miranda, W. R. & Kane, G. C. Diagnosis of Heart Failure With Preserved Ejection Fraction Relies on Detection of Increased Diastolic Filling Pressure, But How? *J. Am. Heart Assoc.* **12**, e028867 (2023).

81. World Health Organization. Haemoglobin concentrations for the diagnosis of anaemia and assessment of severity. *Vitam. Miner. Nutr. Inf. Syst. Geneva Switz. World Health Organ.* 1–6 (2011) doi:2011.

82. Zhang, W. *et al.* Morphometric, Hemodynamic, and Multi-Omics Analyses in Heart Failure Rats with Preserved Ejection Fraction. *Int. J. Mol. Sci.* **21**, 3362 (2020).

83. Peverill, R. E. Understanding preload and preload reserve within the conceptual framework of a limited range of possible left ventricular end-diastolic volumes. *Adv. Physiol. Educ.* **44**, 414–422 (2020).

84. Kosaraju, A., Goyal, A., Grigorova, Y. & Makaryus, A. N. Left Ventricular Ejection Fraction. in *StatPearls* (StatPearls Publishing, 2023).

85. Susic, D. & Frohlich, E. D. The aging hypertensive heart: a brief update. *Nat. Clin. Pract. Cardiovasc. Med.* **5**, 104–110 (2008).

86. A healthy lifestyle - WHO recommendations. https://www.who.int/europe/news-room/fact-sheets/item/a-healthy-lifestyle---who-recommendations.

87. All About Your A1C. *Centers for Disease Control and Prevention* https://bit.ly/2Nc2IA0 (2018).

88. Petrie, J. R., Guzik, T. J. & Touyz, R. M. Diabetes, Hypertension, and Cardiovascular Disease: Clinical Insights and Vascular Mechanisms. *Can. J. Cardiol.* **34**, 575–584 (2018).

89. Jia, G. & Sowers, J. R. Hypertension in Diabetes: An Update of Basic Mechanisms and Clinical Disease. *Hypertens. Dallas Tex 1979* **78**, 1197–1205 (2021).

90. Sun, D. *et al.* Type 2 Diabetes and Hypertension: A Study on Bidirectional Causality. *Circ. Res.* **124**, 930–937 (2019).

91. Badireddy, M. & Baradhi, K. M. Chronic Anemia. in *StatPearls* (StatPearls Publishing, 2023).

92. Bohlius, J., Weingart, O., Trelle, S. & Engert, A. Cancer-related anemia and recombinant human erythropoietin—An updated overview. *Nat. Clin. Pract. Oncol.* **3**, 152–64 (2006).

93. Gela, Y. Y. *et al.* Prevalence of anemia and associated factors among adult hypertensive

patients in Referral Hospitals, Amhara Regional State. *Sci. Rep.* **13**, 14329 (2023).

94. Naito, Y. *et al.* Adaptive response of the heart to long-term anemia induced by iron deficiency. *Am. J. Physiol.-Heart Circ. Physiol.* **296**, H585–H593 (2009).

95. Paul, B., Wilfred, N. C., Woodman, R. & DePasquale, C. Prevalence and Correlates of Anaemia in Essential Hypertension. *Clin. Exp. Pharmacol. Physiol.* **35**, 1461–1464 (2008).

96. Gu, S. *et al.* EPC-Derived Microvesicles Protect Cardiomyocytes from Ang II-Induced Hypertrophy and Apoptosis. *PLOS ONE* **9**, e85396 (2014).

97. Gao, G. *et al.* Rapamycin regulates the balance between cardiomyocyte apoptosis and autophagy in chronic heart failure by inhibiting mTOR signaling. *Int. J. Mol. Med.* **45**, 195–209 (2020).

98. A., P., P., S. R., M., P. R. & K.g., R. Apoptosis in angiotensin II-stimulated hypertrophic cardiac cells -modulation by phenolics rich extract of Boerhavia diffusa L. *Biomed. Pharmacother.* **108**, 1097–1104 (2018).

99. Stuck, B. J., Lenski, M., Böhm, M. & Laufs, U. Metabolic Switch and Hypertrophy of Cardiomyocytes following Treatment with Angiotensin II Are Prevented by AMP-activated Protein Kinase*. *J. Biol. Chem.* **283**, 32562–32569 (2008).

100. Yang, W. *et al.* Involvement of vascular peroxidase 1 in angiotensin II–induced hypertrophy of H9c2 cells. *J. Am. Soc. Hypertens.* **11**, 519-529.e1 (2017).

101. Guan, X.-H. *et al.* CD38 promotes angiotensin II-induced cardiac hypertrophy. *J. Cell. Mol. Med.* **21**, 1492–1502 (2017).

102. Ye, S. *et al.* Celastrol Attenuates Angiotensin II–Induced Cardiac Remodeling by Targeting STAT3. *Circ. Res.* **126**, 1007–1023 (2020).

103. Chen, L. *et al.* STAT3 balances myocyte hypertrophy vis-à-vis autophagy in response to Angiotensin II by modulating the AMPKα/mTOR axis. *PLoS ONE* **12**, e0179835 (2017).

104. Wang, Q., Xu, Y., Gao, Y. & Wang, Q. Actinidia chinensis planch polysaccharide protects against hypoxia-induced apoptosis of cardiomyocytes in vitro. *Mol. Med. Rep.* **18**, 193–201 (2018).

105. Liu, C.-J. *et al.* Lipopolysaccharide induces cellular hypertrophy through calcineurin/NFAT-3 signaling pathway in H9c2 myocardiac cells. *Mol. Cell. Biochem.* **313**, 167–178 (2008).

106. Magi, S. *et al.* Gram-negative endotoxin lipopolysaccharide induces cardiac hypertrophy: Detrimental role of Na+–Ca2+ exchanger. *Eur. J. Pharmacol.* **746**, 31–40 (2015).

107. Li, N. *et al.* Ferritinophagy-mediated ferroptosis is involved in sepsis-induced cardiac injury. *Free Radic. Biol. Med.* **160**, 303–318 (2020).

108. O'Neil, A., Scovelle, A. J., Milner, A. J. & Kavanagh, A. Gender/Sex as a Social Determinant of Cardiovascular Risk. *Circulation* **137**, 854–864 (2018).

109. Garg, P. *et al.* Left ventricular fibrosis and hypertrophy are associated with mortality in heart failure with preserved ejection fraction. *Sci. Rep.* **11**, 617 (2021).

110. Crosier, R. *et al.* Sex Differences in Systemic and Coronary Arterial Hemodynamics in Heart Failure With Preserved Ejection Fraction. *Am. J. Cardiol.* **205**, 87–93 (2023).

111. Rozenbaum, Z. *et al.* Sex differences in heart failure patients assessed by combined echocardiographic and cardiopulmonary exercise testing. *Front. Cardiovasc. Med.* **10**, 1098395 (2023).

112. Shen, S. *et al.* Colchicine alleviates inflammation and improves diastolic dysfunction in heart failure rats with preserved ejection fraction. *Eur. J. Pharmacol.* **929**, 175126 (2022).

113. Saavedra-Alvarez, A., Pereyra, K. V., Toledo, C., Iturriaga, R. & Del Rio, R. Vascular dysfunction in HFpEF: Potential role in the development, maintenance, and progression of the disease. *Front. Cardiovasc. Med.* **9**, 1070935 (2022).

114. Daou, D., Gillette, T. G. & Hill, J. A. Inflammatory Mechanisms in Heart Failure with Preserved Ejection Fraction. *Physiology* **38**, 217–230 (2023).

115. Ballantyne, T. *et al.* Testosterone protects female embryonic heart H9c2 cells against severe metabolic stress by activating estrogen receptors and up-regulating IES SUR2B. *Int. J. Biochem. Cell Biol.* **45**, 283–291 (2013).

116. Altieri, P. *et al.* Testosterone Antagonizes Doxorubicin-Induced Senescence of Cardiomyocytes. *J. Am. Heart Assoc.* **5**, e002383 (2016).

117. Pulendran, B. *et al.* Lipopolysaccharides from Distinct Pathogens Induce Different Classes of Immune Responses In Vivo. *J. Immunol. Baltim. Md 1950* **167**, 5067–5076 (2001).

118. Onódi, Z. *et al.* Systematic transcriptomic and phenotypic characterization of human and murine cardiac myocyte cell lines and primary cardiomyocytes reveals serious limitations and low resemblances to adult cardiac phenotype. *J. Mol. Cell. Cardiol.* **165**, 19–30 (2022).

119. Ren, B. *et al.* Ginsenoside Rg3 attenuates angiotensin II-induced myocardial hypertrophy through repressing NLRP3 inflammasome and oxidative stress via modulating SIRT1/NF-κB pathway. *Int. Immunopharmacol.* **98**, 107841 (2021).

120. Trotta, M. C. *et al.* The Melanocortin MC5R as a New Target for Treatment of High Glucose-Induced Hypertrophy of the Cardiac H9c2 Cells. *Front. Physiol.* **9**, 1475 (2018).

121. Chao, C.-N. *et al.* Tid1-S attenuates LPS-induced cardiac hypertrophy and apoptosis through ER-a mediated modulation of p-PI3K/p-Akt signaling cascade. *J. Cell. Biochem.* **120**, 16703–16710 (2019).

122. Chao, C.-N. *et al.* CHIP attenuates lipopolysaccharide-induced cardiac hypertrophy and apoptosis by promoting NFATc3 proteasomal degradation. *J. Cell. Physiol.* **234**, 20128–20138 (2019).

123. Sun, F., Chen, G., Yang, Y. & Lei, M. Fatty acid-binding protein 4 silencing protects against lipopolysaccharide-induced cardiomyocyte hypertrophy and apoptosis by inhibiting the Toll-like receptor 4–nuclear factor-κB pathway. *J. Int. Med. Res.* **49**, 0300060521998233 (2021).

124. Warren, H. R. *et al.* Genome-wide association analysis identifies novel blood pressure loci and offers biological insights into cardiovascular risk. *Nat. Genet.* **49**, 403–415 (2017).

Appendix A PrestoBlue media compatibility and cell dilution curve

A.

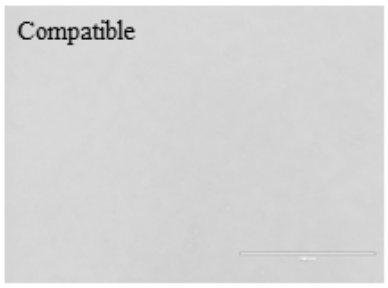

RPMI, No cells, 0% FBS

B.

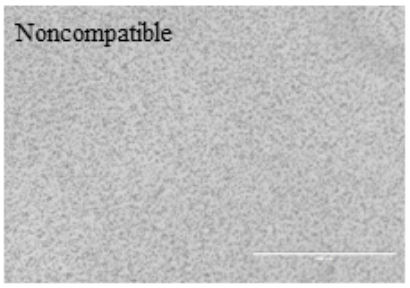

DMEM, No cells, 0% FBS

C.

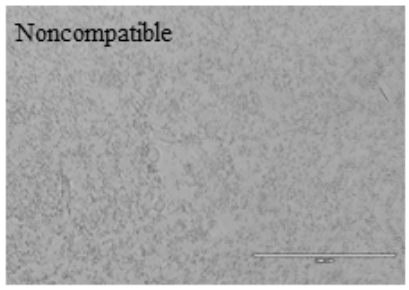

DMEM, Yes cells, 0% FBS

D.

Conditioning			Expiry date: 2022 Aug	Expiry date: 2023 Mar						1% BSA	0.5% BSA	0.1% BSA
Cells		No	No	No	No	No	No	No	No	No	No	No
FBS		0.0%	0.0%	0.0%	0.1%	0.5%	1.0%	5.0%	10.0%	0.0%	0.0%	0.0%
Media	DMEM											
	RPMI											
	MEM											
	EBSS											

Conditioning			Expiry date: 2022 Aug	Expiry date: 2023 Mar						1% BSA	0.5% BSA	0.1% BSA
Cells		Yes	Yes	Yes	Yes	Yes	Yes	Yes	Yes	Yes	Yes	Yes
FBS		0.0%	0.0%	0.0%	0.1%	0.5%	1.0%	5.0%	10.0%	0.0%	0.0%	0.0%
Media	DMEM											
	RPMI											
	MEM											
	EBSS											

Conditioning		Acidified by CO2	Acidified by HCl	GlutaMAX + N2	F12
Cells		No	No	No	No
FBS		0.0%	0.0%	10.0%	10.0%
Media	DMEM				
	RPMI				
	MEM				
	EBSS				

Not Tested
Stable
Unstable

E.

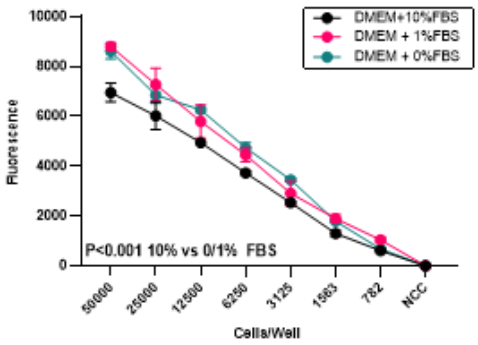

F.

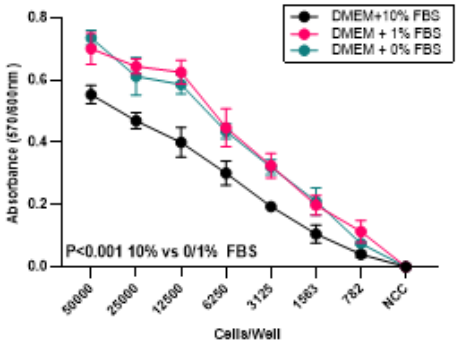

Some cell culture media conditions can make PrestoBlue reagent precipitation/aggregation. (A) Representative phase contrast microscopy of compatible media with PrestoBlue in 96 well. It has RPMI, no cells, 0% FBS. (B) Representative phase contrast microscopy of noncompatible media with PrestoBlue in 96 well. It has DMEM + 0% FBS, no cells, and showed precipitation/aggregation. (C) Representative phase contrast microscopy of noncompatible media with PrestoBlue in 96 well. It has DMEM + 0% FBS, H9c2 cells, and showed precipitation/aggregation. (D) A summary table of all testing have been done on PrestoBlue precipitation/aggregation with different conditioned cell culture media. For DMEM, it has to have minimum 0.1% FBS with cell or 0.5% FBS without cell to avoid precipitation/aggregation. RPMI was safe on either with or without FBS. MEM with 105 FBS was not compatible. This compatibility was not influence by the freshness of media, or acidity, or BSA concentration. To test will the precipitation/aggregation effect on the PrestoBlue readout, a dilation curve with different concentration of FBS in DMEM was tested. (E) showed PrestoBlue Fluorescence readout on DMEM with FBS concentration dependent. (F) showed PrestoBlue absorbance readout on DMEM with FBS concentration dependent. Readouts showed lower concentration of FBS higher the readout, but pattern of the curves are similar. The curve between 12,500 cells/well group and 6,250 cells/well group are parallel, it suggests that 12,500-6,250 cells/well will be the ideal cell seeding number for 96well PrestoBlue cell viability assay.

Appendix B GEO data from genes of interest

Gene name	Control			Mean	SD	HFpEF			Mean	SD
Hmox1	5.83036	6.13357	5.85691	5.94	0.17	6.42975	7.79711	6.84123	7.02	0.70
Hmox2	11.0598	11.0154	11.039	11.04	0.02	11.1083	11.077	11.5032	11.23	0.24
Alas1	14.711	14.0232	14.6416	14.46	0.38	13.5486	14.7	14.8429	14.36	0.71
Alas2	8.12443	6.44889	8.22832	7.60	1.00	6.29646	6.81436	6.27078	6.46	0.31
Hebp1	7.05496	7.18724	7.18241	7.14	0.08	7.63565	8.06103	7.81157	7.84	0.21
Hebp2	6.23754	6.78892	5.82328	6.28	0.48	7.04887	6.56691	6.35078	6.66	0.36
Hrik (eif2ak1)	11.1728	11.194	11.0856	11.15	0.06	11.2909	11.3673	11.3665	11.34	0.04
Perk (eif2ak3)	8.97383	9.61199	8.9107	9.17	0.39	9.90393	9.46897	9.37885	9.58	0.28

GEO datapoints related to heme metabolism genes

Gene name	Control			Mean	SD	HFpEF			Mean	SD
Esrrg	4.69774	4.92334	4.7941	4.81	0.11	5.15512	7.79711	6.84123	7.02	0.70
Ste2	2.98609	3.4121	3.65252	3.35	0.34	2.4594	11.077	11.5032	11.23	0.24
Rerg	7.62608	7.74984	7.63971	7.67	0.07	8.11979	14.7	14.8429	14.36	0.71
Esrra	12.9193	12.3729	12.8755	12.72	0.30	11.7712	6.81436	6.27078	6.46	0.31
Esrrb	3.89165	5.07906	3.88504	4.29	0.69	5.35098	8.06103	7.81157	7.84	0.21
Gper	2.95528	3.03644	4.08586	3.36	0.63	2.4594	6.56691	6.35078	6.66	0.36
Esr1	4.76582	5.39269	4.58082	4.91	0.43	6.77681	11.3673	11.3665	11.34	0.04
Esr2	5.64701	5.35406	5.87547	5.63	0.26	4.45576	9.46897	9.37885	9.58	0.28

GEO datapoints related to estrogen signalling genes

Gene name	Control			Mean	SD	HFpEF			Mean	SD
IL-1b	7.03244	6.25627	6.81811	6.70	0.40	7.67404	6.90233	8.13626	7.57	0.62
IL-6	5.59595	4.76733	5.76358	5.38	0.53	4.91611	5.57618	5.77185	5.42	0.45
IL-10	5.01948	2.7333	4.71913	4.16	1.24	4.36044	5.23976	4.73676	4.78	0.44
Tnf-a	5.01948	2.7333	4.71913	4.16	1.24	6.83716	8.04765	8.7701	7.88	0.98
Nf-kb (p65)	4.61149	4.06791	4.36375	4.35	0.27	4.90835	4.93084	4.91706	4.92	0.01
Tlr4	6.75129	7.00863	6.73081	6.83	0.15	7.24213	7.27602	7.22487	7.25	0.03

GEO datapoints related to inflammation genes

Gene name	Control			Mean	SD	HFpEF			Mean	SD
Nppa	14.3345	15.6863	12.7079	14.24	1.49	15.739	15.5114	15.1573	15.47	0.29
Nppb	14.353	15.0184	14.215	14.53	0.43	14.906	14.5825	14.5973	14.70	0.18
Myh6	14.3779	14.5865	14.711	14.56	0.17	14.917	14.7711	14.139	14.61	0.41
Myh7	14.2683	14.1013	14.2253	14.20	0.09	13.9492	14.3642	14.353	14.22	0.24
Gata4	9.07521	9.36039	9.08587	9.17	0.16	9.13165	8.91183	8.6876	8.91	0.22
Hand2	7.54189	8.22469	7.88215	7.88	0.34	8.58009	8.04013	8.53957	8.39	0.30

GEO datapoints related to hypertrophy genes

Gene name	Control			Mean	SD	HFpEF			Mean	SD
Tlr7	4.07578	4.58818	3.71287	4.13	0.44	5.56877	6.6083	6.21414	6.13	0.52
Diaph3	4.50215	4.74379	4.57322	4.61	0.12	5.44957	6.9262	6.26957	6.22	0.74

Example of two genes analyzed by Zhang et.al. They found these two genes significantly increased compared to control from qPCR, even the log2 fold change were less than 1.